Cellulase saccharification of rooibos biomass pretreated with horseradish peroxidase

By

Mamosela Marriam Mohotloane

Submitted in fulfilment of the requirements for the degree

MASTER OF SCIENCE (BOTANY)

In the Faculty of Natural and Agricultural sciences
Department of Plant Sciences: Botany Division
University of the Free State
Bloemfontein Campus

November 2023

Supervisor: Dr. Mpho Stephen Mafa

Declaration

I, Mamosela Marriam Mohotloane, declare that the Master's Degree research publishable manuscripts/published articles that I herewith submit for the Master's Degree qualification in Botany at the University of the Free State is my independent work, and that I have not previously submitted it for a qualification at another institution of higher education.

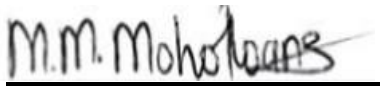

27 November 2023

Mamosela Marriam Mohotloane **Date**

Plant Science Department

Dedicated to:

My mom,
Mpho Margret Mohotloane

&

My sister,
Reamohetswe Mohotloane

,

“Success is no accident. It is hard work, perseverance, learning, studying, sacrifice and most of all, love of what you are doing or learning to do.”– Pelé

Acknowledgements

I would like to express my gratitude to the following institutions:

- University of the Free State, Department of Plant Science and Centre for Graduate Support, for resources and funding that made my studies a success.
- National Research Foundation (NRF) Thuthuka grant for funding my research project.
- Future Professoriate Programme for supporting my appointment as a Lab research assistant in the Carbohydrate and enzymology laboratory (CHEM Lab)

I would like to express my heartfelt gratitude to:

- Dr Mpho S Mafa (my supervisor) for his constant support throughout this project. His impeccable work ethics, kindness, inspiring passion for research and motivation to be the best version of myself. Thank you for believing in me and showing me that any goal is attainable through hard work and determination.
- Prof Brett Ivan Pletschke for his constant support.
- Dr Orbett Alexander for assistance with FTIR and XRD analysis, and valuable feedback.
- Hanlie Grobler for training and assistance with SEM analysis.
- My mom and sister ("my day ones"💕) for their continued love, support, and motivation. My pillars of strength, comfort and encouragement in moments in my life, where i felt uncertainty. You've given me hope to move forward without fearing the unknown. Thank you for believing in me and pushing me to be my best. I wouldn't be where I am without you💕.

I would like to thank God for the strength and guidance to complete my studies.

Table of Contents

List of abbreviations

%	Percent
AA	Auxiliary activity
AAO	Aryl alcohol oxidase
AcME	Acetyl mannan esterases
APX	Ascorbate peroxidase
BEK	Bleached eucalypt kraft pulp
BRF	Brown rot fungi
BWX	Beechwood xylan
C.S	Crystallite size
C1/C4	Carbon number 1 or 4
$Ca(OH)_2$	Calcium hydroxide
CBHI	Cellobiohydrolase-I
CBM	Carbohydrate binding modules
CMC	Carboxymethyl cellulose sodium
CO_2	Carbon dioxide
CrI	Crystallinity index
Cu (II)	Copper(II) oxide
CWDE	Cell wall degrading enzymes
DNS	Dinitrosalicylic acid reagent
DP	Degree of polymerisation
Dyp	Dye decolourising peroxidase
EG1	Endoglucanase-1
EG2	Endoglucanase-2
EGs	Endoglucanases
EXLA	Expansin-like A
EXLB	Expansin-like B
EXLX	Expansin-like X
EXPA	α-expansins
EXPB	β-expansins
FAE-1	Feruloyl esterase
Fe^{2+}	Ferrous ion
FTIR	Fourier transform infrared spectroscopy
FWHM	Full width half maximum

GH	Glycoside hydrolase
GOD	Glyoxal oxidase
GX	Glucuronoxylan
H_2O	Water
H_2O_2	Hydrogen peroxide
H_2SO_4	Sulfuric acid
H_3PO_4	Phosphoric acid
HCl	Hydrochloric acid
HEC	Holocellulolytic enzyme cocktail
HNO_3	Nitric acid
HRP	Horseradish peroxidase
I.P.C.C	Intergovernmental Panel on Climate Change
KOH	Potassium hydroxide
Lac	Laccase
LiP	Lignin peroxidase
LPMO	Lytic polysaccharide monooxygenase
MnP	Manganese peroxidase
NaOH	Sodium hydroxide
nm	Nanometer
NSSC	Neutral sulfite semi-chemical pulp
OH	Hydroxylic group
SBP	Soybean peroxidase
SDS-PAGE	Sodium dodecyl sulfate-polyacrylamide gel electrophoresis
SEM	Scanning electron microscope
SRF	Soft rot fungi
v/v	Volume per volume
VAPs	Value-added products
VP	Versartile peroxidase
w/v	Weight per volme
WAX	Wheat arabinoxylan
WRF	White rot fungi
XRD	X-ray diffraction

List of figures

Appendices

List of tables

Appendices

Research outputs

Conferences

❖ International Conference

Mamosela, M. Mohotloane, Brett, I Pletschke, and Mpho, S. Mafa. HRP pretreatment modifies the structural and chemical properties of rooibos biomass, improving its saccharification by enzyme cocktails. 4th International Conference of Bioresource Technology for Bioenergy, Bioproducts and Environmental Sustainability (BIORESTEC). Italy, 2023 (Poster)

❖ Local conference

Mamosela, M. Mohotloane and Mpho, S. Mafa. Formulation of holocellulolytic enzyme cocktail for hydrolysis of HRP-delignified rooibos bagasse for production of value-added chemicals. The 32nd Annual meeting of the Catalysis Society of South Africa (CATSA). South africa, 2022 (poster)

❖ Science communication: NAS Flash facts Competition

Mamosela, M. Mohotloane and Mpho, S. Mafa. First place winner in the Botany Division during the Plant science departmental flash fact competition and a finalist in the Natural and Agricultural Science faculty competition.

Publications

- ❖ Mohotloane, M.M., Alexander, O., Pletschke, B.I. and Mafa, M.S., (2023). Horseradish peroxidase delignification of fermented rooibos modifies biomass structural and chemical properties and improves holocellulolytic enzyme cocktail efficacy. Biologia 78, 1943–1959. https://doi.org/10.1007/s11756-023-01424-4 (IF: 1.67, Q3)
- ❖ Mohotloane, M.M., Alexander, O., Adoons, V.N., Pletschke, B.I. and Mafa, M.S., 2024. Peroxidase application reduces microcrystalline cellulose recalcitrance towards cellulase hydrolysis in model cellulose substrates and rooibos biomass. Carbohydrate Polymer Technologies and Applications, 7, p.100426. https://doi.org/10.1016/j.carpta.2024.100426 (IF: 5.5, Q1). Note: the manuscript was published during the marking of the dissertation, therefore, the title and the structure of the content underwent review. The publication may slightly differ from the submitted chapter 4.

Summary

Worldwide industrilization has led to economic activities (such as burning of fossil fuels) that enhance greenhouse gas emmissions in the atmostphere, resulting in a phenomenon known as global warming. Therefore, the use of agricultural residues to produce second generation biofuel (2G) can lead to a reduction in carbon dioxide (CO_2) emissions. However, it has been challenging to produce biofuel from agricultural residues, due to the presence of lignin in the plant biomass. Lignin causes non-specific binding of the glycoside hydrolases (GHs) to the biomass, reducing their efficiency. Therefore, it is vital to remove lignin before the production of biofuel. Most chemical methods are effective in removing lignin but are expensive and hazardous to the environment and human health. Hence, there is a need to find cheaper alternative methods that are sustainable, renewable, and environmentally friendly, such as the use of biological pretreatment. This study aimed to delignify fermented rooibos using purified horseradish peroxidase (HRP) and to formulate a holocellulolytic enzyme cocktail for conversion of the delignified fermented rooibos biomass to soluble sugars.

The results indicated that HRP was partially purified, with activity on guaiacol, 8-aminoquinoline, and decolourised methylene blue dye. HRP had a pH optimum of 4.5 and displayed a mesophilic temperature range. It had higher affinity towards guaiacol (Km= 0.082 mg/mL) compared to 8-aminoquinoline (Km= 0.221 mg/mL), but it efficiently catalysed both guaiacol (63436.48 s^{-1}. mg/mL) and 8-aminoquinoline (59189.81 s^{-1}. mg/mL). The partially purified HRP was used to pretreat the fermented rooibos biomass to remove lignin. Scanning electron microscopic (SEM) analysis showed lignin removal, exposed microcrystalline cellulose fibres and the changed structure of the biomass. These observations were corroborated by the Fourier Transform Infrared (FTIR) spectroscopy, which showed reduction of ester-linkages and phenolic functional groups. X-ray diffraction (XRD) analysis confirmed that pretreated biomass had reduced crystallinity compared to the control (untreated) biomass. Cellulose model substrates (Avicel and filter paper) were used to elucidate the mechanisms HRP uses to reduce the crystallinity of cellulose fibres. The results suggest that HRP treatment increased cellulose crystallite sizes from 45 to 47 nm at the 002 lattices in Avicel and decreased from 60.7 to 59.3 nm in filter paper. These modifications enhanced hydrolytic enzymes' accessibility (demonstrated using endoglucanase) to the pretreated rooibos biomass than the control. Commercial cellulases and xylanases were used to formulate the holocellulolytic enzyme cocktail (HEC). The HEC converted the HRP delignified rooibos biomass to soluble

sugars, producing about 95% yield of total reducing sugars at enzymes load of 25 mg /g biomass.

Chapter 1: General introduction

Carbon dioxide is an important gas used in plant photosynthesis and the most abundant greenhouse gas in the atmosphere, mainly regulated by the carbon cycle. However, economic activities (mainly burning fossil fuel) accelerate its accumulation in the atmosphere by producing toxic gases such as carbon monoxide, leading to increased global temperature or what is known as global warming (I.P.C.C 2007; Tian *et al.,* 2018). These toxic gases disrupt the regulation of carbon dioxide emissions. Therefore, several strategies, such as the production of ethanol-based biofuel from forestry or agricultural residues, have been developed to decrease carbon dioxide emissions (Tsegaye *et al.,* 2019; Bhatia *et al.,* 2020; Mafa *et al.,* 2020b; Saravanan *at el.,* 2022). Biofuel (particularly second-generation biofuel) is a form of green energy that can replace fossil fuel and regulate carbon dioxide through the carbon cycle, thus minimizing the greenhouse gas emissions (Olsson and Hahn-Hagerdal 1996; Houghton 2005; I.P.C.C 2007; de Gouvêa *et al.,* 2019).

Second-generation biofuel has been studied for decades in the biorefinery sector, but it continues to be a challenge to close the gap in the circular economy due to the presence of lignin in the plant biomass (also known as lignocellulose) (van Dyk and Pletschke 2012; Bagewadi *et al.,* 2017; Giacobbe *et al.,* 2018; Kumar *et al.,* 2020; Mafa *et al.,* 2020b;). The removal of lignin from the biomass via eco-friendly means and the application of enzyme cocktails to degrade lignocellulose to simple fermentable sugars has been an obstacle, thus resulting in a higher (expensive) price of biofuel compared to petroleum production (Olsson and Harn-Hagerdal 1996). Therefore, it is imperative to do further research on more efficient methods for lignin removal, which will result in a higher conversion of fermentable sugars from lignocellulose degraded with formulated enzyme cocktails (van Dyk and Pletschke 2012; Mafa *et al.,* 2020b; Tiwari *et al.,* 2023).

The major constituents of lignocellulose are cellulose, hemicellulose, and lignin (Malhotra and Suman 2021). Cellulose and hemicellulose (known as holocellulose) are the sources of sugars that can be fermented into ethanol or value-added products (VAP) (van Dyk and Pletschke 2012; Tian *et al.,* 2018; Malgas *et al.,* 2019; Kumar *et al.,* 2020; Malhotra and Suman 2021; Mustafa *et al.,* 2022). Lignin is a phenolic-containing polymer that protects the plant by reinforcing the cell wall (Tian *et al.,* 2018; Kumar *et al.,* 2020; Mnich *et al.,* 2020; Malhotra and Suman 2021; Mustafa *et al.,* 2022). Cell wall reinforcement interrupts the enzyme-

substrate complex, thus inhibiting the conversion of the substrate to sugar products (Bagewadi *et al.,* 2017; Kong *et al.* 2017; Bhatia *et al.,* 2020; Malhotra and Suman 2021; Sheng *et al.,* 2021). Therefore, it is for this reason that lignin must be removed before the lignocellulosic biomass is hydrolysed through enzymatic application (Mnich *et al.,* 2020; Malhotra and Suman 2021; Tiwari *et al.,* 2023). However, the removal of lignin poses a challenge due to the pretreatment methods that have been developed, which are based on the use of chemicals (such as acids and alkaline pretreatment).

These pretreatment methods have limitations; for instance, acid pretreatments are not only expensive to use, but they are toxic to the environment and human health because they produce toxic compounds (Bagewadi *et al.,* 2017; Kong *et al.,* 2017; Agrawal *et al.,* 2019). They also affect the production and fermentation process of the sugars by producing inhibitory products, such as furfural and hydroxymethylfurfural (Badiei *et al.,* 2014; Behera *et al.,* 2014; Bagewadi *et al.,* 2017; Kong *et al.,* 2017; Haldar and Purkait 2021; Malhotra and Suman 2021). Although alkaline pretreatments are cost-effective, they also have limitations, which include the hydrolysis of a higher concentration of hemicellulose affecting the sugar production, and lignin removal is dependent on the amount of lignin present in the biomass (Hendriks and Zeeman 2009; Mafa *et al.,* 2020b). Therefore, we proposed the use of biological pretreatments, which are sustainable and environmentally friendly without affecting the production and fermentation process of the sugar products (Giacobbe *et al.,* 2018; Malhotra and Suman 2021). The literature review aims to provide an overview of biological pretreatments as a method of lignin removal that increases the effectiveness of the holocellulolytic enzyme cocktails during sugar production.

Chapter 2: Literature review

1. Summary of lignocellulose composition

Lignocellulose is considered the most abundant organic resource that makes up the main component of the plant cell wall. The major components of lignocellulosic biomass are cellulose, hemicellulose, and lignin, while pectin, ash content and protein composition is lower (Van Dyk and Pletschke 2012; Calderan-Rodrigues *et al.,* 2019; Mnich *et al.,* 2020). The percentage composition of the major components (cellulose, hemicellulose, and lignin) differs between lignocellulosic sources (Table A2). The percentage content is commonly 30-60%, 20–40%, and 15–25% for cellulose, hemicellulose, and lignin, respectively (Koupaie *et al.,* 2019). Table A2 shows the lignocellulose composition of various biomass materials used for biofuel production.

Cellulose is made up of linear β-D-glucose units linked by β-D-(1→4) glycosidic bonds, forming microcrystalline fibres with small amounts of amorphous cellulose occurring between the fibres (Olsson and Harn-Hagerdal 1996; Silva-Sanzana *et al.,* 2020; Mafa *et al.,* 2021a). Cellulose microcrystalline fibres are directional, as they consist of a reducing end at anomeric carbon (C1) and a nonreducing end at C4 carbon (Mafa *et al.,* 2021a). The microcrystalline cellulose chain bundle is made possible by the inter and intra hydrogen bonding, which forms between adjacent and/or opposite hydroxylic groups (OH) (Crosgrove 2000; Harmsen *et al.,* 2010; Silva-Sanzana *et al.,* 2020). These structural properties make microcrystalline cellulose insoluble in water and recalcitrant to enzymatic hydrolysis (Coseri 2017).

Hemicellulose is composed of a group of polysaccharides containing the β-D-(1→4)-linked backbones of D-glucose, D-mannose, and D-xylose, while the sidechains are composed of L-arabinose, D-galactose and aldoronic acids (Malgas *et al.,* 2019). Hemicelluloses are grouped into classes depending on the sugar residues found in their backbone, such as xyloglucans, xylans (arabinoxylan, glucuronoxylan and arabino-glucuronoxylan), mannans (glucomannan, galactomannan, and galactoglucomannan) and mixed-linked glucans (Olsson and Harn-Hagerdal 1996; Malgas *et al.,* 2019; Malgas *et al.,* 2020; Silva-Sanzana *et al.,* 2020; Mafa *et al.,* 2021b). Additionally, the hemicellulose composition of lignocellulosic material differs depending on the plant species (Olsson and Harn-Hagerdal 1996; Silva-Sanzana *et al.,* 2020). Hence, it is necessary to understand the sample type (dicot or monocot) before choosing the hemicellulolytic enzymes to degrade the hemicellulose content in the biomass.

The complex structure of lignin is made up of monolignols that form subunits in the polymer. The monolignols are known as p-hydroxycinnamyl (coumaryl) alcohol, 4-hydroxy-3-methoxycinnamyl (coniferyl) alcohol, and 3,5-dimethoxy-4-hydroxycinnamyl (sinapyl) alcohol and they form the phenylpropanoid units, namely, p-hydroxyphenyl (H) subunits, guaiacyl (G) subunits, and syringyl (S) subunits, respectively (Koupaie *et al.,* 2019; Chan *et al.,* 2020; Mnich *et al.,* 2020; Weng *et al.,* 2021). The lignin polymer binds to cellulose and hemicellulose resulting in a rigid structure of the plant cell wall and it is mainly found in the cell walls of vascular plants, where it plays a role in growth and development. Additionally, it can protect the plant cells against cell wall degrading enzymes (CWDE) secreted by pathogens and pests due to its insoluble nature (Mnich *et al.,* 2020). Due to its protective nature, lignin causes non-specific substrate-enzyme binding complex, thus inhibiting enzymatic degradation (Kong *et al.,* 2017; Malhotra and Suman 2021). Therefore, it is essential to remove lignin through chemical, mechanical, hydrothermal, or biological pretreatments before cellulose or hemicellulose hydrolysis.

2. Biological pretreatments for sustainable lignin removal

The biological pretreatment is defined as the method that uses biological molecules such as enzymes or microorganisms to achieve a cost-effective, sustainable, and eco-friendly lignocellulosic pretreatment approach (Kong *et al., 2*017; Malhotra and Suman 2021; Mohotloane *et al.,* 2023). The pretreatment is mostly known for the utilisation of microorganisms such as fungi and bacteria, which produce enzymes that remove lignin and decrease the recalcitrant nature of the microcrystalline cellulose (Menon and Rao 2012; Behera *et al.,* 2014; Mustafa *et al.,* 2022). In addition, several studies used recombinant enzymes, crude enzymes, or purified enzymes extracted from microorganisms to remove lignin from the biomass (Giacobbe *et al.,* 2018; Agrawal *et al.,* 2019; Daou *et al.,* 2021). The recent study by Mohotloane *et al.* (2023) demonstrated that some enzymes (peroxidase) sourced from plant material are efficient in removing lignin from the biomass.

There are several reasons biological pretreatments are preferred over other methods. They include high selectivity for the substrate of choice, require low energy to produce high yields of sugar products or lignin removal, do not produce inhibitory products (like black liquor), and reduce loss of polysaccharides from the biomass (Giacobbea *et al.,* 2018; Wagner *et al.,* 2018; Sharma *et al.,* 2019; Hernández-Chaverri *et al.,* 2021; Devi *et al.,* 2022; Mustafa *et al.,* 2022).

However, the reaction conditions require careful monitoring, and the process is slow in terms of fungal pretreatment compared to non-eco-friendly chemical pretreatments. The slow nature of the reaction offers scientists an opportunity to explore technologies that can enhance the reaction to better the system. Hence, there has been a rise in research in this area in the past decade (Harmsen *et al.,* 2010; Limayem and Ricke 2012; Menon and Rao 2012; Hernández-Chaverri *et al.,* 2021; Mustafa *et al.,* 2022). The types of biological pretreatments include microbial (known as fungal, bacterial, microbial consortia and ensiling) and enzymatic. Table 2.1 summarizes the benefits and limitations of biological pretreatments in contrast to the developed (chemical, mechanical and physical) pretreatments.

Table 2.1: The advantages and limitation of the developed pretreatment methods and their effect on the biomass

Type Pretreatment	**Description**	**Pretreatment time**	**Effects on biomass structure**	**Advantage**	**Disadvantage**	**References**
Chemical						
Acids	• Pretreatment with dilute or strong acids, with a concentration of 4% and 70-77%, respectively. • The most used acids can be inorganic or organic such as H_2SO_4, HCl, H_3PO_4, HNO_3, fumaric and maleic acids. • Dilute acids require a temperature range of 130-210°C, while 40-100°C for strong acids	20-90 minutes	• Enlarged surface area that enhances biomass digestibility, resulting in the removal of hemicellulose. • Lignin modification.	• It is a well-studied technique. • High reaction rate. • Requires high temperature and pressure.	• Low lignin digestion. • Increased formation of inhibitors. • Corrosive and toxic to the environment and human health. • Requires neutralization.	Kumar *et al.* (2020); Haldar and Purkait (2021)
Alkali	• Alkaline pretreatment uses chemicals such as NaOH, KOH and $Ca(OH)_2$	Several minutes to hours	• Lignin degradation. • Enlarged surface area, leading to hemicellulose digestion.	• Efficient in biomass containing low lignin content. • Requires low temperature and pressure. • Enhanced downstream hydrolysis.	• Requires longer reaction time. • Neutralization may be difficult.	Hendriks and Zeeman (2009); Kumar *et al.* (2020); Mafa *et al.* (2020)
Ozonolysis	• The use of ozone gas that is applied to the biomass at a particular flow rate	15-90 minutes	• Mostly selective for lignin digestion.	• Formation of inhibitors is relatively low.	• On-site production and use of ozone gas is extremely expensive.	Zabed *et al.* (2016)

				• Functions at room temperature and atmospheric pressure.	• The use of ozone gas poses safety issue due to its flammability and toxicity.	
Ionic liquid	• Application of ionic liquids on lignocellulose biomass (such as N-methyl morpholine-N-oxide monohydrate) • The ionic liquids remain liquids at temperatures that are not above 100°C	30-60 minutes	• Enlarged surface area that results in better cellulose and hemicellulose digestion. • Efficient lignin removal.	• Easy to recycle and re use. • Consumes low energy, even at high biomass loading.	• Recovery of ironic liquids Is necessary. • Increasing the costs.	Li *et al.* (2011); Kumar *et al.* (2020); Li *et al.* (2022); Sidana *et al.* (2022)
Organosolv	• A cocktail of organic liquids and water at a ratio of 1:1 • Mineral acids can be used as organosolv as they improve lignin removal	30 minutes	• Complete digestion of hemicellulose and lignin. However, cellulose remains in a solid form.	• Neutral conditions are required for low cellulose loss. • Functions at low temperature and pressure. • Produces pure cellulose yields. • Efficient in biomass containing high lignin content.	• Removal of solvents is not necessary. • Although the method is expensive. • Results in the production of inhibitors.	Tayyab *et al.* (2018); Sidana *et al.* (2022)
Physical						
Mechanical	• The grinding, milling, chipping of biomass material to a small to fine size	A few minutes (Approximately 1-10 min)	• Enlarged surface area, increased porosity and decrease in cellulose crystallinity, improved	• Easy to use. • Improves mass and heat transfer in the downstream processes (hydrolysis and fermentation).	• Requires high energy during processing. • Without the removal of lignin.	Zabed *et al.* (2016); Koupaie *et al.* (2019)

			accessibility to enzymes.	• Resulting in high hydrolysis yield.	• The method is not economically practical.	
Irradiation	• The use of microwave, gamma, electron beam irradiation and ultrasonic treatment	Minutes to hours	• Incomplete removal of lignin that enhanced surface area leading to: • A decrease in cellulose crystallinity. • Complete digestion of hemicellulose.	• Efficient at high energy input. • Improving the rate of the downstream enzymatic hydrolysis.	• The method is not environmentally friendly. • With low rate of biomass modification. • Resulting in high costs.	Bhutto *et al.* (2017); Hassan *et al.* (2018)
Physicochemical						
Steam explosion	• An example is the use of an autoclave which uses high-temperature and pressure steam that autohydrolysis the biomass with or without an acid catalyst. • The temperature and pressure of the steam is about 160-260°C and 5-50 atm, respectively.	Several minutes (around 5 min)	• Modification of lignin structure, resulting in complete digestion of lignin. • Enlarged surface area, resulting in accessibility to hemicellulose digestion.	• No requirement for recycling or implication on the environmental costs. • Shorter reaction time, at low energy input.	• Produces inhibitory compounds. • Leading to loss of sugar products after hydrolysis.	Auxenfans *et al.* (2017); Kumar *et al.* (2020)
Liquid hot water	• The hydrolysis of biomass using higher temperatures of about 180-220°C and pressure	15 minutes	• Complete digestion of lignin. • Enlarged surface area, leading to	• Minimal to no formation of inhibitory compounds. • Leading to the high recovery of sugars.	• Requires a lot of water and energy input for processing. • Resulting in high costs	Luo *et al.* (2019)

			hemicellulose digestion.	• Which is achieved without the need for catalysts or chemicals.	• However, it produces low fermentable sugars	
Wet oxidation	• Application of air or oxygen on the lignocellulose biomass • The methods require high temperature of 140-210° and pressure of about 20.0mpa	5-120 minutes	• Lignin degradation. • Enlarged surface area, leading to reduced cellulose recalcitrance.	• Inexpensive capital costs. • Effective lignin removal and carbohydrate recovery. • Increased accessibility to enzymatic digestion.	• Expensive materials for the reactor are required. • With high energy input. • However, there's low recovery of hemicellulose.	Bhutto *et al.* (2017)
Supercritical fluid	• The commonly used supercritical fluid is CO_2, which uses moderate critical temperature and pressure	20 minutes	• Successful lignin removal that increased the surface area leading to. • Accessibility to cellulose digestion.	• Low operational costs. • With low temperature requirement for high solid loads. • However, results in minimal sugar degradation.	• The utilities required may increase the costs. • Outputs may be affected.	Bhutto *et al.* (2017); Hernández-Chaverri *et al.* (2021),
Ammonia fibre explosion (AFEX)	• Application of liquid ammonia on lignocellulose biomass at a temperature of 60-120°C and 3mpa pressure for the duration of 30 minutes followed by the decompression step	30-60 minutes	• Modification of lignin structure leading to the removal of lignin. • Enlarged surface area, increasing accessibility to cellulose and hemicellulose digestion.	• It is only effective for biomass that contains low lignin content.	• The equipment and ammonia required in the processes are expensive.	Koupaie *et al.* (2019); Kumar *et al.* (2020)

Biological						
Fungal	• The fungal pretreatment method is based on the incorporation of single cells or species of basidiomycetes or ascomycetes fungi with the lignocellulolytic biomass using the classic cultivation techniques, namely, submerged culture or solid-state.	Weeks to months	• It is effective in lignin removal, but the method results in a greater loss of the holocellulose.	• The pretreatment and downstream recovery costs are low. • The method requires less energy and reagents. • There's little to no waste generation and formation of inhibitors.	• The method requires long incubation time. • It results in a loss of carbohydrates.	Kumar *et al.* (2020); Hernández-Chaverri *et al.* (2021); Maity *et al.* (2021)
Bacterial	• The method subjects the lignocellulosic biomass to lignin-degrading enzymes such as Actinomycetes, α-proteobacteria and γ-proteobacteria	Several days	• It is less effective for lignin removal due to the complexity of the lignin structure thus most bacterial strains are suited for holocellulose degradation.	• Bacteria growth is more rapid than fungi. • The method is more effective than fungi, with a shorter incubation time. • It is easier to genetically manipulate bacteria, and it has higher adaptability than fungi. • It also has little to no formation of inhibitors.	• The method is less effective in degrading lignin compared to fungi.	Kumar *et al.* (2020)
Microbial consortium	• The microbial consortia pretreatment incorporates co-culture systems that are made up of pure cultures, which can be fungal-fungal or bacterial-bacterial, or bacterial-fungal combinations	Several days	• The method has been most effective in the production of biogas, as it has the capability of degrading macromolecules and reducing biomass	• The complex combination of the microbial communities increases hydrolysis by facilitating biomass accessibility to the enzymes.	• The environmental changes may affect the adaptability of the individual strains.	Kumar *et al.* (2020)

			crystallinity, thus enhancing biomass degradability.	• The method results in enhanced productivity at a lower incubation time compared to fungi. • Metabolites that are needed for the breakdown of lignin are produced stable and continuously.		
Ensiling	• The use of lactic acid bacteria or a mixture of lactic acid and hydrolytic enzymes	Weeks to months	• The method was developed for the preservation of lignocellulose biomass during biogas production	• Little to no waste is generated. • The method is used for crop storage, which can be achieved at moderate environmental conditions. • Downstream costs are very low.	• The incubation time is longer, which may result in a loss of the polysaccharides (mainly cellulose and hemicelluloses).	Sun *et al.* (2021)
Enzymatic	• The use of crude or purified enzymes, either as cocktails or single enzymes for biomass degradation. The enzymes are sourced from bacteria, fungi and plants, and the most common enzymes are ligninases, laccases and peroxidases.	Hours to a few days	• The method is effective in the removal of lignin and the hydrolyses of the holocellulose resulting in increased sugar production.	• The method is most effective in the hydrolysis of macromolecules that assists in further conversion processes at a lower incubation time compared to fungal and bacterial pretreatment.	• There is a higher cost in the production and purification of enzymes. • The ligninolytic enzymes lack stability during industrial processes.	Malhotra and Suman (2021); Singhania *et al.* (2022); Mohotloane *et al.* (2023)

Extensive research has been done on fungi as a method of lignocellulose pretreatment, particularly basidiomycetes which have been identified as lignin-degrading fungi (Chandel *et al.,* 2015). The exploration of the fungal pretreatment isolated three types of fungi namely: white-rot (WRF), brown-rot (BRF) and soft-rot (SRF), which have different lignin degrading capabilities (Sharma *et al.,* 2019; Zabed *et al.,* 2019). White-rot fungi are known for their efficiency in the complete removal of lignin and subsequent degradation of the holocellulose, due to their selective ability to degrade biomass utilising their extracellular enzymatic systems (Abraham *et al.,* 2020). Whereas, soft-rot fungi perform incomplete removal of lignin, leading to faster degradation of the holocellulose, due to the presence of a wide range of cellulolytic enzymes (Shirkavand *et al.,* 2016). In contrast, BRF are more of the holocellulose degrading fungi, with little to no effect on lignin. However, it has been proposed that lignin modification is successful through the fenton reaction, where BRF utilises the hydrogen peroxide (H_2O_2) produced during hemicellulose degradation (Shirkavand *et al.,* 2016; Tian *et al.,* 2018; Zabed *et al.,* 2019). The hydrogen peroxide combined with iron (Fe^{2+}) is able to cleave lignin and this is mediated by the free radical reactions (Schilling *et al.,* 2012; Shirkavand *et al.,* 2016; Tian *et al.,* 2018; Zabed *et al.,* 2019). Additionally, BRF uses two degradation systems, the enzymatic Fenton-like reaction and non-enzymatic fenton reaction to degrade lignocellulose (Schilling *et al.,* 2012; Shirkavand *et al.,* 2016).

Although fungal pretreatment has been shown to be effective in its lignin removal capability, it requires a longer pretreatment time, which results in a greater loss of the holocellulose, thus decreasing the soluble sugars produced (Zabed *et al.,* 2019; Kumar *et al.,* 2020; Hernández-Chaverri *et al.,* 2021). It is for this reason that the bacterial strains are studied for lignocellulose pretreatment as they required less pretreatment time because of their rapid growth rate and metabolic activities (Kumar *et al.,* 2020). However, the lignin degradation by bacterial strains is less effective as it depends on the composition of the biomass. Lignin has been proven to be a complex and tough structure to degrade than hemicellulose and cellulose (Sharma *et al.,* 2019; Singhania *et al.,* 2022). Therefore, most bacterial strains are suited for cellulose degradation as they are known to produce cellulases (Shi *et al.,* 2009; Sharma *et al.,* 2019).

The microbial pretreatment of lignocellulose biomass at optimum conditions is a fairly established method, however, the longer reaction time that results in the loss of holocellulose prompted researchers to develop a method that requires less time and produced more sugar products. Thus, gave rise to enzymatic pretreatment, which is the use of crude, purified or

partially purified enzymes, either as cocktails or single enzymes for biomass degradation. These enzymes are sourced from bacteria, fungi and plants, and the most common enzymes are known as ligninases, laccases and peroxidases (Malhotra and Suman 2021). The enzymatic pretreatment process contains two mechanisms of action: 1. As ligninolytic enzymes for lignin removal and 2. As hydrolytic enzymes for the degradation of the holocellulose. This section highlights the microbial pretreatment such as fungi and bacteria, however, subsequent sections focus on reviewing the enzymatic (laccase and peroxidase) pretreatments on the lignocellulose.

2.1 Ligninolytic enzymes for delignification of lignocellulose

Ligninolytic enzymes are extracellular enzymes that initiate biochemical reactions catalysing the lignin polymer into monolignols (Sharma *et al.,* 2019; Zabed *et al.,* 2019). The most studied enzymes are laccases, lignin peroxidase, manganese peroxidase and versatile peroxidase sources from fungi, bacteria, and plants. The source, properties and mechanisms of action differentiate these enzymes from each other (Kumar and Chandra 2020).

2.1.1 Laccases

Laccases (oxygen oxidoreductase, EC 1.10.3.2) are known as multi-copper proteins that contain four copper atoms in the catalytic centre, which plays a role during catalysis resulting in the reduction of oxygen to water (Nargotra *et al.,* 2022). The four copper atoms are categorized as type I (T1), type II (T2) and type III (T3) according to their absorption spectra or electron paramagnetic resonance. The T1 is detected by its absorption at 600-610 nm, due to its copper-cysteine covalent bond. Additionally, this site contains a high redox potential, which is responsible for substrate oxidation (Malhotra and Suman 2021). Laccases catalyse various phenolic or non-phenolic substrates by utilising oxygen as a co-factor, and is found in a wide range of sources, including fungi, bacteria, and plants (Agrawal *et al.,* 2018; Abraham *et al.,* 2020). However, most studies were performed using fungal laccases compared to those produced by the bacteria (Baruah *et al.,* 2018). Laccase uses a direct or indirect mechanism in the catalysis of the phenolic and non-phenolic substrates [(Figure 2.1), (Malhotra and Suman 2021)].

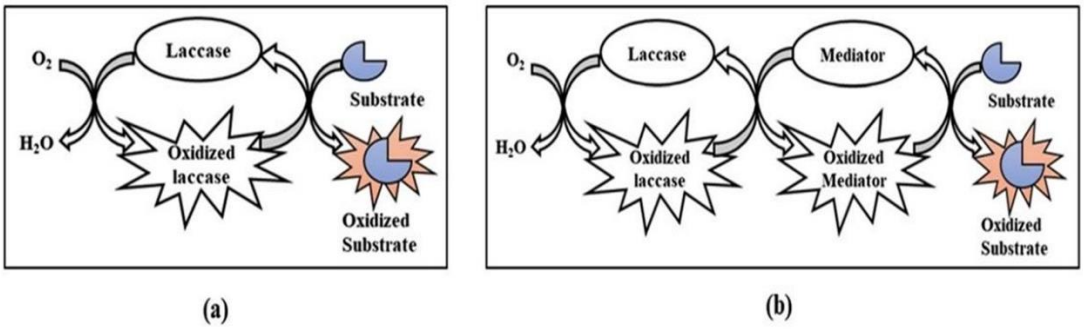

Figure 2.1: The illustration of the direct (a) and indirect (b) mechanism laccases utilise in the catalysis of phenolic and non-phenolic compounds (Malhotra and Suman 2021).

The direct mechanism is described as the interaction of the substrate with the copper centre of laccase resulting in a formation of a radical, which is only successful if the ionisation potential of the substrate is lower than that of the T1 copper ion redox potential. Hence, the method is suited for phenolic-containing compounds as they have low ionisation potential (Figure 2.1a). However, non-phenolic containing compounds have a high ionisation potential than the T1 copper ion redox potential. Therefore, laccases are unable to perform the catalysis on their own; they require a mediator [such as 1-hydroxybenzotriazole (HBT), *N*-hydroxyphthalimide (HPI) and violuric acid (VLA)] containing a low molecular weight to drive the catalytic activity. The indirect mechanism occurs in two steps; firstly, the mediator is oxidised by the laccase, then secondly, the resulting oxidised mediator leads to the oxidation of the substrate, thus returning the mediator to its initial unoxidised form (Figure 2.1b). The oxidation of the non-phenolic compound is a non-enzymatic reaction promoted by a laccase oxidised mediator (Chaurasia *et al.,* 2013; Agrawal *et al.,* 2018; Malhotra and Suman 2021). Some studies have attributed the industrial and biotechnological application importance of laccases to their lower/lesser range of substrate specificity (Agrawal *et al.,* 2019). In contrast, other studies showed that laccases have broad substrate specificity (Giacobbe *et al.,* 2018; Malhotra and Suman 2021). The authors argue that broad substrate specificity of laccase made its use appealing in many industries, such as biogas, bioethanol, clinical application, bleaching fibres and food.

Laccases particularly play a role in lignin degradation reactions that enhance yield production during hydrolysis and fermentation processes because of lignin modification, leading to increased biomass porosity (Giacobbe *et al.,* 2018). Bagewadi *et al.* (2017) demonstrated that a laccase produced from *Trichoderma harzianum* strain HZN10

effectively delignified saw dust. Similarly, laccase pretreatment effectively removed lignin, which led to the efficient hydrolysis of the holocellulose resulting in about 80% soluble sugars production yield (Giacobbe *et al.,* 2018). Along with lignin removal, laccase pretreatment has been shown to modify the structural properties of the microfibres. These modifications enhanced surface area, exposure of pores and reduce hydrophobic properties of the biomass, which increase the activities of the glycoside hydrolases (GHs). Studies demonstrated that the delignification of various biomass with laccase resulted in high production of sugar during simultaneous pretreatment and hydrolysis (Avanthi and Banerjee 2016; Banerjee *et al,* 2019; Rajeswari and Jacob 2020). However, the drawback in simultaneous pretreatment and hydrolysis is the reduction of cellulase and β-glucosidase activity leading to low soluble sugar production.

2.1.2 Peroxidases

Some lignin-degrading enzymes have no ability to degrade lignin by themselves but produce the reactive oxygen species (ROS) or reducing compound necessary to initiate activities of lignin degrading enzymes (Singhania *et al.,* 2022). Examples of these enzymes are glyoxal oxidase (GOD) (EC 1.2.3.5), aryl alcohol oxidase (AAO) (EC 1.1.3.7), heme-thiolate haloperoxidases [(EC 1.11.2.1) classified under unspecific peroxygenases], glucose dehydrogenase (EC 1.1.99.10) and pyranose 2-oxidase (EC 1.1.3.10). These enzymes are known as lignin-degrading auxiliary enzymes, and their function is to generate H_2O_2, which activates reactions catalysed by peroxidases during lignin breakdown (Kumar and Chandra 2020; Singhania *et al.,* 2022). Peroxidases are proteins that contain a heme-group that facilitates the oxidation of organic substrates by reducing H_2O_2 into H_2O (Bilal *et al.,* 2018; Morsi *et al.,* 2020; Mohotloane *et al.,* 2023). Peroxidases are produced by many sources, including bacteria, fungi, and plants, which belong to the peroxidase catalase superfamily (PCATS) (Battistuzz *et al.,* 2010; Pandey *et al.,* 2017).

Peroxidases are further subdivided into three classes (Class I, II and III) (Jouili *et al.,* 2011). Class I peroxidases are produced from bacteria, these include cytochrome C peroxidase (CCP; EC 1.11.1.5), ascorbate peroxidase (APX; EC 1.11.1.11) and catalase-peroxidase (CP; EC 1.11.1.6) (Twala *et al.,* 2020; de Oliveira *et al.,* 2021). Although catalase-peroxidase is closely related to Cytochrome C peroxidase and ascorbate peroxidase evolutionary, it is known to be bifunctional enzyme, acting as catalase and peroxidase (Pandey *et al.,* 2017). On the other hand, Class II peroxidases are produced by fungi, and

these include lignin peroxidase (LiP; EC 1.11.1.14), manganese peroxidase (MnP; EC 1.11.1.13) and versatile peroxidase (VP; EC 1.11.1.16). Lastly, Class III peroxidases are found in the plant kingdom, and examples include horseradish peroxidase (HRP), and soybean peroxidase (SBP) (Pandey *et al.,* 2017; de Oliveira *et al.,* 2021).

Peroxidase use a similar mechanism for catalysis, even though they oxidise different substrates. The main mechanism of peroxidases is a series of steps, resulting in the formation of compound I and II (Figure 2.2). The process involved the iron (Fe^{3+}) or ferric resting state of the enzyme, which reacts with the oxidising agent H_2O_2, resulting in the reduction of H_2O_2 to form water and the Fe^{3+} that is oxidised to form compound I (Fe^{4+} known as the oxyferryl center). The oxidised compound I accepts an electron from the substrate, forming compound II (known as the oxyferryl heme intermediate) and a substrate-free radical (Hiner *et al.,* 2002; Pandey *et al.,* 2017). Compound II interacts again with one substrate molecule, which reduces compound II back to the ferric resting state. However, an excess supply of H_2O_2 results in a formation of a complex containing an oxygen molecule bound to the ferrous iron (known as compound III) present in peroxidase (such as MnP, VP and HRP), [(Figure 2.2); (Kumar and Chandra 2020; de Oliveira *et al.,* 2021)]

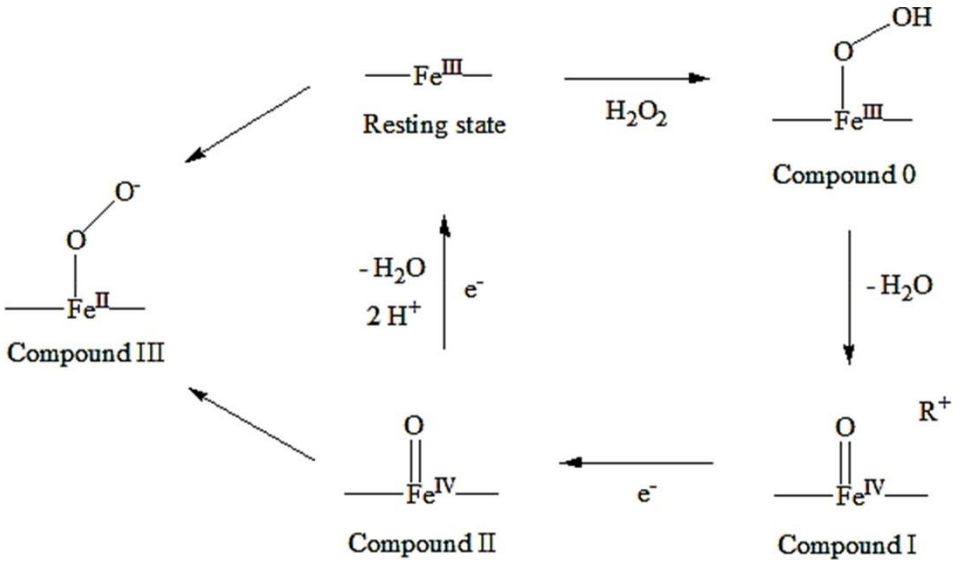

Figure 2.2: The Illustration of the mechanism of action of peroxidases (de Oliveira *et al.,* 2021)

The peroxidases sourced from plants have a few physiological functions including cell wall lignin cross-linking (Mafa *et al.,* 2022; Mafa *et al.,* 2023). As indicated earlier in this section

most fungal and bacterial ligninolytic enzymes (including peroxidase) were reported to effectively remove lignin from the biomass samples. In addition, my MSc findings for objective 1 and 2, demonstrated that partially HRP effectively removed lignin and displayed the cellulose activity, leading to decreased microcrystalline cellulose recalcitrance (Mohotloane *et al.,* 2023). Interestingly, these findings correlated with the observations made by Min *et al.* (2022) that peroxidases appear to be more than just lignin-degrading enzymes, because their MnP sourced from WRF *Phanerochaete chrysosporium* had cellulase-xylanase enzyme degrading capabilities as it resulted in high amounts of soluble reducing sugars produced from CMC, Avicel and xylan substrates.

2.1.3 Are there differences between lignin (LiP) and versatile peroxidase (VP)?

Lignin and versatile peroxidase enzymes both belong to the oxidoreductase family that are secreted by fungi and some bacteria (Kumar and Chandra 2020; Singhania *et al.,* 2022). In addition, these enzymes share some functions; for instances the VP possess activities of MnP and LiP. Also, all the peroxidases are classified under Auxiliary Activity Family 2 in CAZy database (AA2: http://www.cazy.org/AA2_characterized.html). It is unclear if LiP, and VP can be used at the same time to pretreat the lignocellulose biomass for lignin removal. Could these two peroxidases show synergism and improve the lignin removal? To answer this question and assess the possibility of synergism between the LiP and VP, extensive research was conducted on peroxidase assays to compare the differences or similarities between these enzymes (Table 2.2)

Table 2.2: Comparisons of LiP and VP activity assays similarities and differences.

Lignin peroxidase	**Versatile peroxidase**
Principle	
LiP (EC 1.11.1.14) are associated with lignin degradation, and they were first discovered in white-rot fungi (*Phanerochaete chrysosporium*). Additionally, LiP functions in the presence of H_2O_2 to catalyse the degradation of lignin (Singhania *et al.,* 2022). Lignin peroxidases utilise the two-step mechanism (that results in the formation of compound I and II) to catalyse the oxidation of phenolic and non-phenolic	VPs (EC 1.11.1.16) known as the hybrid peroxidases are also produced by white-rot fungi and they exhibit similar molecular structure to LiP and MnP (Singhania *et al.,* 2022). The versatile peroxidases follow the two-step mechanism forming compound I and II in oxidation of phenolic and non-phenolic compounds. However, the presence of excess H_2O_2, it results in the formation of compound III.

compounds (Kumar and Chandra). According to Expasy enzyme database [accessed 14 November 2023], LiP in the presence of excess H_2O_2 results in the formation of compound III. Additionally, Ghodake *et al.* (2009), demonstrated that lignin peroxidase sourced from *Acinetobacter calcoaceticus* NCIM 2890 had the ability to oxidise manganese (Mn^{2+}).	
Procedure	
Similarities between LiP and VP*	
1. The oxidation of veratryl alcohol was determined at a concertation ranging from 0.4 to 17 mM, buffering conditions pH 1 or 3 (0.1 M, 0.2 M and 20 mM sodium tartrate, HCl-KCl, and succinate, respectively) and H_2O_2 added at concentrations ranging from 0.2 to 40 mM. The reactions were measured at 310 nm (a few studies used 285 and 300 nm) (Yang *et al.,* 2005; Sugiura *et al.,* 2003; Ghodake *et al.,* 2009).	1. Veratryl alcohol oxidation was determined at the concentration of 0.4 to 2 mM, with the addition of 100 mM sodium tartrate buffer at pH 3 and H_2O_2 concentration ranging from 0.1 to 0.54 mM. The reactions were measured at 310 nm (Taboada-Puig *et al.,* 2011; Ravichandran *et al.,* 2019)
2. MnP activity was determined using 1 mM $MnSO_4$, with the addition of 50 mM sodium tartrate buffer (pH 4.5) and the reaction was started with 10 mM H_2O_2. The formation of Mn^{3+} was determined by monitoring the absorbance at 238 nm (Ghodake *et al.,* 2009)	2. MnP activity was determined using 0.5 or 1 mM $MnSO_4$ added to 100 mM malonate buffer (pH 4.5) or sodium tartrate buffer (pH 5) and the reaction was initiated with H_2O_2 at a concentration of 0.1 or 0.4 mM. The formation of Mn^{3+} was determined by monitoring the absorbance read at 238 or 270 nm (Taboada-Puig *et al.,* 2011; Ravichandran *et al.,* 2019).
3. The oxidation of 2, 6-dimethoxyphenol with a concentration of 49.6 mM was measured by adding 20 mM succinate buffer pH 3.0 and about 0.2 mM H_2O_2 was	3. The oxidation of 2, 6-dimethoxyphenol was determined at a concentration of 0.1 or 1 mM, added 50 mM malonate buffer pH 4.5- or 100 mM sodium tartrate buffer pH

added to initiate the reaction. The change in absorbance was recorded at 470 nm (Sugiura *et al.,* 2003).	3 and H_2O_2 (0.1 or 0.4 mM) was used to initiate the reaction the presence of $MnSO_4$. The change in absorbance was read at 468 nm (Taboada-Puig *et al.,* 2011; Ravichandran *et al.,* 2019).
Differences between LiP and VP*	
1. Lignin peroxidase activity was measured using 2,2'-azino-di-[3-ethyl-benzthiazoline-(6)-sulphonic acid] (ABTS) with the addition of 20 mM 4-aminoantipyrine, 50 mM Tris–HCl buffer containing 1 mM $MnCl_2$ at **pH 8,5** and 0.33 mM H_2O_2. The absorbance was measures every 30s for 4 minutes to determine the increase in absorbance at **510 nm** (Rekik *et al.,* 2015).	1. 2,2'-azino-bis [3-ethylbenzothiazoline-6-sulfonic acid] (ABTS), was used to determine versatile peroxidase activity using substrate concentrations ranging from 0.1 to 5 mM. The reactions were initiated by adding H_2O_2 (0.1 or 0.4 mM) in buffering systems of 100 mM sodium acetate buffer **pH 4.5 or 5** and the change in absorbance was measured at **436 nm**, or **420 nm** (Min *et al.,* 2010; Taboada-Puig *et al.,* 2011; Ravichandran *et al.,* 2019).
2. Decolorization of textile dyes was determined using 100 µg Reactive red M5B as substrate, with the addition of 50 mM potassium phosphate buffer **pH 7.0**, 40 mM H_2O_2, and 2.5 mM tryptophan (TRP) as the stabilizing agent. The reaction was measured at 598nm (Ghodake *et al.,* 2009)	2. The degradation of azo dye reactive black 5 was determined using 10 µM of the substrate added to 100 mM sodium tartrate buffer **pH 3**. The reaction was initiated by adding 0.1 mM H_2O_2 and measured as the decrease in absorbance at 598 nm (Ravichandran *et al.,* 2019).
3. Lignin peroxidase activity was measured using o-dianisidine, guaiacol, 4-chlorophenol, and 2,4,6-trichlorophenol as substrates with concentrations ranging from 10 to 40 mM. The reactions included 20mM 4-aminoantipyrine, 50 mM Tris–	3. The demethylation of methylene blue dye (MB) to determine lignin peroxidase activity and the oxidation of MBTH (3-methyl-2-benzothi-azolinone hydrozone) together with DMAB (3-(dimethylamino) benzoic acid) form azo

HCl buffer containing 1 mM $MnCl_2$at **pH 8.5** and 0.33mM H_2O_2. The absorbance was measures every 30s for 4 minutes to determine the increase in absorbance at 510 nm (Rekik *et al.,* 2015). 4. Ghodake *et al.* (2009), also assayed lignin peroxidase activity on tryptophan (TRP), L-Dopa, *n*-propanol, mimosine, 8-hydroxyquinone substrates at 10 mM concentration, with 0.2 M HCl–KCl buffer **pH 1.0** and 40 mM H_2O_2 as a co-substrate. The changes in absorbance were measured at 305, 300, 300, 303, 310 nm, respectively. 5. Sugiura *et al.* (2003), determined lignin peroxidase activity using the concentration of benzyl alcohol, anisalcohol and guaiacol substrates ranging from 1.8 to 26.6 mM, with 20 mM succinate buffer **pH 3** and 0.2 mM H_2O_2. The change in absorbance was measured over time at 285, 280 and 470 nm, respectively.	dye (blue colour) was used to determine MnP. The substrate concentrations for MB, MBTH and DMAB were 40 µM, 70 µM and 1 mM, respectively. The MBTH and DMAB reaction were conducted in the presence of $MnSO_4$ ranging from 0.3 to 2.0 mM concentration. The reactions were initiated by 0.1 mM H_2O_2, in reaction mixture buffered by 0.1 M sodium tartrate buffer pH 3.5 or 4.5. The change in absorbance were recorded at 664 and 590 nm for LiP and MnP (Ertan *et al.,* 2012).

***** All the reactions were measured using kinetic mode of UV-VIS spectrophotometer. # The reactions were conducted at temperatures ranging from 25 to 37 °C and the absorbances were measured over time between 3 to 10 minutes.

The LiP and VP assays show similarities, with minor differences. Therefore, we postulate that these enzymes can be use in a synergistic manner to remove lignin from the biomass. For instance, both enzymes have a similar mechanism even though VP is a bifunctional enzyme (containing both LiP and MnP). Additionally, both enzymes catalyse a range of substrates with diverse chemical properties. Throughout the literature it was observed that most studies did not determine MnP activity when performing lignin peroxidase activity assays, except for a few studies by Sugiura *et al.* (2003) and Ghodake *et al.* (2009). Both studies showed that LiP (sourced from *Acinetobacter calcoaceticus* NCIM 2890 and *Phanerochaete sordida* YK-624)

had MnP activity by determining the oxidation of Manganese substrates. Additionally, Ghodake *et al.* (2009) proposed the LiP from *Acinetobacter calcoaceticus* NCIM 2890 was a versatile peroxidase because it displayed activity on various substrates including ten textile dyes. Thus, these findings could be an indication that LiP and VP are similar enzymes and perhaps can be considered for synergistic assays in future studies.

2.2 Hydrolytic enzymes for degradation of hemicellulose and cellulose

Enzymes that hydrolyse cellulose and hemicellulose are classified under GH family, which is a big subfamily of the carbohydrates active enzymes (CAzymes) documented in CAZy (http://www.cazy.org/Home.html). These enzymes are produced by a broad range of organisms, including but not limited to fungi, bacteria, plants (Van Dyk and Pletschke 2012; Bhattacharya *et al*., 2015). The hydrolysis of cellulose polysaccharides into β-D-glucose monomers requires cellulases, which are classified into exo-1,4-β-glucanases also known as cellobiohydrolases (CBHI and CBHII), endo-1,4-β-glucanases (EC 3.2.1.4) and β-glucosidases (EC 3.2.1.21). Endoglucanases hydrolyse the amorphous region of cellulose chains, while the CBHs act on the crystalline region of the cellulose (Malgas *et al.,* 2020a; Mafa *et al.,* 2021a). There are two CBHs, i.e., CBHI (EC 3.2.1.176) which breakdown the cellulose chain from the reducing ends (C1) and CBHII (EC 3.2.1.91) hydrolyse the cellulose from the non-reducing ends (C4). The oligosaccharides or disaccharides produced by the endoglucanase and CBHIs are further hydrolysed to glucose by β-glucosidase. It is well known that in the biological systems (cells) or *in vitro* assays, cellulases mainly work in synergy during the conversion of cellulose to glucose units, although they act on different chain length (degree of polymerization: DP) and display different substrate affinities (Mafa *et al.,* 2021a; Zhou *et al.,* 2021). In contrast, Thoresen *et al.* (2021) demonstrated that some endo-exo cellulases do not show synergism due to the differences in their substrate affinities.

Unlike cellulose, the degradation of hemicellulose requires a more complex enzyme consortium, which include the main enzymes that breaks down xylan into monomers. To degrade the xylan backbone chain, xylanases (EC 3.2.1.8) and xylosidase (EC 3.2. 1.37) are generally used with assistance from debranching enzymes (L-arabinofuranosidases, α-D-glucuronidases and esterases) (Mafa *et al.,* 2021; Malgas 2021b). For mannan backbone chain degradation to mannose, mannanases (EC 3.2.1.78) and mannosidase (EC 3.2.1.25) are required, and once again the debranching enzymes assist to remove the side chain from mannan (Van Dyk and Pletschke, 2012; Malgas *et al.,* 2015; Malgas *et al* , 2019; Mafa and Malgas

2023). The breakdown of the glycosidic and ester bonds in the side chains or branches of the chain is facilitated by α-L-arabinofuranosidase (EC 3.2.1.55), β-glucuronidase (EC 3.2.1.139), acetylxylan esterase (EC 3.1.1.72), ferulic acid esterase (EC 3.1.1.73) and/or glucuronyl esterases (EC 3.1.1) (Huang *et al.,* 2019; Malgas *et al.,* 2021).

Xylanases belonging to family GH10 and GH11 of glycoside hydrolases are the main enzymes responsible for the breakdown of the β-1,4-glycosidic bonds. Xylanases from family GH10 are known to target and cleave the branched xylans, while GH11 xylanases breakdown the xylans found in the backbone of the hemicellulose (Malgas *et al.,* 2019). In contrast, β-1,4-linked mannan backbone is hydrolysed by endo-mannanases to produce oligomers which are further degraded to produce mannose subunits, while α-L-arabinofuranosidase and α-L-arabinases function together to cleave the arabinan situated in the side chains attached to the xylan backbone to produce arabinose (Wu *et al.,* 2022). Due to the complexity of the hemicellulose structure, a consortium of xylan enzymes functions synergistically to produce monomeric products. The synergy between the enzymes is characterised by two modes of action: homeosynergy and heterosynergy. Homeosynergy is the synergy between two enzymes that cleave the backbone or two enzymes that cleave the side chain, and heterosynergy is the synergy between a backbone and side chain cleaving enzymes (Amit *et al.,* 2018; Malgas *et al.,* 2019).

2.3 Carbohydrate active non-hydrolytic and oxidative/reductase enzymes

Non-hydrolytic or oxidative proteins are auxiliary enzymes that increase the activity of hydrolytic enzymes, these are lytic polysaccharide monooxygenases (LMPOs), swollenins, expansins and carbohydrate binding modules (CBM) (Kim *et al*., 2014; Adsul *et al*., 2020; Mafa and Malgas 2023). The auxiliary enzymes improve biomass accessibility to hydrolytic enzymes (GHs) and in this section, we address the contribution of LPMO and expansins activities towards cellulose loosening.

2.3.1 Lytic polysaccharide monooxygenase (LPMOs) de-crystallises cellulose.

The microcrystalline fibres can be recalcitrant to enzymatic hydrolysis due to their physicochemical properties. However, there is accumulating evidence showing that LPMOs reduce the recalcitrant nature of cellulose, and improves cellulase activity (Harris *et al.,* 2010; Cragg *et al.,* 2015; Eijsink *et al.,* 2019; Moon *et al.,* 2022). LPMOs are copper containing enzymes that function in the degradation of the insoluble cellulose by utilising the oxidative

reaction, which involves the cleaving of glycosidic bonds. Thus, modifying the cellulose structure, resulting in the enhanced accessibility of the hydrolytic enzymes (such as endoglucanases (EGs), (CBHs) and β-glucosidase) to the biomass (Forsberg *et al.,* 2019; Singhania *et al.,* 2021; de Gouvêa *et al.,* 2019). These enzymes are sourced from bacteria and are classified as auxiliary activities (AA), which belong to several families. The first LPMOs to be characterised were initially classified as GH61 and CBM33 family, which are now known as AA9 and AA10, respectively (Walton and Davies 2016; Calderaro *et al.,* 2021). Other families include AA11, AA13, and the recently discovered AA14, AA15 and AA16 (de Gouvêa *et al.,* 2019; Singhania *et al.,* 2021; Calderaro *et al.,* 2021). These LPMO families modify different polysaccharides, such as cellulose, xylan, chitin, and starch (de Gouvêa *et al.,* 2019). LPMOs (particularly family AA9 and white-rot fungi sourced LPMOs) have also been associated with the facilitation of lignin removal by acting as auxiliary enzymes that are known to produce H_2O_2 required by lignin degrading peroxidase (Li *et al.,* 2019; Tõlgo *et al.,* 2022). Given that LPMOs are among the currently scientific buzzing word, the only focus is on microcrystalline cellulose modifying LPMO Family AA9 and AA10; which cleave the glycosidic bonds at carbon 1 (C1) and carbon 4 (C4) (de Gouvêa *et al.,* 2019; Forsberg *et al.,* 2019; Singhania *et al.,* 2021).

Although the reaction mechanism of LPMOs remains unclear, it has been proposed that the reaction begins with the reduction of the Cu (II) (contained within the LPMO copper center) to Cu(I), due to an external electron donor leading to the activation of the dioxygen molecule. The dioxygen molecule removes a hydrogen molecule from either C1 or C4 of the microcrystalline cellulose, replacing it with the hydroxyl group in the formed substrate radical. Thus, resulting in the cleavage of the glycosidic bonds, which reduce the crystallinity of cellulose (Vaaje-Kolstad *et al.,* 2017; Forsberg *et al.,* 2019; Singhania *et al.,* 2021; Nargotra *et al.,* 2022).
The mechanism of LPMOs in cellulose modification or cleavage is region specific, particularly family AA9 has been shown cleave C1 and C4 separately or simultaneously and they are classified as type 1 (C1 cleaving), type 2 (C4 cleaving) and type 3 (C1 and C4 cleaving) LPMOs (Meier *et al.,* 2017; Chylenski *et al.,* 2019 Singhania *et al.,* 2021). This ability to cleave microcrystalline cellulose could explain its proposed synergy with cellulases resulting in increased cellulose degradation (Vermaas *et al.,* 2015). Filiatrault-Chastel *et al.* (2019) demonstrated that AA16 LPMOs sourced from *Aspergillus aculeatus* showed activity on the C1 region of cellulose and increased *T. reesei* CBHI activity on cellulose degradation. Additionally, de Gouvêa *et al.* (2019) showed that the incorporation of *Aspergillus fumigatus*

LPMO in the hydrolysis of sugarcane bagasse (SEB) improved the cellulase cocktail efficacy by 22% compared to the use of the cocktail alone. A thermostable MtEG5 endoglucanase that was multifunction showed synergistic capabilities when combined with MtLPMO by the increasing sugar yield production. Thus, validating the LPMO ability to de-crystallise and synergize with cellulases resulting in improved hydrolytic activity (Karnaouri *et al.,* 2017).

2.3.2 Expansins decrease the cellulose crystallinity via fibre chain loosening.

Non-hydrolytic enzymes that possess the ability to break the intra- and inter-hydrogen bonds of microcrystalline cellulose (or between cellulose fibres) resulting in a decreased crystallinity and loosened cellulose fibres are known as expansins (Wu *et al.,* 2022; Cosgrove 2022). Expansins are classified into two groups that have a similar cell wall loosening activity: namely α (EXPA) and β (EXPB) expansins (Baker *et al.,* 2000). Additionally, there are other subfamilies sourced from plants [expansin-like A (EXLA) and expansin-like B (EXLB)] and non-plants [expansin-like X (EXLX)] (Imai *et al.,* 2023; Georgelis *et al.,* 2015). The α-expansins are a smaller family found in Arabidopsis, while the β-expansins are a larger family found in grasses (Cosgrove 2000). These families are typically found in the plant cell wall, and they play a significant role in several physiological processes, however, they function in cellulose modification by cleaving hydrogen bonds within cellulose, and between cellulose and hemicellulose (Cosgrove 2000; Mafa and Malgas 2023; Imai *et al.,* 2023;).

Imai *et al.* (2023) reported that EXPB and EXLX seem to have a similar structure to family GH-45 endoglucanases, however the similarity does not imply that expansins have hydrolase activity because they mainly function in inducing stress relaxation and extension of plant cell walls without hydrolysing the cellulose fibres. Duan *et al*. (2018) demonstrated that the *Bacillus subtilis* expansins (BsEXLX1) increased the enzyme accessibility to cellulose by breaking the hydrogen bonds, which lead to increased surface area and reduced crystallinity index. Other studies showed that *Bacillus subtilis* expansins (BsEXLX1) effectively synergized with cellulases on the hydrolysis of filter paper shown by the activity that was 5 times higher than the cellulases alone (Zhang *et al*., 2021). These studies demonstrate that expansins decrystallise and loosen cellulose substrates, improving cellulose degradation and release of soluble sugars that are important for producing biofuel and value-added products upon fermentation.

2.4 Model of synergism: interplay between enzymatic pretreatment and biomass hydrolysis.

Enzyme synergism is a process that occurs when oxidative enzymes in combination with hydrolytic enzymes work together in the catalysis of different components of the lignocellulose resulting in enhanced product production (Van Dyk, J.S. and Pletschke, B., 2012; Malgas *et al.,* 2021). There are two types of synergistic systems, namely, simultaneous, and sequential. Simultaneous synergy entails the use of various enzymes in a reaction at the same time, while sequential synergy requires a step-by-step addition of enzymes depending on their efficacy and lignocellulose substrate targets (Mafa *et al.,* 2021a).

Due to the complexity of lignocellulose, particularly the presence of lignin, most studies use the sequential system together with the simultaneous system, beginning with the biomass pretreatment for lignin removal, then the subsequent hydrolysis of the holocellulose with enzyme cocktails (containing cellulases and xylanases) for enhanced production of sugar products (Mohotloane *et al.,* 2023; Schmitz *et al*., 2022). To improve the system, we propose the use of the sequential system for lignin removal by using LiP, VP and HRP individually or in synergistic combinations. The delignified biomass can be subsequently subjected to GH enzymes that hydrolyse the hemicellulose and cellulose in a simultaneous manner. As mentioned above lignin is a complex polymer that resist GH enzymes degradation by causing non-specific binding of the GH enzymes (Harmsen *et al.,* 2010; Mnich *et al.,* 2020). Thus, biological pretreatments (enzyme use) should remove lignin, followed by holocellulolytic biomass hydrolysis with GHs enzymes.

Lignin is made up of monolignols that are connected by the intra-polymer linkages (ether or carbon-to-carbon linkages), while the inter-polymer linkages between lignin and the polysaccharides are hydrogen bonds, ether bonds and covalent bonds (Harmsen *et al.,* 2010). For instance, G-units of lignin or ferulic acids forms ester bonds that cross-link lignin with hemicellulose, which are responsible for the recalcitrance towards enzymatic degradation (Mnich *et al.,* 2020).

Ligninolytic enzymes such as phenol oxidases (laccase) and heme peroxidases (lignin, manganese, and versatile peroxidase) as previously mentioned, undergo oxidative reactions that produce free radicals which are involved in cleaving ether, carbon-carbon bonds and breakdown of the aromatic rings. Therefore, dislodging the lignin from the polysaccharides and releasing the lignin fragments (Chan *et al.,* 2020; Weng *et al.,* 2021). Zhang *et al.* (2022) showed that laccase, lignin peroxidase and manganese peroxidase can be used in combination

for complete removal of lignin from corn stover. The authors highlighted that the laccase initiated the reaction by producing intermediates that are further catalysed by LiP and MnP, resulting in the destruction of the lignin structure. Interestingly, HRP was found to remove relatively about 80% of lignin from rooibos biomass, while also reducing the recalcitrant nature of cellulose (Mohotloane *et al.,* 2023). Further removal of the lignin from the polysaccharides can be achieved by the catalysis of the ester bonds between lignin and hemicellulose by utilising ferulic acid esterase [CE1; EC 3.1.1.73] (Schmitz *et al.,* 2022). These studies show that the LiP, VP, MnP and HRP can be used as effective biological pre-treatment technology for lignin removal but retain higher content of holocellulose.

Following lignin removal and biomass washing processes, the hemicellulose component of the biomass should be degraded in the sequential synergy. Choices of enzymes used to degrade polysaccharides are vital because monocots and dicots have different types of hemicellulose, i.e., xylan, xyloglucan, mannan, and β-glucans. For instance, xylanases are crucial enzymes required for the degradation of xylan, particularly endo-1,4-β-D-xylanases (EC 3.2.1.8) and 1,4-β-D-xylosidases (EC 3.2.1.37). The xylanase from family GH11, which function in cleaving the glycosidic bonds contained in the backbone of xylan to produce short oligosaccharides. These oligosaccharides can further be degraded into xylose monomers by xylosidases (Malgas *et al.,* 2021). The debranching of the arabinobiose or arabinose involve the combination of α-L-arabinofuranosidase (EC3.2.1.55), while the debranching of glucuronic acid from xylose structure is facilitated by α-D-glucuronidases (EC 3.2.1.131). Mafa *et al.* (2021b) demonstrated that feruloyl esterase (FAE-1) can synergise with xylanases from family GH10 to effectively remove the arabinoxylan contained within cereal feedstock. Although the FAE-1 does not break down sugar molecules themselves, it functions in the cleavage of the ester bonds that link ferulic acid and arabinoxylan.

Hemicellulose structures are also known to contain mannan residues, which are classified under four subfamilies that are homo or hetero polysaccharides. The homo polysaccharide is the linear mannan, while the hetero polysaccharides are the glucomannan, galactomannan and galactoglucomannan (Mafa and Malgas 2023). Due to the various components of the mannan structure, homeo or hetero-synergistic systems can be used during hydrolysis and synergistic properties of mannan have been extensively reviewed by Malgas *et al.* (2015). However, Mafa and Malgas (2023) proposed an updated model which incorporates the use of oxidative or non-hydrolytic enzymes such as LPMO, expansins and swollens, which function in the decrystallization of cellulose, thus enhancing the hydrolytic activity of acetyl mannan esterases

(AcME) and other GH enzymes. Similar to lignin, we propose the biomass wash step to remove the hemicellulose fragments that maybe still be attached, thus leaving the cellulose for further hydrolysis.

The most abundant polysaccharide in lignocellulosic biomass is cellulose. The microcrystalline fibres are recalcitrant to enzymatic degradation, while the amorphous region is easily degraded by the enzymes (Adsul *et al.,* 2020). The CBHs are responsible for hydrolysing the microcrystalline cellulose regions and amorphous regions are hydrolysed by the endoglucanases. The oligomers produced are further hydrolysed by β-glucosidase (Andlar *et al.,* 2018; Keller *et al.,* 2021; Fernandes *et al*., 2022). However, enzymes such as LPMOs and expansins play an important role in reducing the recalcitrance of crystalline cellulose. LPMOs have been shown to synergize with cellulases, however caution should be taken when combining CBHs with LPMOs because the mechanism of the enzymes is region specific (Vermaas *et al.,* 2015; Filiatrault-Chastel *et al.,* 2019). For examples, LPMOs that act on the C1 region of the cellulase show anti-synergism when combined with CBHI, which acts on the same region, as previously mentioned (Keller *et al.,* 2021). Therefore, this can be avoided by combing the C1 cleaving LPMO with the C4 cleaving CHBII. Although the proposed sequential synergism maybe efficient in the hydrolysis of the lignocellulose, it may be expensive due to the use of various enzymes. Therefore, simultaneous synergism maybe beneficial as it is a combination of lignocellulolytic enzymes used at the same time. Schmitz *et al*. (2022) studied the degree of synergy between xylanases, ferulic acid esterase and laccase using sequential and simultaneous application and the findings showed that the simultaneous addition of the enzymes resulted in a higher degree of synergy compared to sequential.

3. State of the art technology used to characterise the pretreatment effect on biomass

Pretreatment methods that aid the removal of lignin or de-crystallization of cellulose induce chemical and structural modification to the lignocellulose biomass. These effects can be analysed using various techniques, however for the purpose of the review, we focused on the use of scanning electron microscopy (SEM), Fourier Transform Infrared Spectroscopy (FTIR) and X-ray diffraction (XRD) analysis.

3.1 Biomass topological analysis using scanning electron microscopy (SEM)

Scanning electron microscopy (SEM) is a powerful tool used to study the surface topology. The advantage of using SEM is that it has a large focal length, which allows researchers to

view the surface of the sample in focus in any specific area at a time using different magnifications, regardless of the texture (roughness or smoothness) of the sample (Vernon-Parry, 2000; Zhou *et al.,* 2007). SEM analysis can be used to determine the efficacy of the pre-treatment, i.e., lignin modification results in the formation of the droplets or flakes on the surface of biomass samples; or complete lignin removal increases surface porosity and exposure of the holocellulose (Ling *et al,* 2019). Rajak and Banerjee (2015) demonstrated that laccase (sourced from *Pleurotus* sp) could modify lignin on wasteland weed (*Saccharum spontaneum)* biomass samples. The authors used the SEM analysis to show the effect of the pretreatment on the surface topology of the biomass (Figure 2.3). The untreated biomass (a) shows a smooth, intact layer of lignocellulose, while the treated biomass (b) displayed a rough and flaky surface containing sheets or pieces of lignin. These modifications resulted in increased hydrolytic enzyme accessibility to holocellulose and increased sugar production. Similarly, a follow up study conducted using laccase sourced from *Lentinus squarrosulus* MR13 on the same wasteland weed yielded similar results, showing that the pretreatment degraded the lignin layer (displayed by the rough layer) resulting in exposure to the holocellulose, thus increasing hydrolytic enzyme accessibility to biomass (Rajak and Banerjee 2016).

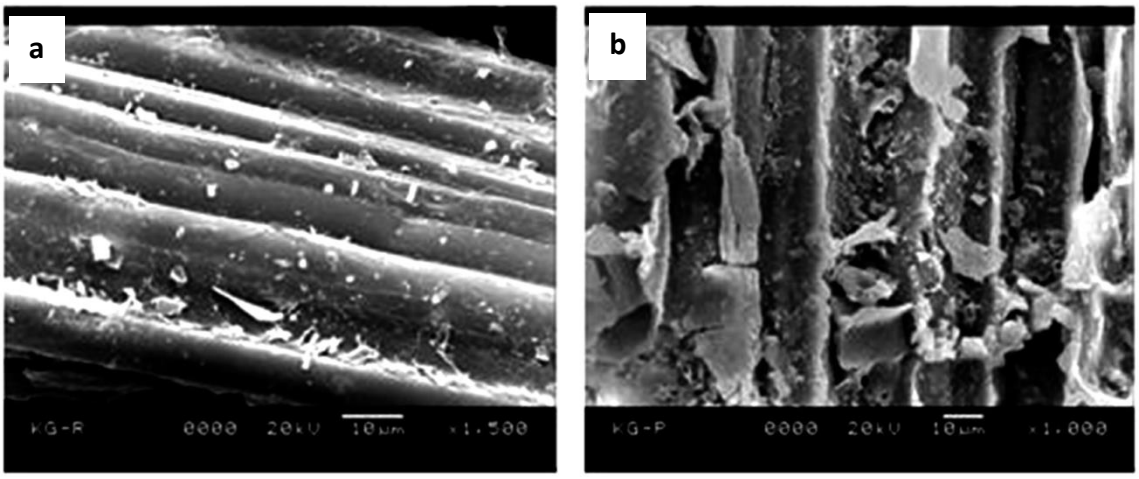

Figure 2.3: SEM images (a) untreated raw substrate (b) delignified substrate (Rajak and Banerjee 2015).

3.2 Measuring the chemical functional groups of the biomass using FTIR analysis

Understanding the chemical properties of the materials provides insight into the chemical and structural differences observed after pretreatment. FTIR mainly identifies the chemical functional groups within a sample by utilising infrared radiation. This technique provides a

spectrum that shows absorbance/transmittance readings versus the wavenumber, which results from the infrared absorption made by every functional group in the sample (Khan *et al,* 2018). The chemical functional groups of the plant biomass components can be identified between 700 to 3600 (1/cm) wavenumber as illustrated in Table A3. The findings are either represented in a form of a table or graph, showing the absorbances or transmittance (%) of the region of choice (Colom *et al.,* 2003; Waghmare *et al.,* 2018; Zhang *et al.,* 2019). For instance, Figure 2.4 shows an FTIR analysis conducted to determine the effect of the pretreatment on the biomass samples and the three regions of interest widely reported in the literature (Table A3). These regions of interest show the chemical functional groups belonging to the OH group region (inter and intra hydrogen linkages), phenolics/lignin region and glycosidic bonds/holocellulose regions (Figure 2.4). The regions correspond to the following wavenumbers ranging between 3600–3000, 1800–1500 and 1200–900 (1/cm), respectively (Figure 2.4). A successful lignocellulose pretreatment would show a reduction in the peaks at wavenumbers between 1700-1500 and 1700-1780 (1/cm) belonging to lignin/phenolic and ester linkages, respectively. The lower absorbance is an indication of the breakdown of ester linkages between lignin and hemicellulose and the carbon-carbon bonds, thus leading to lignin removal. Additionally, the reduction at peak 1113 (1/cm) shows the cleaving of inter or intra ether or glycosidic linkages within and between lignin, hemicellulose, and cellulose. Therefore, indicating lignin removal and separation of the hemicellulose and cellulose which enhances the accessibility of the enzymes to the biomass. However, if the pretreatment is unsuccessful the peaks at those regions would be similar to the control, showing no change in the pretreated samples. In contrast, the peak at 3600-3000 (1/cm) belonging to the inter or intra hydrogen bonds can either decrease or increase depending on the effect of the pretreatment on the microcrystalline fibres. A decrease in the peak indicates cleaving of the hydrogen bonds which is shown by a lower crystallinity index in the pretreated sample compared to the control. While an increase in the peak indicates remodelling of the hydrogen bond network, which can be shown by an increase in the crystallinity index. However, the increase or decrease in the crystallinity index does not specify the solubility of pretreated sample.

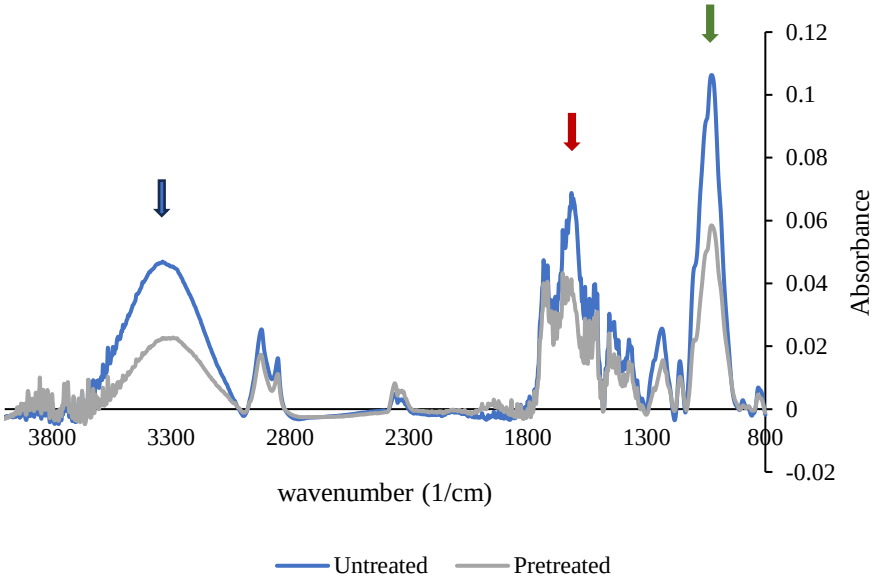

Figure 2.4: FTIR analysis showing three regions of interest, OH group region (inter or intra hydrogen bonds), phenolics/lignin region and glycosidic bonds/holocellulose regions represented by blue, red and green arrows, respectively.

3.3 Determination of cellulose crystallinity using X-ray diffraction (XRD)

X-ray diffraction is a technique mostly used to provide insight into the physical properties of the crystalline nature of cellulose. It can be used to determine the crystallinity index (CrI), distance between the crystals and size of the crystals in the tested sample (Ling *et al,* 2019; Yu *et al,* 2020). Most studies use the Segal/Parks peak height method to measure the CrI of the cellulose in various lignocellulose biomasses (Segal *et al.,* 1959; Park *et al.,* 2010). However, the CrI does not account for the amorphous and crystalline material, therefore other factors such as crystallite sizes, d-spacing and Full Width Half Maximum (FWHM) play a role in the crystalline nature of cellulose (Park *et al.,* 2010; Cheng *et al.,* 2011; Ling *et al.,* 2017; Ren *et al.,* 2022). Cellulose material from different sources have varying diffraction patterns, leading to different CrI (Garvey *et al.,* 2005).

Figure 2.5 is an example of diffraction patterns with peaks labelled to indicate their crystal lattice assignment of the crystalline cellulose model substrate before and after pretreatment. The number of the resolved diffraction peaks differs in the Avicel and filter paper biomass. Avicel shows three resolved peaks, while filter paper has four narrow peaks. Garvey *et al.* (2005) demonstrated that filter paper has four narrow resolved peaks when compared to neutral

sulfite semi-chemical pulp (NSSC) and bleached eucalypt kraft pulp (BEK) samples. The changes in the XRD spectra of the samples during pretreatment can be determined using the Segal/park peak height method, which measures the CrI (%) by using the ratio between the height at peak 002 ((I_{002}) and height of the minimum (I_{AM}) found between the 002 and the 101 peaks. However, this method does not determine of the amount of the crystalline and amorphous material in the cellulose sample (Park *et al.,* 2010).

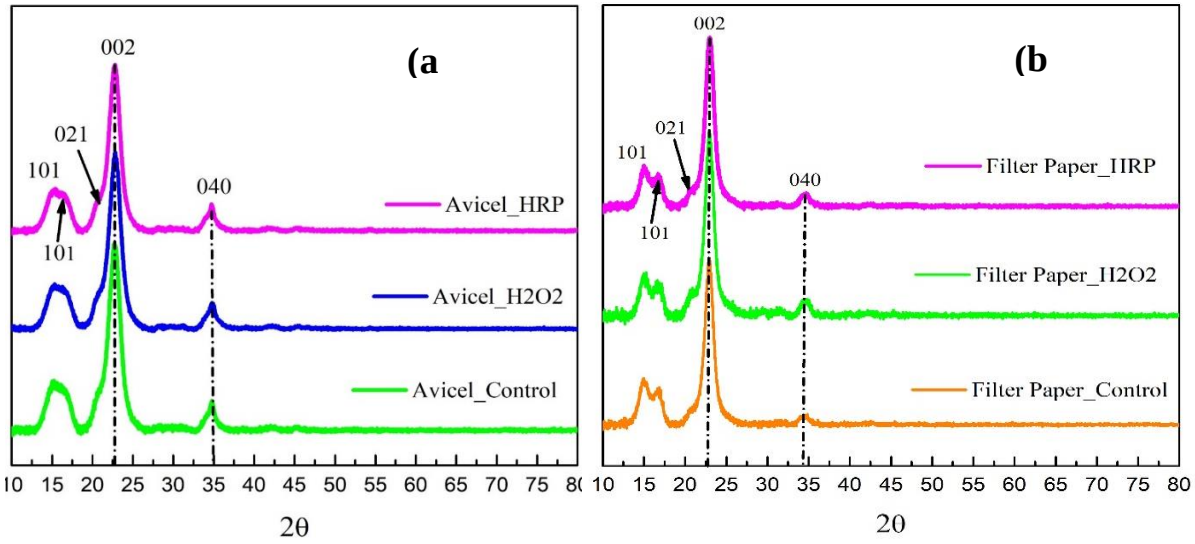

Figure 2.5: X-ray powder diffractograms of (a) Avicel, and (b) Filter Paper samples.

The computational method that can separate amorphous and crystalline contributions to the diffraction spectrum to accurately measure the crystallinity index (%) is known as the deconvolution method, which uses a curve-fitting process [Figure 2.6; Park *et al.,* 2010]. The shape and number of peaks are used to make the assumptions for the curve fitting. Curve fitting the XRD spectra requires the use of the Gaussian, Lorentzian and Voigt functions that can result in a separation of five or four crystalline peaks (Park *et al.,* 2010, Ling *et al.,* 2017). Figure 2.6 shows the curve fitting of the Avicel control using five Gaussian crystal peaks. The crystallinity index (CrI) is calculated from the ratio of the area of all crystalline peaks to the total area.

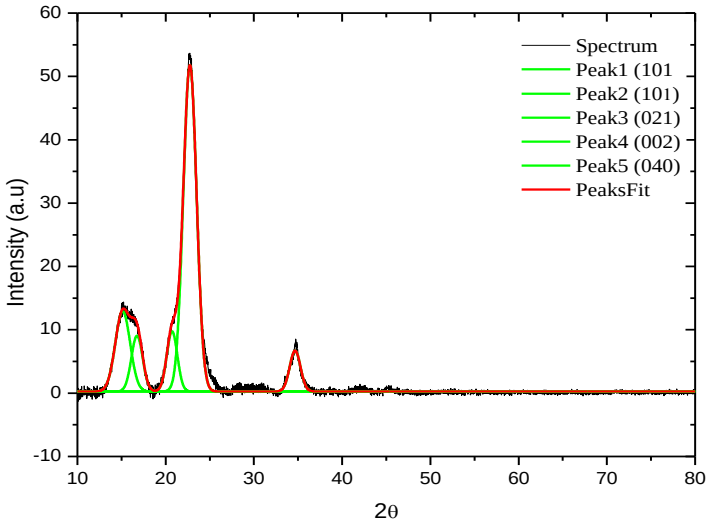

Figure 2.6: The Gaussian functions used to fit the X-ray diffraction data from a Avicel Control.

To comprehensively determine the crystalline nature of a cellulose in biomass samples, factors such as lattice spacing (d-spacing), which describe the distance between the crystallites and the crystallite size can be used to understand the evolution of the peak morphology. The changes in the d-spacing and crystallite size at 101 and $10\bar{1}$ plane indicates the structural property of cellulose. For instance, a perfect crystallite size of between 0.384 and 0.3866 nm, and a larger d-spacing at 002 plane is an indication of a compact biomass, which can be differentiated by two resolved peaks. Thus, implying increased recalcitrance to endoglucanase hydrolysis (Ju *et al.,* 2015). Whereas a decrease in the crystallite size at the 101-lattice plane as a result of a breakdown of the intermolecular hydrogen bonds, which is associated with the increase in the distance between the crystals represented by one broad peak, could have a direct implication to the ability of endoglucanase to hydrolyse microcrystalline cellulose (Figure 2.6; Ling *et al.,* 2017; Ren *et al.,* 2022).

4. Problem Statement

Several investigations have demonstrated that rooibos tea has the potential to be applied as a source of complex phenolic compounds that can be used beyond the tea industry. For instance, Hübsch *et al.* (2014) demonstrated that the rooibos extracts had antibacterial activity. Additionally, the application of ferulic acid esterase, pectinase, ß-glucanase, and xylanase on rooibos biomass improved the extraction of phytochemicals (Coetzee *et al.,* 2014). The enzyme phytochemical extracts contain flavone and iso-orientin, which have pharmaceutical value. The

use of cellulase and xylanase biocatalysts improved the concentration of soluble solids extracted from rooibos (Pengilly *et al.,* 2008). However, there is a knowledge gap regarding the innovative use of rooibos residue from tea extraction processes. According to the rooibos council (https://sarooibos.co.za/industry-statistics/) close to 14000 tons of rooibos is produced annually in South Africa and about 6000 tons of the rooibos is exported Therefore, the amount of rooibos residue left after tea processing is measured in tons per annum, and the fact that rooibos is a woody fynbos plant, suggests that it can be suitable for biofuel production. Thus, the current MSc research project addresses the knowledge gap regarding the use of rooibos as a potential sustainable bioresource for producing value added chemicals/products.

5. Aims and objectives.

The aims of the MSc project were to comprehensively characterise the horseradish peroxidase (HRP) and use it to delignify rooibos biomass. In addition, to formulate a holocellulolytic enzyme-cocktail (using cellulases and xylanase) that catalyse the production of soluble sugars from the HRP delignified fermented rooibos.

The study's objectives were to

1. Extract, purify and physicochemically characterise HRP.
2. Apply purified HRP on fermented rooibos bagasse for lignin removal; and characterise the delignified biomass.
3. To probe the HRP activity on cellulose model substrates (decrystallizing cellulose)
4. Formulate a holocellulolytic enzyme cocktail (HEC) with cellulases and xylanases, and its application for effective hydrolysis of the delignified rooibos biomass.
5. Apply HEC for conversion of pretreated rooibos residues into soluble sugars.

Chapter 3: Published Article

Horseradish peroxidase delignification of fermented rooibos modifies biomass structural and chemical properties, and improves holocellulolytic enzyme cocktail efficacy

Mamosela Marriam Mohotloane[1], Orbett Alexander[2], Brett Ivan Pletschke[3], and Mpho Stephen Mafa[1*]

[1]Carbohydrates and Enzymology Laboratory (CHEM-LAB), Department of Plant Sciences, University of the
Free State, P.O. Box 339, Bloemfontein 9300, South Africa.
[2]Department of Chemistry, University of the Free State, Qwa-Qwa Campus, South Africa.
[3]Enzyme Science Programme (ESP), Department of Biochemistry and Microbiology, Rhodes University, Makhanda 6140, South Africa.
* Corresponding author contacts: mafams@ufs.ac.za
https://doi.org/10.1007/s11756-023-01424-4

Abstract

The purpose of the study was to pretreat fermented rooibos biomass with partially purified horseradish peroxidase (HRP) for lignin removal and to convert delignified biomass to soluble sugars through saccharification with a formulated holocellulolytic enzyme cocktail (HEC). HRP enzyme was extracted from the horseradish root tissue and was partially purified by membrane filters and characterised biochemically. HRP enzyme was used to pretreat the fermented rooibos biomass to remove lignin before hydrolysing it with the HEC. Our findings indicated that HRP is versatile because it displayed activity on guaiacol, 8-aminoquinoline, and decolourised methylene blue dye. HRP had a pH optimum of 4.5 and displayed a mesophilic temperature range. The kinetics studies indicated that HRP displayed a higher affinity towards guaiacol (K_m= 0.082 mg/mL) followed by 8-aminoquinoline (K_m= 0.221 mg/mL). However, the catalytic efficiency revealed that the enzyme hydrolysed guaiacol (63436.48 s^{-1}. mg/mL) and 8-aminoquinoline (59189.81 s^{-1}. mg/mL) efficiently. HRP pretreatment of rooibos biomass significantly removed lignin content and increased pores on the surface as visualised with SEM. FTIR validated the SEM results by showing reductions at 3324.81, 1615.16 and 1018.75 cm^{-1}, corresponding to crystalline cellulose, lignin and holocellulose regions, respectively. HRP pretreated biomass had the lowest crystallinity index of 11.2% compared to 20% of the

control. HRP delignified rooibos biomass was hydrolysed effectively by the HEC, which released about 10% yield of soluble sugars compared to 6% of control. We conclude that HRP pretreatment significantly modified the structural and chemical properties of the biomass, making it more accessible to hydrolytic enzymes.

Keywords: Enzyme cocktail; enzymatic biomass-pretreatment; HRP-activity; rooibos biomass; LPMO-activity

Abbreviations

BWX: beechwood xylan
CBHI: Cellobiohydrolase-I from *Hypocrea jecorina*
CMC: carboxymethyl cellulose sodium
DNS: Dinitro Salicylic Acid reagent
DP: Degree of polymerisation
Dyp: dye decolourising peroxidase
EG1: Endoglucanase1 from *Aspergillus niger*,
EG2: Endoglucanase2 from *Aspergillus* sp.
EGs: Endoglucanases
FTIR: Fourier Transform Infrared Spectroscopy
H_2O_2: Hydrogen peroxide
HRP: horseradish peroxidase
I.P.C.C: Intergovernmental Panel on Climate Change
LiP: lignin peroxidase
LPMO: lytic polysaccharide monooxygenase
MnP: manganese peroxidase
SDS-PAGE: Sodium dodecyl sulfate-polyacrylamide gel electrophoresis
SEM: Scanning electron microscopic
VAPs: Value-added products
WAX: arabinoxylan
XRD: X-ray diffraction

1. Introduction

Economic activities such as burning fossil fuels (coal, oil and gas) enhance the greenhouse effect leading to global warming. Hence, biofuel production from agricultural residues is one of the preferred renewable fuels because it can decrease carbon monoxide emissions (I.P.C.C 2007; Houghton 2005). Plants can use the emissions of carbon dioxide from the biofuel during photosynthesis resulting in an ecofriendly process known as the carbon cycle (I.P.C.C 2007). The biorefinery sector continues to investigate cheaper methods for producing second generation biofuel and value-added products (VAPs) from agricultural residues, which have the potential to produce simple sugars that can be fermented into ethanol (Olsson and Hahn-Hagerdal 1996; Mafa *et al.* 2021). However, removing lignin from the biomass via ecofriendly means and using enzyme cocktails to degrade lignocellulose to simple sugars has been a challenge, resulting in a higher price for biofuel than petroleum production (Olsson and Hahn-Hagerdal 1996). These observations prompt more research that probes newer, efficient and environmentally friendly methods to remove lignin from lignocellulose or formations of enzyme cocktails with superior biomass conversion to fermentable sugars (Mafa *et al.* 2021; Van Dyk and Pletschke 2012).

Agricultural wastes such as rooibos (*Aspalathus linearis*) residues are carbon-rich biomass that can be used to produce second-generation biofuels without affecting food supply due to their high abundance (Kong *et al*. 2017; Malhotra and Suman 2021). Rooibos is part of the fynbos vegetation found in the Western Cape and Northern Cape Provinces of South Africa (Joubert and Schulz 2006; Lotter and Maitre 2014). It is one of the major drinks consumed as a ready-made tea (iced tea), or as a hot tea (Joubert and Schulz 2006). The production of iced tea results in tons of rooibos bagasse produced annually, and the manufacturing companies typically dispose of the waste by burning, dumping it into landfills or using it as compost (kondo *et al*. 2007). We propose that some of the rooibos residues disposed of annually can be used to produce biofuel and VAPs through enzymatic degradation.

The physiological and biochemical features of the rooibos plant make it an attractive biomass source. Rooibos is a shrub (woody plant) that grows along the ground and can reach 2 m in length (Joubert and Schulz 2006; Lotter and Maitre 2014). Pengilly *et al*. (2008) demonstrated that soluble sugars (e.g., xylose, glucose, arabinose, and galactose) were easily extracted from rooibos samples by boiling in water. Compared to black tea (*Camellia sinensis*), rooibos contains lower tannin content, which forms part of lignin in most dicots (Joubert and de Beer

2011). A study by Dossou-Yovo *et al*. (2021) showed that rooibos contains about 45% soluble matter, 37% holocellulose, 9% soluble lignin, and 82% of the rooibos biomass is hydrolysable. Other studies argue that the holocellulose constitutes the major content (Malhotra and Suman 2021), where cellulose forms 36-61%, and hemicellulose constitutes 13-39% (Olsson and Harn-Hagerdal 1996; Calderan-Rodrigues *et al*. 2019).

Cellulose and hemicellulose are hydrolysed by glycoside hydrolases (GHs) that constitude main-chain cleaving and debranching enzymes to produce sugars that can be fermented to produce ethanol or VAP (van Dyk and Pletschke 2012; Malgas *et al*. 2019; Mafa *et al.* 2021). However, the presence of lignin can lead to non-specific substrate-binding of holocellulolytic enzymes or inhibits the enzymatic degradation of cellulose and hemicellulose (Malhotra and Suman 2021; Kong *et al*. 2017). Lignin is a polymer comprised of randomly linked hydroxycinnamyl alcohols such as *p*-coumaryl alcohol, coniferyl alcohol, and sinapyl alcohol (Mnich *et al*. 2020). Due to its protective nature, lignin must be removed before the lignocellulosic biomass is hydrolysed through enzymatic application. Generally, lignin removal results in a higher enzymatic biomass conversion rate with a higher yield of soluble sugars. (Mnich *et al*. 2020; Mafa *et al*. 2020; Van Dyk and Pletschke 2012).

Most of the developed pretreatment methods used to remove lignin include chemicals (particularly acid pretreatments) which are expensive and produce toxic compounds, such as black liquor, that are detrimental to the environment and human health (Kong *et al*. 2017; Bagewadi *et al*. 2017). Additionally, pretreatment methods alter the lignin and hemicellulose structure during lignin degradation and produce inhibitory compounds, such as furfural and hydroxymethylfurfural, which impede enzymatic hydrolysis and the fermentation process (Kong *et al*. 2017; Harmsen *et al*. 2010). In contrast, the use of alkaline pretreatments, such as sodium hydroxide, is cost-effective compared to acid pretreatment. Alkaline pretreatments lower the degree of polymerisation (DP) and cellulose crystallinity, as a result, increases the efficacy of the enzymes that hydrolysis carbohydrates (Mafa *et al*. 2020; Hendriks and Zeeman 2009). However, the limitation of alkaline pretreatment is that the method's efficacy depends on the amount of lignin present in the biomass, and it can also hydrolyse hemicellulose content at higher concentration (Mafa *et al*. 2020; Hendriks and Zeeman 2009). The biological approach for lignin removal (including the use of ligninase, peroxidase, laccase and carbohydrate esterase enzymes or microbes), is a cheaper alternative that is sustainable,

environmentally friendly and effective without the loss of polysaccharides and the production of inhibitory compounds (Giacobbea *et al*. 2018).

Biological pre-treatments use enzymes produced by microorganisms and plants to remove lignin from the biomass. Enzymes that remove lignin are known as ligninolytic enzymes, which include lignin peroxidase (LiP, EC 1.11.1.14), manganese peroxidase (MnP, EC 1.11.1.13), versatile peroxidase EC 1.11.1.16), and dye decolourising peroxidase (DyP, EC 1.11.1.19) (Malhotra and Suman 2021; Biko *et al*. 2022). The current study will focus on the use of horseradish peroxidase to delignify rooibos bagasse. The peroxidases (EC 1.11.1.7) require H_2O_2 as a co-substrate to initiate the reaction for lignin degradation, and in the same reaction, H_2O_2 is converted to water (Sarika *et al*. 2015; Rad *et al*. 2007; Lavery *et al*. 2010; Liu *et al*. 2013). Ligninolytic enzymes, such as peroxidase from horseradish roots (*Armoracia rusticana)*, are heme-containing enzymes used in immunohistochemistry, the treatment of waste containing phenolic compounds, removal of colour from waste or the removal of peroxide from industrial waste (Miranda and Cascone 1995; Lavery *et al*. 2010; Liu *et al*. 2013; Sarika *et al*. 2015). The need for cheaper biofuel and other VAPs produced from lignocellulosic material is the driving force behind the search for cheaper and eco-friendly de-lignification process of the biomass. The aims of the study are to comprehensively characterise horseradish peroxidase (HRP) and use it to de-lignify rooibos biomass. Secondly, to formulate a holocellulolytic enzyme cocktail and apply it to the de-lignified rooibos to convert it to soluble sugars.

2. Materials and methods

2.1. Materials

Rooibos samples were supplied by rooibos limited (Clanwilliam, Western Cape, South Africa). The horseradish root was provided by Mr Barry Newton and Mr John Parr from Yaxham farm situated in Tweespruit, Free State, South Africa. The SDS-page prestained protein ladder was purchased from Thermo fisher scientific. The commercial cellulases and xylanase enzymes such as xylanase from *Aspergillus oryzae*, endoglucanase1 (EG1) from *Aspergillus niger*, endoglucanase2 (EG2) from *Aspergillus* sp., β-glucosidase from *Aspergillus niger* and CBHI from *Hypocrea jecorina* were all purchased from Sigma (3050 spruce street, St Louis, MO, USA). The commercial substrates, such as guaiacol, avicel, 8-aminoquinoline, glucuronoxylan and carboxymethyl cellulose sodium (CMC) were purchased from Sigma (3050 spruce street,

St Louis, MO, USA), whereas beechwood xylan and wheat arabinoxylan were purchased from Megazyme, (Wicklow, Ireland) and methylene blue dye was supplied by protea laboratories. All the analytical chemicals used in the study were purchased from Sigma (3050 spruce street, St Louis, MO, USA), unless stated differently.

2.2. Extraction of horseradish peroxidase (HRP)

Horseradish peroxidase (HRP) was extracted from 300 g root tissue of horseradish. The root was chopped into 5 cm pieces, transferred into an electric industrial blender (Mellerware: optima jug blender), and homogenised into a fine paste after adding 500 mL of 50 mM sodium phosphate buffer at pH 6. The homogenate was transferred into 50 mL falcon tubes and incubated on ice for 30 minutes. The ice-cool samples were filtered using a cheese cloth. The resulting supernatant was transferred into clean falcon tubes and allowed to sediment for 16 hours at 4°C. After 16 hours, samples were centrifuged at 15 000 x*g* for 30 minutes, and the supernatant was collected in a clean beaker, and then filtered using a 0.45µm, white 47mm gridded sterile (Millipore) filter. A volume of 400 mL of the filtrate (HRP) was collected in clean Falcon tubes and stored at 4°C for further use.

2.3. HRP purification analysis

About 50 mL crude HRP was added to a 30 kDa, 20-100 mL, 4pk Pierce^{TM} protein concentrator PES (Thermoscientific, United Kingdom) for partial purification. The samples were centrifuged at 4250 x*g* for 30 minutes, the flow-through and the retained samples were collected in 50 mL falcon tube. The protein concentration of the partially purified HRP enzyme was determined using Bradford's method (Bradford 1976). The enzyme purity was determined with 12% (w/v) sodium dodecyl sulfate-polyacrylamide gel electrophoresis (SDS-PAGE) according to Laemmli (1970). The proteins were loaded on stacking gel wells and separated for 2 hours at 118 V. After separation, the gel was stained overnight using the Coomassie-staining solution (40% methanol, 10% acetic acid, and 0.025% Coomassie Brilliant Blue G250), and destained using a destaining solution (40% methanol and 10% glacial acetic acid).

2.4. HRP substrate specificity assay

HRP substrate specificity assays were conducted using guaiacol, methylene blue and 8-aminoquinoline. About 1.5 mM of guaiacol substrate was dissolved in 50 mM sodium citrate buffer pH 4.5, and 0.5% (v/v) H_2O_2 and used to test HRP activity. Firstly, we varied HRP concentrations as follows, 1.6 µg/mL, 4.7 µg/mL, 7.8 µg/mL and 16 µg/mL but kept the

concentration of the substrate constant. The kinetic absorbance was measured as the rate of the reaction for 3 minutes at 470 nm. Once the HRP activity on guaiacol was established, about 0.68 mg/mL of HRP was used to demethylate methylene blue dye by dissolving about 1.5 mM methylene blue dye in 50 mM sodium citrate buffer pH 4.5, which was added to HRP, and 0.5% (v/v) H_2O_2. The reactions were incubated for 16 hours and the absorbance was measured at 666 nm. The third reaction to test the versatility of HRP was performed using 1.5 mM of 8-aminoquinoline dissolved in 50 mM sodium citrate buffer pH 4.5, then added to 4.7 µg/mL of HRP and 0.5% (v/v) H_2O_2. The reactions were incubated at 37ºC for 20 minutes and the absorbance was measured at 520 nm. All the reactions were performed in triplicate and absorbance readings were performed on an ultraviolet-visible spectrophotometer (Varian Cary 100 Bio UV-Visible). The extinction coefficient of guaiacol and 8-aminoquinoline were 26.6 mM $.cm^{-1}$ and 6.58 mol/L $.cm^{-1}$, respectively.

2.5. HRP biochemical characterisation

Biochemical characterisation studies were performed to determine the HRP pH optimum, pH stability and thermostability using guaiacol as a substrate. pH optimum studies were assayed using 1.5 mM guaiacol dissolved in different buffers, i.e., 50 mM sodium citrate buffer for pH 4 to 5.5; 50 mM sodium phosphate buffer for pH 6 to 7.5; 50 mM for Tri-HCL buffer for pH 8 to 9) and 4.7 µg/mL of the HRP and 0.5% (v/v) H_2O_2. For pH stability studies, the enzyme was incubated for 16 hours in different buffers with varying pH, and the reactions were conducted as mentioned above. Similarly, for thermostability assays, the enzyme was incubated at 37, 50 and 70°C for 1, 5, and 16 hours to initiate the reaction as mentioned above. All reactions were conducted in triplicate, and the absorbance was measured at 470 nm.

2.6. HRP enzyme kinetic studies

The kinetics studies were conducted using 8-aminoquinoline and guaiacol substrates. HRP kinetic constants were determined using various concentrations (0.1, 0.25, 0.5, 0.75, 1, 1.25, 1.5 mM) of 8-aminoquinoline and guaiacol substrate. Each reaction in 1 mL consisted of the substrate dissolved in 50 mM sodium citrate buffer at pH 4.5, 4.7 µg/mL of the HRP-enzyme and 0.5% (v/v) H_2O_2. For 8-aminoquinoline, the reactions were incubated for 20 minutes at 37ºC, and the absorbance readings were taken at 520 nm. For guaiacol, the reactions were measured as the rate of the reaction at 470nm. The reactions were carried out in triplicate and the readings were taken using a spectrophotometer (Varian Cary 100 Bio UV-Visible). After calculation, the reaction rate was converted to mg/mL for the determination of the Michaelis-

Menten constant (K_M), V_{max}, catalytic constant (k_{cat}) and catalytic efficiency using the Lineweaver-Burk plot and Solver analysis in Microsoft Excel (Version 2016).

2.7. Fermented rooibos biomass pretreatment with HRP for lignin removal

About 2.5 g of soluble sugar-free fermented rooibos samples were dissolved in 50 mM sodium citrate buffer pH 4.5. The lignin removal reaction was conducted by adding 0.5 mg/mL HRP-enzyme and 1% (v/v) H_2O_2 in the tubes containing the rooibos biomass. The reaction period was 24 hours, and samples were incubated in a water bath set at 37°C followed by mixing with vortex every 6 hours. Additions of enzyme and H_2O_2 were performed in triplicate (at 0, 6 and 12 hour incubation) in the reaction. There were two reaction controls that were performed in the same conditions as the HRP pretreatment reaction, except that first control contained rooibos biomass and buffer only, and the second control reaction contained rooibos biomass and 1% (v/v) H_2O_2 only. After the lignin removal reaction, the samples were centrifuged at 4 000 x*g* for 15 min and the supernatant was removed and frozen at -20°C for later use, while the rooibos material was dried at 60°C for 72 hours and stored in an airtight container at room temperature for later use.

2.8. Rooibos biomass analysis with FTIR

Chemical (functional group) analysis of the untreated or pretreated fermented rooibos biomass samples was analysed with Fourier Transform Infrared (FTIR) Spectroscopy. The FTIR spectra of the fermented rooibos control (untreated), and H_2O_2 or HRP pretreated samples were measured at room temperature using an UATR-FTIR instrument (Thermo scientific, USA). All FTIR spectra were collected in absorbance mode at a spectrum resolution of 4 cm^{-1}, with 32 co-added scans per sample over the range of 4000 to 650 cm^{-1}. Peaks' functional groups were assigned according to Mafa *et al*. (2020).

2.9. X-ray diffraction (XRD) analysis of rooibos biomass

The XRD technique was used to determine the HRP-pretreatment effect on the crystallinity of the fermented rooibos biomass. Once again, 1% (v/v) H_2O_2 pretreated biomass and untreated rooibos biomass were used as controls. The Bruker diffractometer (USA) was used to do XRD using Cu Ka radiation at 40 kV and 130 mA at Coupled 2θ/Theta scanning angle and a speed of 0.5º/minute. Sample's crystallinity index was calculated according to Park *et al*. (2010).

2.10. Determination of rooibos biomass topology with SEM

To determine the effect of HRP-pretreatment on rooibos biomass topology and the controls, completely dry samples were analysed with scanning electron microscopy (SEM). Samples were mounted on aluminium pin stubs using double sided carbon tape and coated with Iridium (±10 nm) for conductivity using a Leica EM ACE600 coating system. Specimens were imaged at 5 kV using a JSM-7800F Extreme-resolution Analytical Field Emission SEM (Tokyo, Japan). The samples with different magnification ranging between 100 to 1000 times were used to analyse the samples and photos were taken with a built-in camera to document the results.

2.11. The effect of HRP on microcrystalline cellulose

About 2.5 g of Avicel samples were dissolved in 50 mM sodium citrate buffer pH 4.5. The reaction was conducted as described in the lignin removal method to determine the effect of the HRP pretreatment on the microcrystalline cellulose. After 24-hour incubation, each of the sample was mixed by vortexing and placed in a falcon tube stand to determine the sedimentation rate according to Koskela et al. (2022) with modification. Photographs were taken (using a cell phone) every min for 10 min and after 10 min the distance of the sedimentation was measured in millimetre (mm). After the determination of the sedimentation, the samples were centrifuged at 4 000 x *g* for 15 minutes and the supernatant was removed and stored at -20°C for later use, while the Avicel insoluble material was dried at 60°C for 72 hours and stored in an airtight container at room temperature for later use. The supernatant was used to determine the soluble reducing sugars using DNS method (Miller 1959). The readings were taken at 540 nm on an ultraviolet-visible spectrophotometer (Varian Cary 100 Bio UV-Visible). Enzyme activity was also conducted using EG1 (from *A. niger*) and EG2 (from *Aspergillus* sp.), and β-glucosidase (from *A. niger*) and HRP pretreated Avicel was used a substrate. Each reaction assays for the cellulase activity consisted of about 1% (w/v) substrate (pretreated Avicel dissolved in 50 mM sodium phosphate buffer pH5) added to 0.143 mg/mL for EG1, 0.33 mg/mL for EG2, and 0.25 mg/mL for β-glucosidase of the enzymes. All the reactions were incubated at 37ºC for about 2 hours. After the completion of the reactions, samples were centrifuged at 5 000 x *g* and total reducing sugars were also detected with the DNS method.

2.12. Holocellulolytic enzymes substrate specificity assay

Substrate specific assays were conducted using wheat arabinoxylan (WAX), beechwood xylan (BWX), which represent the hemicellulosic content of lignocellulose; and carboxymethyl cellulose sodium (CMC) represented the amorphous cellulose content, while microcrystalline

cellulose was represented by Avicel or filter paper. Each reaction assay for the xylanase activity consisted of 1% (w/v) WAX and BWX dissolved in 50 mM sodium phosphate buffer pH 6 and 0.143 mg/mL of xylanase and EG1, or 0.246 mg/mL of EG2. In the case of cellulase two experimental regimes were used; for the CHBI activity, about 0.024 mg/mL of enzyme was added to 1% (w/v) Avicel or 3 discs of filter paper hydrated in 50 mM sodium phosphate buffer pH6, and endoglucanase activities were assayed using 1% (w/v) CMC dissolved in 50 mM sodium phosphate buffer at pH6. All the reactions were incubated for an hour at 37ºC, except for the reaction where enzymes degraded Avicel and filter paper, the reactions were incubated for about 5 hours. All the experiments were conducted in triplicate. The enzyme activity was measured using the DNS method as mentioned in the previous section.

2.13. Formulation of the cellulolytic cocktail

The most effective endoglucanase enzyme core set was determined using 1% (w/v) of CMC or 3-discs of filter paper dissolved in 50 mM sodium citrate buffer pH 5 and enzyme-loading combinations (100, 75, 50, 25, 0%) of EG1 and EG2 were kept at constant concentration of 0.143 mg/mL. The reactions contained 1% (w/v) CMC, 0.143 mg/mL enzyme (EG1 and EG2 combinations) and 0.0143 of β-glucosidase, and the reactions were incubated for an hour at 37ºC. After the completion of the reactions, reducing sugars were detected using the DNS method. The most effective EG1:EG2 combination (i.e., 25%:75%) was further used in combination with CBHI to determine the cellulolytic cocktail using 1% (w/v) Avicel or 3-discs of filter paper dissolved in 50 mM sodium citrate buffer pH5. The experimental setup was similar to the one used to develop the most effective EG1:EG2 core sets.

2.14. Application of the holocellulolytic enzyme cocktail on the delignified rooibos biomass

The cellulolytic enzyme cocktails (consisting of EG1, EG2, CBHI and β-glucosidase) did not show a superior hydrolytic effect compared to EG1, EG2 and β-glucosidase. As a result, the holocellulolytic enzyme cocktail was formulated by investigating the additive effect of xylanase on the most effective EG1:EG2 enzyme core set. The xylanase additive effect was determined using 1% (w/v) of the de-lignified or control rooibos biomass that was hydrated by 50 mM sodium citrate buffer at pH 5. The best EG1:EG2 (25%:75%) was used at a constant concentration of 0.143 mg/mL and 0.0143 mg/mL β-glucosidase, while the xylanase concentration varied at 0.1, 0.5, 0.75 and 1 mg/mL. The reactions were incubated for 24 hours at 37ºC. All experiments were performed in triplicate. After the completion of the reactions,

reducing sugars were detected using the DNS method as described in the effect of HRP on microcrystalline cellulose section.

2.15. Data analysis

All the data (excluding the SDS-page and sedimentation data) was analysed in Excel and used to generate graphs and tables. One-way ANOVA was used to calculate the significant differences between treatments where necessary. Solver was used to determine the kinetic constants of the HRP enzyme.

3. Results

3.1. HRP partial purification and substrate specificity

Post extraction of HRP from the root of horseradish plant, the enzyme was partially purified and concentrated. The SDS-PAGE analysis showed intense bands with a molecular weight of 44, 48 and 66 kDa (Fig. 3.1). These bands were visible in the crude HRP samples, partially pure HRP and the dialyzed samples. It is important to note that after dialyzing the concentrated partially pure HRP samples, a few of the bands between the 48 and 60 kDa and a few bands above 60 kDa disappeared from the gel. These observations indicated that we partially purified the HRP enzyme which was used in the follow-up studies.

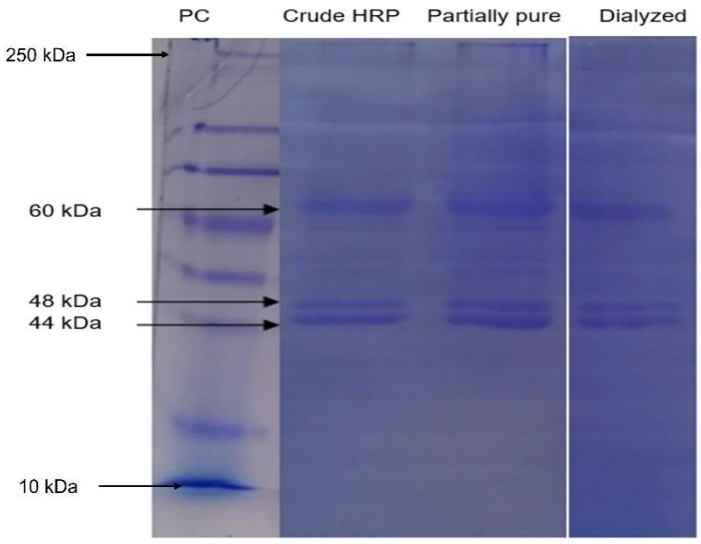

Figure 3.1: Determination of HRP partial purity with SDS-PAGE. Lane 1 (PC) represents the protein standard (prestained protein ladder), lane 2 represents crude protein extracted from the horseradish root, lane 3 represents HRP enzyme partially purified with 30 kDa cut-off filters and Lane 4 shows the profile of a further dialyzed partially pure HRP.

Substrate specificity assays were conducted to determine the partially purified HRP enzymes' activities. The enzymes showed extremely high activity on the guaiacol substrate- as a result, this substrate was used to determine the correct HRP concentration for further analysis. The results showed that 4.7 µg/mL concentration of the HRP was sufficient as it did not convert guaiacol to tetraguaiacol more rapidly as did 16 µg/mL (Fig. 3.2a). So, a concentration of 4.7 µg/mL was used for downstream analysis and to test the HRP activity on one other substrate (Fig. 3.2c). The enzyme decolourised the methylene blue dye by significantly reducing the absorbance values (Fig. 3.2b). Also, the HRP enzyme efficiently converted 8-aminoquinoline to form a quinoline dye (Fig. 3.2c), and the activity of the HRP enzyme was significantly different from when H_2O_2 was present alone. The assays showed that HRP is a versatile enzyme because it had activity on all three tested substrates.

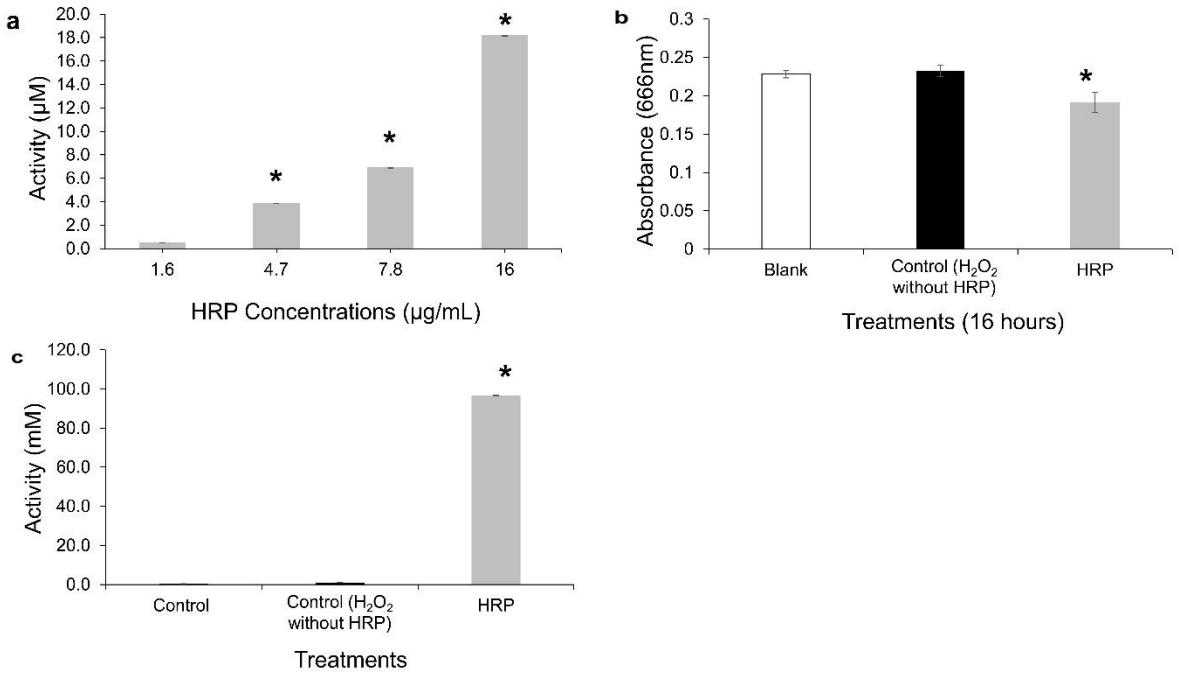

Figure 3.2: represents the activity of the peroxidase enzyme on, a) guaiacol substrate at different enzyme concentrations, b) on Methylene Blue dye and c) on 8 aminoquinoline. The values represent the means ± standard deviation. The * represents significant differences between enzyme concentrations or treatments detected with ANOVA ($p<0.05$).

3.2. Biochemical properties and kinetics parameters of the HRP enzyme

Guaiacol is a model substrate for peroxidase, and it was used to optimize the HRP enzyme biochemical conditions. HRP displayed a pH optimum at 4.5 (Table 3.1), however at pH 4 and

5.5 the enzyme displayed more than 80% relative activity indicating that the enzyme favoured acidic conditions but gradually lost activity as the conditions became more basic. For pH stability studies, the enzyme still demonstrated high activity at pH 4.5, while it lost between 30 and 40% of its activity at pH 4, and at pH 5 to 7, and lost more than 50% of its activity in the basic range. Thus pH 4.5 was taken as the optimum pH condition for the HRP-enzyme.

The thermostability studies for HRP was conducted by incubating the enzyme at 37, 50, and 70°C for 1, 5 and 16 hours, respectively. The enzyme had high activity at 37°C for all three-time points (Table 3.1), and at 50°C, it had an activity of more than 80% after 1 hour of incubation, but gradually lost activity at 50°C after 5 hours incubation followed by 16 hour incubation. At 70°C the enzyme lost activity at all the time points. Thus, 37°C was taken as the temperature at which the HRP enzymes showed optimal activity.

Table 3.1. The HRP Biochemical properties and kinetic parameters

Substrates	**Biochemical properties (optimum conditions)**			**Kinetics**			
	pH optima	pH stability range	Thermostability studies	K_M (mg/mL)	V_{max} (mg/mL.min^{-1})	k_{cat} (s^{-1})	Coefficient constant (s^{-1}. mg/mL)
Guaiacol	4[#]; 4.5; 5.5[#]	4.5 and 6.5[#]	37°C	0.082	0.404	5185.45	63436.48
8-Aminoquinoline	Not tested	Not tested	Not tested	0.221	1.022	13096.86	59189.81

[#]indicates the pH conditions where HRP enzyme displayed more that 80% relative activity All experiments were perfomed in triplicate.

Kinetics studies showed the rate at which HRP catalysed guaiacol and 8-aminoquinoline substrate into products, as well as HRP's affinity towards the substrates. The K_m values were 0.082 and 0.221 mg/mL for guaiacol and 8-aminoquinoline substrates, respectively (Table 3.1). These results indicate that HRP enzyme has a higher affinity toward guaiacol compared to 8-aminoquinoline. However, the enzyme displayed a higher V_{max} (1.022 mg/mL.min $^{-1}$) when it catalyse 8-amniquinoline, which was 3.5 fold higher than the V_{max} (0.404 mg/mL.min $^{-1}$) it

displayed during the catalysis of guaiacol. k_{cat} values of 5185.45 s^{-1} for guaiacol and 13096.86 s^{-1} for 8-aminoquinoline were recorded. The HRP displayed a catalytic efficiency value of about 63436.48 s^{-1}. mg/mL for guaiacol and 59189.81 s^{-1}. mg/mL for 8-aminoquinoline. The catalytic efficiency values were higher when HRP catalysed guaiacol, compared to when it catalysed 8-aminoquinoline. The results showed that HRP enzyme has a higher affinity for guaiacol compared to 8-aminoquinoline, but the enzyme catalysed guaiacol and 8-aminoquinoline efficiently.

3.3. **Structural, and physicochemical characterization of HRP-treated rooibos biomass**

After confirming the substrate specificity, optimum biochemical properties and kinetics parameters for the HRP enzyme, it was used to delignify the rooibos biomass. SEM topological studies were employed to determine the lignin removal efficacy of the HRP enzyme. The control (the untreated rooibos biomass) had a rough surface with a thick layer of lignin covering cellulose and hemicellulose of fermented rooibos, which was visible under 300x and 800x magnification (Fig. 3.3). The biomass treated with 1% (v/v) H_2O_2, had a smoother surface that still contained pieces of the lignin layer visible on the biomass. Also, a few pores appeared on the biomass after H_2O_2 pre-treatment. Interestingly, the biomass treated with HRP showed a significant removal of lignin layer from the fermented rooibos biomass, such that the fibres (holocellulose) were exposed, suggesting that relatively more than 80% of the lignin layer was removed or catalysed by HRP to phenolic compounds compared to the control. Lastly, the HRP-treated rooibos biomass was more porous compared to the control and H_2O_2 pretreatment. Increased, pores on the HRP-treated rooibos surface could grant hydrolytic enzymes more access to the biomass, which could lead to increased soluble sugars production.

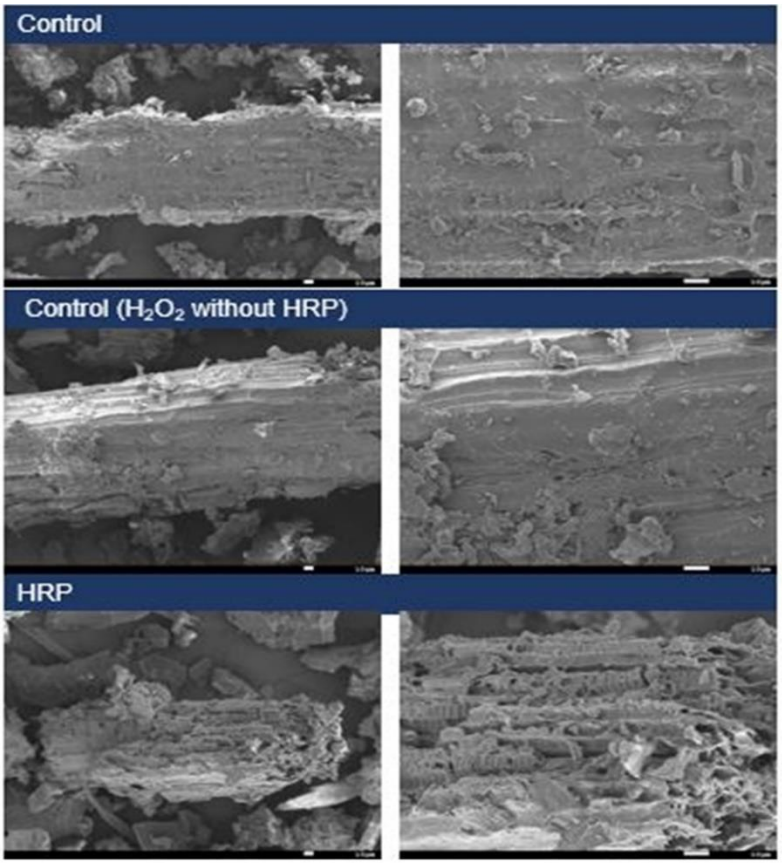

Figure 3.3: The determination of the impact of HRP treatment biomass topology using scanning electron microscopy. The topological structure of the samples were determined at 300x (left images) and 800x (right images) magnification; scale bar for all images is 10 µm.

Changes in the chemical functional groups in the untreated or pretreated fermented rooibos biomass samples were analysed with FTIR. The FTIR results corroborated the SEM findings because it was clear from the FTIR analysis that HRP pretreatment had an effect on the structural and chemical features of the rooibos biomass (Fig. 3.4). The control (untreated) biomass showed a high peak at 3324.81 cm^{-1} (red asterisk) which represent the OH groups, inter- and intra-hydrogen bonds found in the microcrystalline cellulose region of the biomass. The rooibos biomass pretreated with H_2O_2 also had a high peak at the same wavenumber as untreated samples, while the HRP pretreated samples showed a significant decrease in the absorbance at 3324.81 cm^{-1}. The observations suggest untreated and H_2O_2 pretreated biomass had higher crystallinity compared to HRP-treated biomass. In addition, the control (untreated) biomass showed the highest peak at the phenolic content range (1615.16 cm^{-1}), indicating the substantial presence of lignin in the samples. The second higher peak at the phenolic content range was that of H_2O_2, followed by HRP pretreated biomass with significantly reduced peak

in the phenolic content region compared to the control (yellow asterisk above peak 1615.16 in Fig. 3.4). Once again, the results indicated that HRP pretreatment had a significant effect by removing the lignin from the biomass. There was a minimal difference between control and H_2O_2 pretreated biomass at the holocellulose region (1018.75 cm^{-1}). However, the HRP pretreated biomass had a reduced holocellulose peak at 1018.75 cm^{-1} (green asterisk in Fig. 3.4). The FTIR findings reveals that HRP-enzyme treatment had significantly modified the chemical and structural features of fermented rooibos biomass.

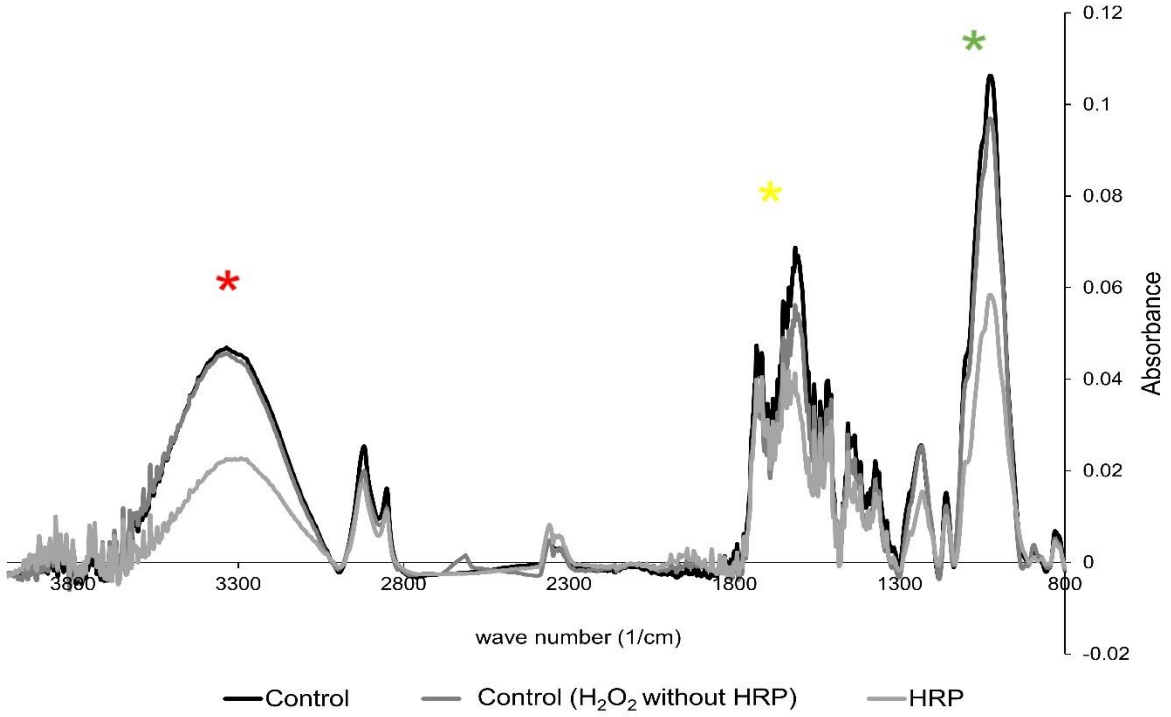

Figure 3. 4: Effects of horseradish peroxidase (HRP) enzyme on the chemical functional groups of fermented rooibos samples using FTIR analysis. The HRP-pretreated rooibos FTIR spectrum was compared to that of the control and H_2O_2 pretreated biomass. Three regions of interest, OH group region, phenolics/lignin region and glycosidic bonds/holocellulose regions are represented by red, yellow and green asterik, respectively.

The SEM and FTIR findings were supported by XRD analysis of the HRP-pretreated rooibos biomass. The untreated biomass displayed a higher crystallinity index of 20.4%, while the H_2O_2 pretreated biomass had a reduction of 3.2% crystallinity index than the control (Fig. 3.5). However, the HRP pretreated biomass showed that the pretreatment had an effect on the microcrystalline cellulose as it led to a reduction of 9.2% in the crystallinity index. Taken together, the SEM, FTIR and XRD analysis demonstrated that the HRP-pretreatment significantly modified structural and chemical features of the rooibos biomass.

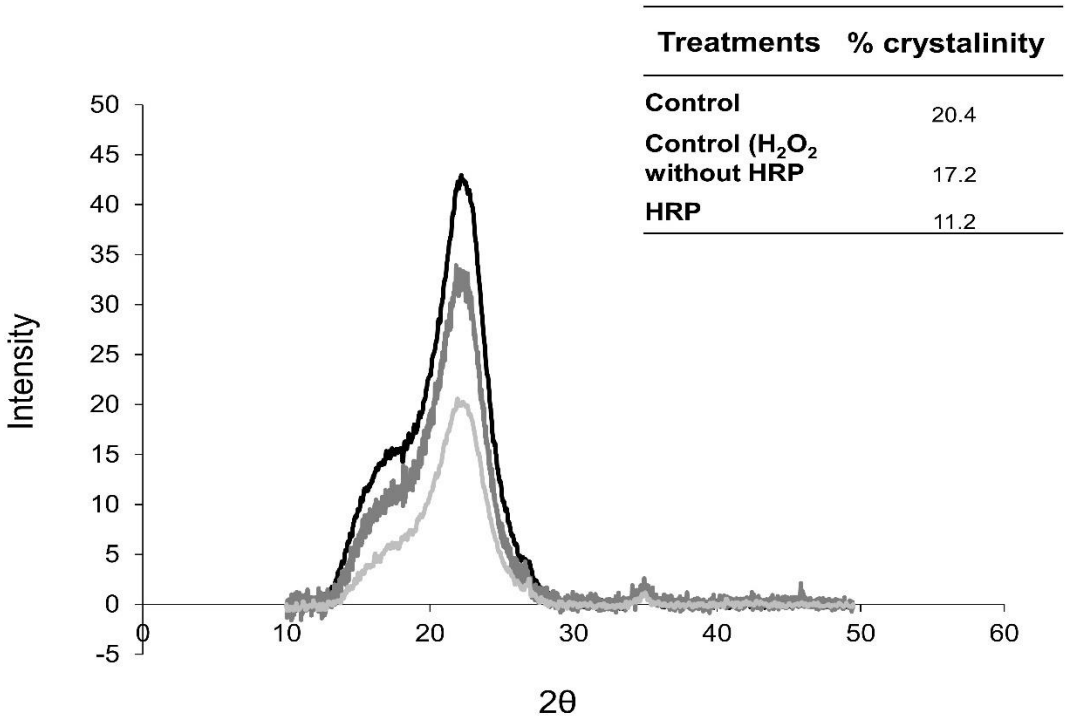

Figure 3.5: The determination of the HRP-pretreatment effect on the crystallinity of cellulose in the fermented rooibos biomass using X-ray diffraction analysis. Colour of the peaks represent control-black, control (H_2O_2 without HRP)-dark gray and HRP-light gray.

3.4. The effect of HRP on microcrystalline cellulose

The significant decrease in the crystallinity, lignin and holocellulose content after HRP pretreatment (shown by SEM, FTIR and XRD analysis), suggests that the HRP-enzyme hydrolysed the lignin and holocellulose content. As a result, we further investigated the effects of HRP enzyme on the microcrystalline cellulose using Avicel as a suitable substrate. The reducing sugars produced during the Avicel pretreament was determined using the hydrolysate (supernatant) collected after the 24 hour reaction. Fig. 3.6 showed that HRP pretreatment produced the highest level of reducing sugar content compared to the control and H_2O_2 pretreatment, which had residual activity. The HRP application produced 6 fold higher total reducing sugars compared to the H_2O_2 pretreated sample; and 10 fold higher total reducing sugars compared to the control. The residual total reducing sugars detected in the control samples and H_2O_2 treated samples could be due to auto-hydrolysis of avicel substrate during incubation at 37℃ for 24 hours.

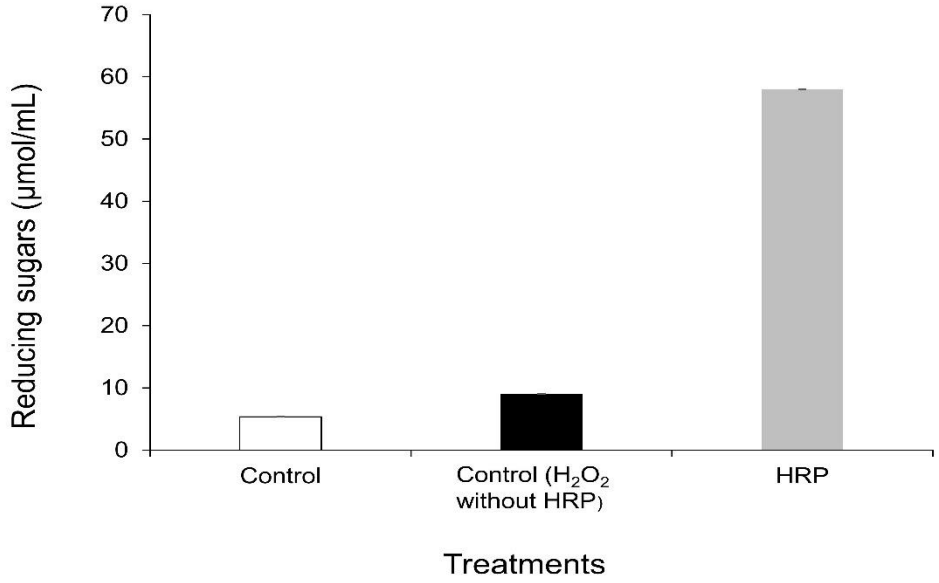

Figure 3.6: The reducing sugars produced by horseradish peroxidase (HRP) during Avicel pretreatment. The untreated and H_2O_2 pretreatment samples were used to compare the HRP activity on Avicel substrate. The values represent the means ± standard deviation. The * represents significant differences between enzyme concentrations or treatments detected with ANOVA ($p<0.05$).

Additionally, sedimentation studies were performed to validate the HRP enzyme activity on the Avicel substrate. Fig. 3.7 demonstrates that the rate of Avicel sedimentation after the HRP-pretreament reaction was significantly slower compared to the control (untreated) and H_2O_2 pretreated Avicel biomass. Avicel sedimented rapidly in the control leaving a clear liquid on top measuring 1.6 cm and a similar response was observed in the H_2O_2 Avicel with the clear liquid measuring 1.7 cm after 10 minutes. Interestingly, the HRP pretreated Avicel had a slow sedimentation rate, resulting in a sedimentation distance that was not significantly different between 3, 5 and 7 minutes (Fig. 3.7 b to d). Only after 10 minutes sedimentation distance was about 0.9 cm, suggesting that the HRP-pretreatment had an effect on the structural and physicochemical properties of cellulose.

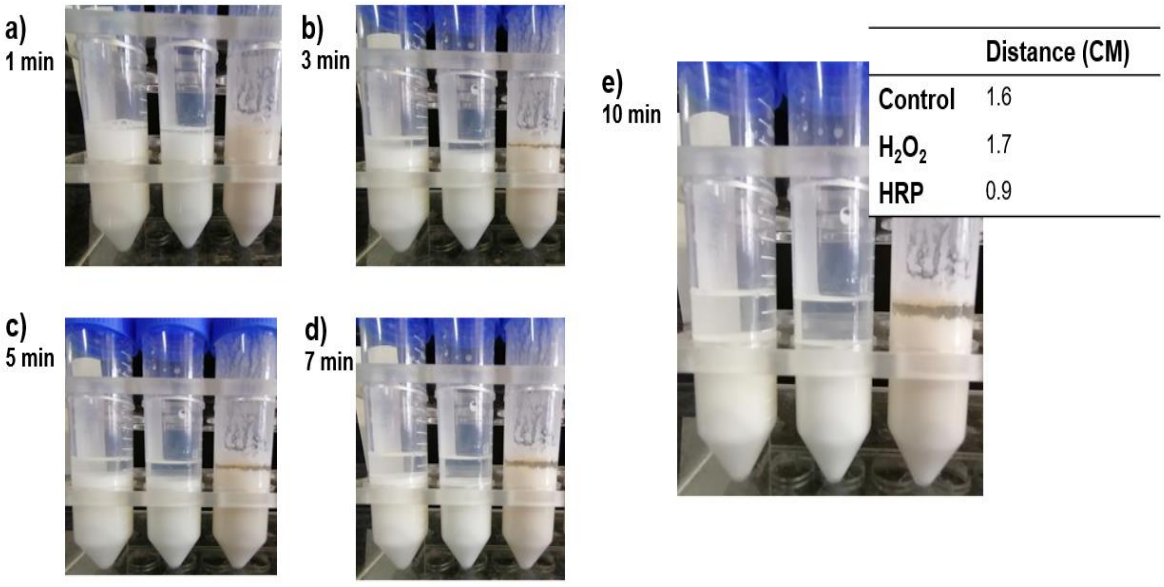

Figure 3.7: The sedimentation rate of horseradish peroxidase (HRP) pretreatment, H_2O_2 pretreatment and control Avicel after one minute (a), three minutes (b), five minutes (c), seven minutes (d), ten minutes (e) 10 minutes. The clear liquid on top of Avicel used was to measure sedimentation distance covered.

EG1, EG2 and β-glucosidase hydrolysis assays were used to determine the impact of HRP pretreatment on the structural and chemical properties of Avicel. The EG1 and EG2 showed high activity in the HRP pretreated Avicel compared to control (untreated) and H_2O_2 pretreated samples (Fig. 3.8). After HRP pretreatment EG1 showed more than 2 fold activity on Avicel compared to control and H_2O_2 treated samples, respectively. EG2 displayed about 1.2 fold higher activity when it hydrolysed the HRP-treated samples compared to control and H_2O_2 treated Avicel. EGs are known to show little-to-no activity on Avicel, due to its crystalline nature, which makes it recalcitrant to enzymatic hydrolysis. However, the findings reveals that HRP-treatment had an effect on reducing the recalcitrance of Avicel, resulting in the increased EGs activities on the modified Avicel. β-glucosidase displayed low activity as expected, because it usually hydrolyse disaccharides or shorted oligosaccharides (with a DP less than 5) into monosaccharides, indicating that the polymers produced during HRP pretreatment had higher degrees of polymerisation (long oligosaccharides).

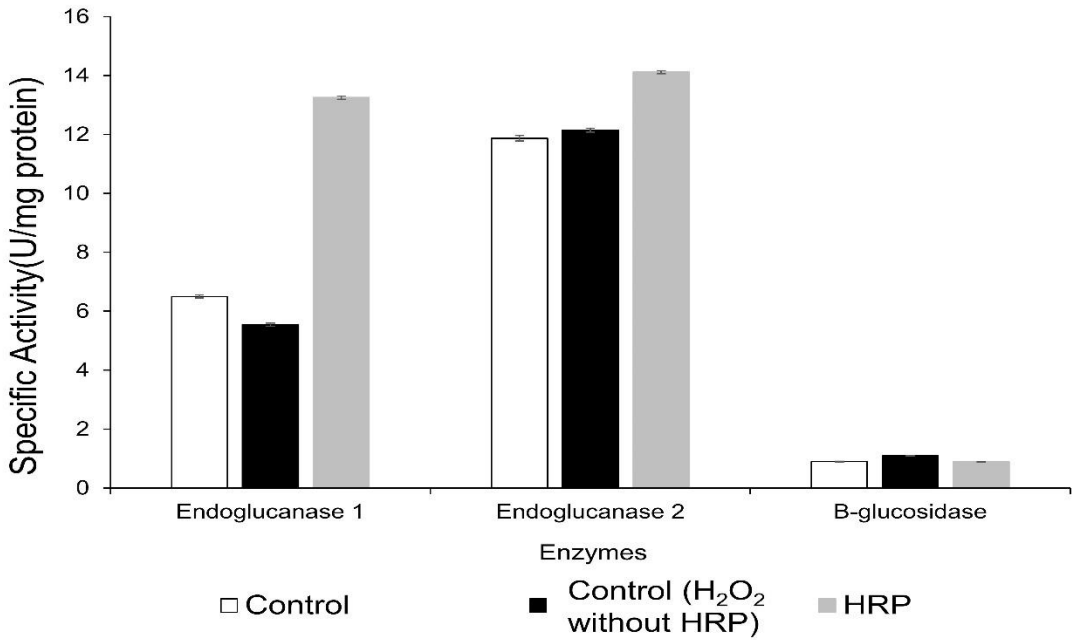

Figure 3.8: The effects of HRP-pretreatment on the microcrystalline cellulose substrate (Avicel) measured as a function of endoglucanase-1 (EG1), Endoglucanase-2 (EG2) or β-glucosidase. The values represent the means ± standard deviation. The U represent units, which is equal to μmol.h^{-1}. The * represents significant differences of EGs activity on pretreated Avicel; detected with ANOVA ($p<0.05$).

3.5. Substrate specificity of holocellulolytic enzymes

Before the formulation of the holocellulolytic enzyme cocktail for hydrolysis of rooibos biomass, we determined the specific activities of commercial EG1, EG2, CBH and xylanase. Fig. 3.9a shows that xylanase enzyme had higher activity on BWX followed by WAX and GX. EG1 enzyme also displayed a higher activity on BWX and had the same amount of activity on WAX and GX. It is important to note that EG1 displayed relatively similar results on all xylan substrates, while EG2 displayed 3 fold lower activity on xylan substrates compared to the xylanase (Fig. 3.9a). Cellulolytic substrate specificity revealed that CBHI had the overall highest activity on both substrates that represents the microcrystalline cellulose. It showed more than 3 fold higher activity on filter paper and Avicel compared to the activity of EG1, EG2, and xylanase. While CBHI has the overall highest activity on CMC (Fig. 3.9b). Both endoglucases exhibited the second highest activity on CMC, compared to xylanase.

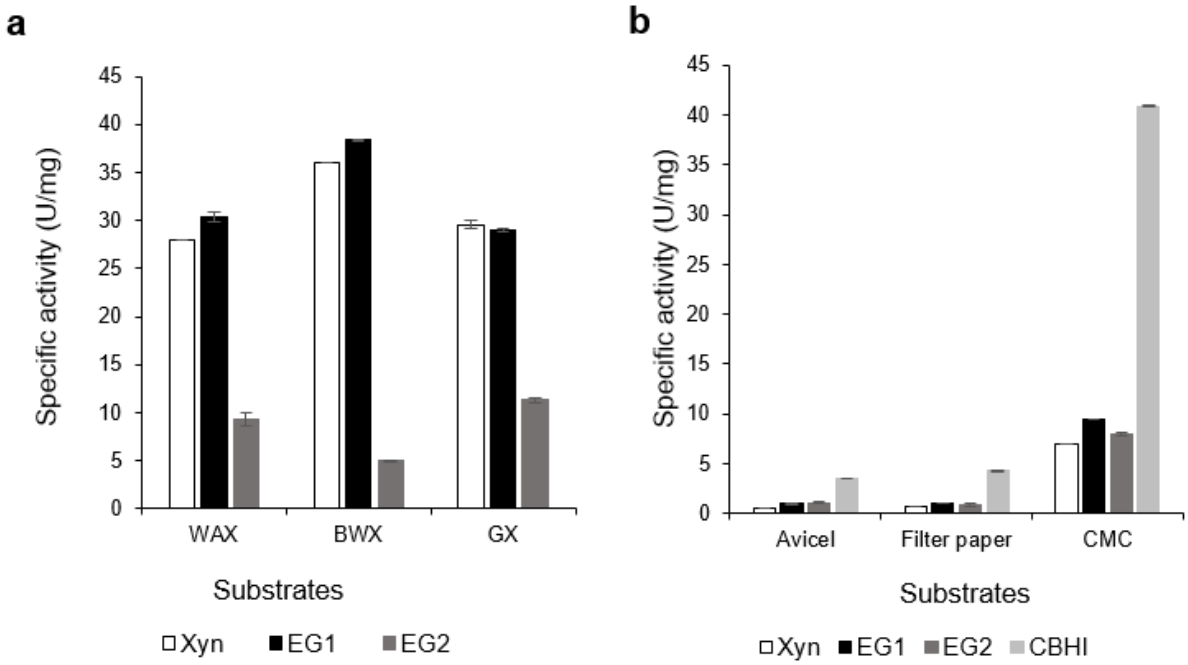

Figure 3.9: Substrate specific activity of the cellulases and xylanases on the xylan and cellulose substrates. In a) xylanase, endoglucanase-1 (EG1) and endoglucanase-2 (EG2) activity tested on Beechwood-xylan (BWX), wheat arabinoxylan (WAX) and glucuronoxylan (GX) substrates. In b), xylanase, CBHI, EG1 and EG2 activity was tested on Avicel, filter paper and carboxymethyl cellulose sodium (CMC) substrates. The U represent units, which is equal to $\mu mol.h^{-1}$

3.6. Endoglucanase binary synergy

The most effective endoglucanase combination was determined by using varying combinations of the EG enzymes. β-glucosidase was applied at 10% (v/v) relative to the total concentration of the EGs. The most effective combination of EGs was 25% EG1 and 75% EG2, as this combination had a significantly ($p<0.05$) higher specific activity compared to other combinations (Fig. 3.10). The next best combination of EGs that had significantly higher activity was 50% EG1 and 50% EG2. The enzyme combination 25% EG1 and 75% EG2 was selected for the formulation of the cellulase cocktail.

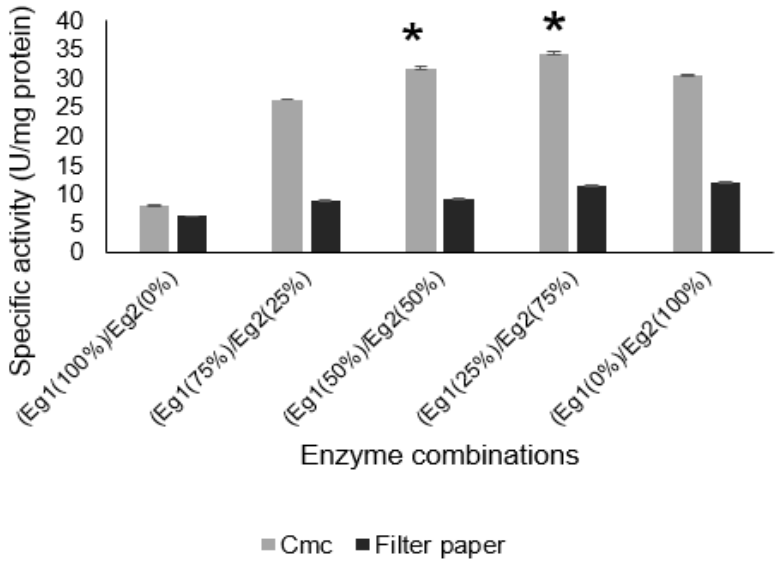

Figure 3.10: Formulations of the endoglucanase cocktail using different combinations of endoglucanase 1 (EG1) and endoglucanase 2 (EG2). The U represent units, which is equal to μmol.h^{-1}. The * represents significant differences of EGs activity on pretreated Avicel detected with ANOVA ($p<0.05$)

3.7. Cellulase enzyme cocktail

The most effective cellulase combination was formulated by using varying combinations of the selected endoglucanase enzyme core-set and exoglucanase (CBHI) as shown in Fig. 3.11. The concentration of the enzymes was kept constant at 0.84 mg/mL and β-glucosidase application concentration was 0.084 mg/mL. The endoglucanase enzyme core set dosed at 100% showed significantly ($p<0.05$) higher activity compared to any CBHI and EGs combinations (Fig. 3.11). The next best combination was a 75% endoglucanase and 25% exoglucanase combination, which showed second significantly ($p<0.05$) higher activity (Fig. 3.11). However, we anticipated that the best activity would be observed where all three cellulase enzymes were combined.

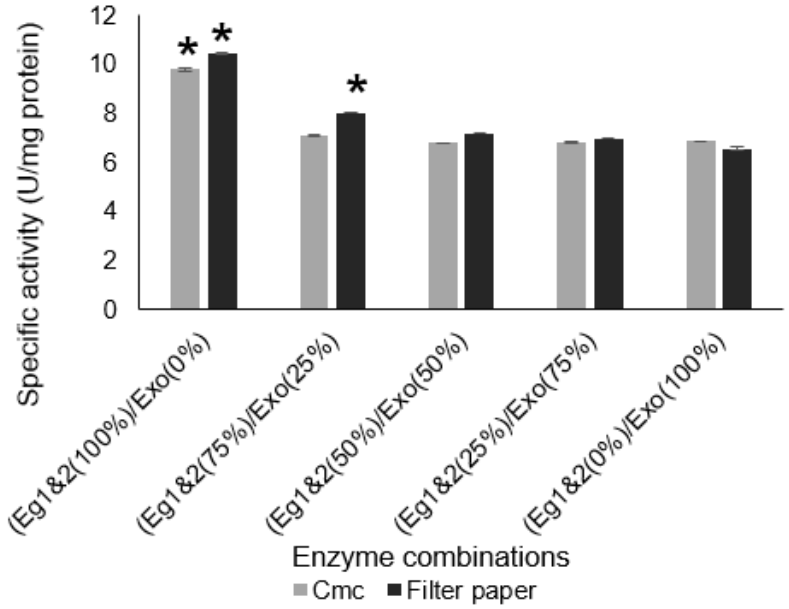

Figure 3.11: Formulation of the cellulase cocktail composed of two endoglucanases (EG1 and EG2) and exoglucanase (Exo). All experiments were performed in triplicate, the values and error bars represent the means ± SD, respectively. The U represent units, which is equal to μmol.h^{-1}. The * represents significant differences of EGs and exoglucanase combination on CMC or filter papers detected with ANOVA ($p<0.05$)

3.8. Additive effect of xylanase on the rooibos biomass hydrolysis

The additive effect of xylanase enzyme on enhancing the cellulase cocktail activity was tested using rooibos biomass. The final volume and the concentration of the endoglucanase combination was kept constant at 1 mg/mL, and the substrate loading at 1% (w/v), respectively. The fermented rooibos biomass was treated with peroxidase enzyme to remove the lignin content, while the control substrate was only subjected to buffer without peroxidase. Xylanase enzyme was used by increasing the concentration from 0.1 to 1 mg/mL. Fig. 3.12a shows the combined activity of the selected EG enzyme cocktail and xylanase was significantly higher ($p<0.5$) at 0.5 mg/mL xylanase enzyme loading. Thereafter, the activity did not change, indicating that 0.5 mg/mL xylanase enzyme loading was an ideal concentration to have maximum effect on hydrolysis of the rooibos biomass. However, the fermented biomass treated with peroxidase had the overall highest activity, which may give an indication that lignin was indeed removed, thus increasing the efficiency of enzyme hydrolysis. Another indication that the removal of lignin increased the efficiency of the enzymes is displayed in Fig. 3.12b, where the yield produced in the biomass treated with peroxidase was higher by 10% compared to the

6% in the control. It also indicated that 0.5 mg/mL of xylanase, in addition to the endoglucanase cocktail, is required in order to produce more sugar products.

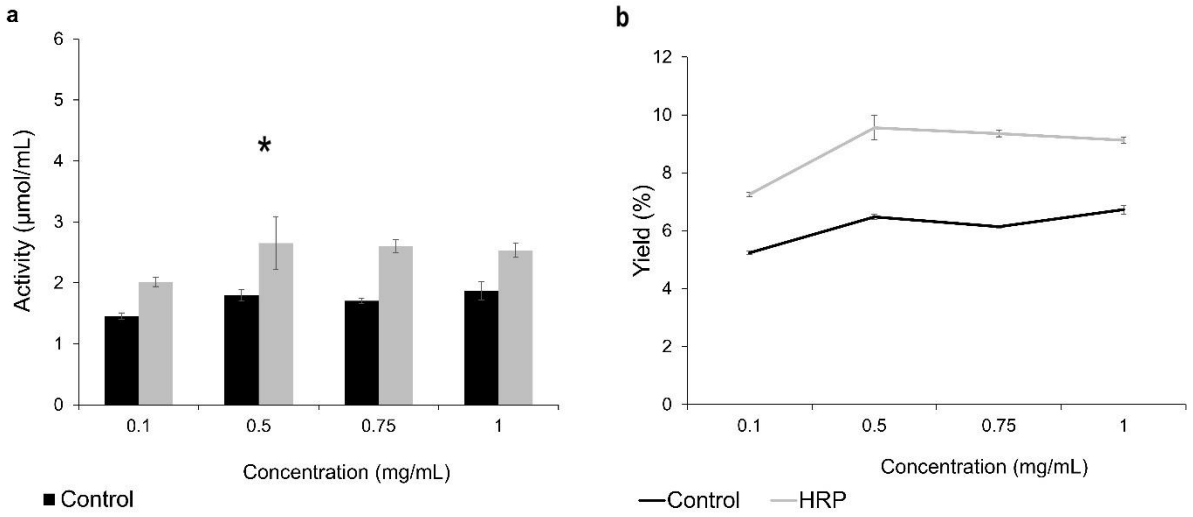

Figure 3.12: The additive effect of xylanase on the endoglucanase cocktail activity (a) and reducing sugar yield (b) during fermented rooibos biomass hydrolysis. The values and error bars represent the means ± SD, respectively. The * represents significant differences of holocellulolytic enzyme cocktail activity on fermented rooibos detected with ANOVA ($p<0.05$). Concentration is in mg/mL.

4. Discussion

The partially pure horseradish peroxidase contained bands with molecular weights of 44, 48 and 66 kDa, which were similar to molecular weight of horseradish peroxidase reported by Paul and Stigbrand (1970). Peroxidase from sycamore maple and peanuts contained bands of 42 and 40-42 kDa molecular weight, respectively (Dean *et al*. 1994; Chibbar and Van Huystee 1984). Duarte-Vázquez *et al*. (2007) reported that peroxidases typically sourced from plants have a molecular weight of between 30 to 60 kDa. These studies suggest that the three intense bands observed on the SDS-PAGE in our study could be isozymes of horseradish peroxidase. In addition, the partially pure HRP showed versatility as it hydrolysed three tested substrates. The enzyme in the presence of the co-substrate H_2O_2 converted the model substrate guaiacol to tetra-guaiacol, which is measured as the change in absorbance overtime (Fig. SI1), similar to the HRP enzyme reported by Lavery *et al*. (2010). The enzyme also acts as a decolourizing agent by removing colour from methylene blue dye. Bholay *et al*. (2012) proposed that bacterial peroxidase with decolourizing activity showed lignin modifying activity. The 8-aminoquinoline is mainly used as an antimalaria agent (Strother *et al*. 1981), however, it is

similar to the 4-aminoantipyrine-phenol substrate that acts as a hydrogen donor in the presence of hydrogen peroxide and HRP, resulting in the production of the quinone chromogen. Our studies also found 8-aminoquinoline was hydrolysed by HRP enzyme to produce quinoline dye (Fig. SI2), giving an intense pink colour formation (Sarika *et al*. 2015). We propose that 44, 48 and 66 kDa protein bands on the SDS-PAGE gel could be the HRP-isozymes, which contribute to the versatile nature of this enzyme. We are conducting follow-up studies to identify and verify if this protein band are isozyme of the HRP.

Biochemical studies showed that the HRP pH optimum was 4.5, which is within the pH range of peroxidases reported in literature; for instance, date-palm peroxidases showed an optimum pH at pH 4.5 (Al-Bagmi *et al*. 2019), while other peroxidases have optimum pH from 4 to 6 (Sarika *et al*. 2015; Biko et al., 2022). The HRP enzyme is not thermostable, because the enzyme lost activity at 50 and 70℃ within one hour of incubation and was only stable at 37℃. However, peroxidase from *Moringa oleifera L*. leaves was stable at 55℃ (Khatun *et al*. 2012). The K_m value represents the affinity or possible degree at which an enzyme tends to bind to a substrate. HRP displayed higher affinity for guaiacol compared to 8-aminoquinoline, but catalytic efficiency was relatively higher in both substrates. These implies that the HRP is effective in producing more products at a faster rate during catalysis of both substrates (Sulyman *et al*. 2020).

After successfully characterising HRP and confirming its versatility in hydrolysing three substrates, we used it to delignify fermented rooibos biomass. The SEM results showed the efficacy of HRP pretreatment in removing lignin from the fermented rooibos biomass. The HRP pretreatment removed the thick rough layer of lignin, exposing the pores and fibres of the biomass, which generally increase the area accessible to enzymes for hydrolysis. Similar studies on the pretreatment of corn stover with lignin degrading fungi and isolated *Trametes hirsuta* yj9, showed that the pretreatments removed lignin and increased biomass conversion to simple sugar (Su *et al*. 2018; Sun *et al*. 2011). Liu *et al*. (2022) also used bactetrial (*Raoultella ornithinolytica* RS-1) pretreatment to remove lignin from the corn stover. It was shown that the RS-1 strain was successful in removing lignin because it secreted lignin-peroxidase, manganese-peroxidase and unclassified peroxidase (Liu *et al*. 2022). The studies validated our SEM findings, which showed that HRP-pretreatment modified or removed the lignin from rooiboss biomass.

The FTIR results validated the claim that HRP pretreatment removed lignin from the rooibos biomass. Liu *et al*. (2022) also found that biological pretreatment of the corn stover decreased the peak at 1630 cm^{-1}, which corresponded to the C = O stretching vibration of aromatic rings in lignin. Our findings also showed a similar trend because the HRP pretreated rooibos biomass had a significant decrease at 1625 cm^{-1}. At 1718 cm^{-1} corresponding to ester bonds (lignin hemicellulose conjugation region) peak slightly increase in the HRP pretreated rooiboss biomass compared to H_2O_2 control, suggesting that the products of lignin degradation increased. In addition, the pretreatment of rice straw with renewable bioionic liquids showed a decrease in the phenolic content, indicating the removal of lignin (Hou *et al*. 2013). Additionally, the FTIR analysis show the broad peak between 3000 cm^{-1} and 3500 cm^{-1} corresponding to OH stretching vibration and intra/inter hydrogen bonds was significantly reduced in the HRP-treated biomass. The region (3000-3500 cm^{-1}) is generally assigned to microcrystalline cellulose (Mafa *et al*. 2020), so the decreased peak at this region indicate that HRP treatment modified the microcrystalline cellulose of rooibos biomass. The XRD results confirmed a decrease in the crystallinity of cellulose due to the HRP pretreament. Other studies also used FTIR analysis to show that pretreatment of corn stover with lignin degrading fungi or bacteria had an increased cellulose and hemicellulose content, and XRD analysis displayed a reduction in the crystallinity of cellulose (Su *et al*. 2018; Lui et al. 2022).

The SEM, FTIR and XRD results indicated that the HRP pre-treatment also hydrolysed the holocellulose content of the rooibos. This observation implies that the HRP enzyme also possesses lytic polysaccharide monooxygenase-like (LPMO-like) activity, which catalyse the holocellulose content (cellulose or hemicellulose) of the biomass (Walton and Davies 2016; Meier *et al*. 2018). Further analyses were conducted by pretreating microcrystalline model substrate (Avicel) with the HRP enzyme. The results showed that the hydrolysate from the pretreatment contained reducing sugars produced by the HRP enzyme. Additionally, the sedimentation study showed that HRP pretreatment modified the structure of Avicel. We propose that HRP decreased recalcitrance of cellulose towards enzymatic hydrolysis because after HRP-pretreatment the Avicel was effectively hydrolysed by endoglucanases (Fig. SI3). Eijsink *et al.* (2019) argued that LPMOs require the presence of a reductant (e.g., H_2O_2) to catalyse recalcitrant polysaccharides to produce oxidised oligosaccharides. The authors detected both reducing sugars and oxidised sugars, and the presences of reducing sugars was attributed to contamination. Interestingly, manganese peroxidase sourced from *Phanerochaete chrysosporium* that degraded lignin from the biomass, could also produce high amount of

soluble reducing sugars froms CMC, Avicel and xylan substrates (Min *et al*. 2022). The manganese peroxidase from Min *et al*. (2022) and HRP used in our study have similar properties such as, LPMO-like activity, cellulase activity boosting effects and reduced the recalcitrance of Avicel. We are conducting additional studies to establish the LPMO mechanism employed by the HRP enzyme during cellulose hydrolysis.

The HRP-pretreated rooibos biomass was hydrolysed by the holocellulolytic enzyme cocktail. Commercial enzymes used to formulate the enzyme cocktail were analysed with binary synergy assays (for endoglucanases) and ternary synergy assays as described by (Mafa *et al*., 2021 and Thoresen *et al*., 2021). Synergy studies of the two endoglucanases were used to formulate the best endoglucanase enzyme core set. The endoglucanase enzymes hydrolyse glycosidic bonds in the amorphous region of cellulose, while the exoglucanase (CBHI) enzyme hydrolyses glycosidic bonds from the reducing-end region of the microcrystalline cellulose (Van Dyk and Pletschke, 2012, Zhang and Zhang, 2013, Mafa et al., 2021). Thus, CMC was used as the substrate for endoglucanase synergy studies, which demonstrated that the best endoglucanase combination was 25% EG1 and 75% EG2. This EGs combination was used along with CBHI to formulate the cellulase cocktail. The results were not expected because the EGs combination at 100% enzyme dose had higher activity than the combinations of EGs and CBHI on Avicel or filter paper. Thoresen et al. (2021) demonstrated that CBHs and endoglucanases do not always display synergy. As a result, some EG and CBH combinations don't produce higher concentration of soluble sugars, the phenomena is called anti-synergy (Thoresen et al. 2021; Mafa et al., 2021). Therefore, the best EGs combination were used to convert the HRP de-lignified rooibos biomass.

EGs combination was supplemented with various concentrations of xylanase and the enzyme cocktail was used to hydrolyse the delignified rooibos. The removal of lignin allowed the holocellulolytic enzyme cocktail to convert the rooibos biomass to soluble sugars better than control. In addition, the holocellulolytic enzyme cocktail yielded 10% soluble sugars during the hydrolysis of delignified rooibos biomass which was about 2 fold higher compare to the yield of soluble sugars produced from the control. Eijsink et al. (2019) demonstrated that the use of LPMOs together with commercial cellulases enzymes resulted in a 10% yield of glucose produced from the lignocellulose biomass. The manganese peroxidase had boosting effects on the cellulase activity that degraded CMC, such that about 75% of CMC was converted to glucose (Min et al. 2022). In addition, a bacterial strain that secreted three types of peroxidases

was used to pretreat corn stover and thereafter, used commercial cellulase and β-glucose to convert 20% of pretreated corn stover to soluble sugars (Liu *et al*. 2022). These studies support our observation that the HRP pretreated rooibos biomass was efficiently degraded by the holocellulolytic enzyme cocktail.

5. Conclusion

Horseradish peroxidase (HRP) is a versatile enzyme with activity on multiple substrates. It also displays LPMO-like activity that produces significant amounts of reducing sugars from Avicel. Additionally, the LPMO-like activity of HRP decreased Avicel's recalcitrance against endoglucanase enzymes - as a result, endoglucanases showed higher activity on HRP-treated Avicel. Furthermore, SEM analysis showed that HRP pretreatment removed lignin from fermented rooibos biomass, increased pores on the biomass surfaces, and there were visible signs that it degraded holocellulose content. To the best of our knowledge, this is the second study reporting on versatile peroxidase that possesses LPMO-like activity and can remove lignin from lignocellulose substrate after Min et al. (2022). We are working on elucidating the LPMO mechanisms employed by HRP to produce reducing sugars from microcrystalline cellulose. The efficacy of HRP pretreatment on rooibos biomass was confirmed by FTIR and XRD analysis, which showed a decreased crystallinity, reduced holocellulose content, and a reduction in lignin from fermented rooibos biomass. Finally, saccharification of HRP pretreatment rooibos biomass with holocellulolytic enzyme cocktail released more reducing sugars and resulted in about a 10% yield compared to the control. Thus, we recommend the use of HRP pretreatment over chemical pretreatment because it removes lignin and reduces the crystallinity of lignocellulosic biomass.

Acknowledgements:

This research was supported by University of the Free State, Department of Plant Science and Centre for Graduate Support. This research was also partially supported by the South African National Research Foundation through a Thuthuka grant to Dr. Mpho S Mafa.

Author Contribution

MMM and MSM designed the research; MMM conducted the experiment;

MSM, MMM, OA, and BIP analysed the data and wrote the paper; and MSM had primary responsibility for the final content.

Funding

Ms MMM received MSc bursary from University of the Free State Centre for Graduate Support, MSMS received the central research fund (CRF) from the Dean of Natural and Agricultural Sciences and NRF-Thuthuka grants

Data Availability

Available upon request

Consent for publication

All authors have read and approved the final manuscript.

Competing Interests

Authors do not have any competing interests

6. References

Al-Bagmi MS, Khan MS, Ismael MA, Al-Senaidy AM, Bacha A.B, Husain FM, Alamery SF (2019) An efficient methodology for the purification of date palm peroxidase: Stability comparison with horseradish peroxidase (HRP). Saudi J. Biol. Sci. 26:301-307. https://doi.org/10.1016/j.sjbs.2018.04.002

Bagewadi ZK, Mulla SI, Ninnekar HZ (2017) Optimization of laccase production and its application in delignification of biomass. IJROWA 6:351-365. https://doi.org/10.1007/s40093-017-0184-4

Bholay AD, Borkhataria BV, Jadhav PU, Palekar KS, Dhalkari MV, Nalawade PM (2012) Bacterial Lignin Peroxidase: A Tool for Biobleaching and Biodegradation of Industrial Effluents. Univers. j. environ. res. technol. 2:58-64

Biko OD, Viljoen-Bloom M, van Zyl WH (2022) Medium optimization for enhanced production of recombinant lignin peroxidase in Pichia pastoris. Biotechnol. Lett. 45:105-113. https://doi.org/10.1007/s10529-022-03321-3

Bradford MM (1976). A rapid and sensitive method for the quantification of microgram quantities of protein utilizing the principle of protein-dye binding. Anal. Biochem. 72:248-254. https://doi.org/10.1016/0003-2697(76)90527-3

Calderan-Rodrigues MJ, Fonseca JG, de Moraes FE, VazSetem L, CarmanhanisBegossi A, Labate CA (2019) Plant cell wall proteomics: A focus on monocot species, Brachypodiumdistachyon, Saccharum spp. and Oryza sativa. Int. J. Mol. Sci 20:1975. https:// doi:10.3390/ijms20081975

Dean JFD, Sterjiades R, Eriksson KEL (1994) Purification, characterization of an anionic peroxidase from sycamore maple (Acer pseudoplatanus) cell suspension cultures. Physiol Plant 92:233–240. https://doi.org/10.1111/j.1399-3054.1994.tb05331.x

Dossou-Yovo W, Parent SÉ, Ziadi N, Parent É, Parent LÉ (2021) Tea Bag Index to Assess Carbon Decomposition Rate in Cranberry Agroecosystems. Soil syst 5:44. https://doi.org/10.3390/soilsystems5030044

Duarte-Vázquez MA, García-Padilla S, García-Almendárez BE, Regalado C (2007) Purification of natural plant peroxidases and their physiological roles. Funct. plant sci. biotechnol 1:18-31.

Eijsink VG, Petrovic D, Forsberg Z, Mekasha S, Røhr ÅK, Várnai A, Bissaro B, Vaaje-Kolstad G (2019) On the functional characterization of lytic polysaccharide monooxygenases (LPMOs). Biotechnol. Biofuels 12:1-16. https://doi.org/10.1186/s13068-019-1392-0

Giacobbe S, Pezzella C, Lettera V, Sannia G, Piscitelli A (2018) Laccase pretreatment for agrofood wastes valorization. Bioresour. Technol. 265:59-65 https://doi.org/10.1016/j.biortech.2018.05.108.

Harmsen PF, Huijgen W, Bermudez L, Bakker R (2010) Literature review of physical and chemical pretreatment processes for lignocellulosic biomass. Wageningen UR-Food & Biobased Research.

Hendriks ATWM, Zeeman G (2009) Pretreatments to enhance the digestibility of lignocellulosic biomass. Bioresour. Technol. 100:10-18. https://doi:10.1016/j.biortech.2008.05.027

Hou XD, Li N, Zong MH (2013) Renewable bio ionic liquids-water mixtures-mediated selective removal of lignin from rice straw: Visualization of changes in composition and cell wall structure. Biotechnol. Bioeng. 110:1895-1902. https://doi.org/10.1002/bit.24862

Houghton J (2005) Global warming. Rep. Prog. Phys. 68:1343. https://doi:10.1088/0034-4885/68/6/R02

I.P.C.C., (2007) Climate change 2007: The physical science basis. Agenda 6(07), p.333.
Joubert E, Schulz H (2006) Production and quality aspects of rooibos tea and related products. J. Appl. Bot. Food Qual. 80:138-144.

Khatun S, Ashraduzzaman M, Karim MR, Pervin F, Absar N, Rosma A (2012) Purification and characterization of peroxidase from Moringa oleifera L. leaves. Bioresources 7:3237-3251.
Kondo M, Hidaka M, Kita K, Yokota H (2007) Ensiled green tea and black tea waste as protein supplement for goats. Options méditerr., Sér 74:165-169.

Kong W, Fu X, Wang L, Alhujaily A, Zhang J, Ma F, Zhang X, Yu H (2017) A novel and efficient fungal delignification strategy based on versatile peroxidase for lignocellulose bioconversion. Biotechnol. Biofuels 10:1-15. https://doi 10.1186/s13068-017-0906-x

Koskela S, Zha L, Wang S, Yan M, Zhou Q (2022) Hemicellulose content affects the properties of cellulose nanofibrils produced from softwood pulp fibres by LPMO. Green Chem. 24:7137-7147. https://doi: 10.1039/d2gc02237k

Laemmli UK (1970) Cleavage of structural proteins during the assembly of the head of bacteriophage T4. nature 227:680-685.

Lavery CB, MacInnis MC, MacDonald MJ, Williams JB, Spencer CA, Burke AA, Irwin DJ, D'Cunha GB (2010) Purification of peroxidase from horseradish (Armoracia rusticana) roots. J. Agric. Food Chem 58:8471-8476. https://doi.org/10.1021/jf100786h

Liu G, Han D, Yang S (2022) Combinations of mild chemical and bacterial pretreatment for improving enzymatic saccharification of corn stover. Biotechnol. Biotechnol. Equip. 36:598-608. https://doi.org/10.1080/13102818.2022.2112910

Liu J, Yang B, Chen C (2013) A novel membrane-based process to isolate peroxidase from horseradish roots: optimisation of operating parameters. Bioprocess Biosyst Eng 36:251-257. https://doi 10.1007/s00449-012-0781-6

Lotter D, le Maitre D (2014) Modelling the distribution of Aspalathus linearis (Rooibos tea): implications of climate change for livelihoods dependent on both cultivation and harvesting from the wild. Ecol. Evol 4:1209–1221. https://doi.org/10.1002/ece3.985

Mafa MS, Malgas S, Bhattacharya A, Rashamuse K, Pletschke BI (2020) The effects of alkaline pretreatment on agricultural biomasses (corn cob and sweet sorghum bagasse) and their hydrolysis by a termite-derived enzyme cocktail. Agronomy 10:1211. https://doi:10.3390/agronomy10081211

Mafa MS, Malgas S, Pletschke BI (2021b) Feruloyl esterase (FAE-1) sourced from a termite hindgut and GH10 xylanases synergy improves degradation of arabinoxylan. AMB Express 11:1-9. https://doi.org/10.1186/s13568-021-01180-1

Mafa MS, Malgas S, Rashamuse K, Pletschke BI (2020a) Delineating functional properties of a cello-oligosaccharide and β-glucan specific cellobiohydrolase (GH5_38): Its synergism with Cel6A and Cel7A for β-(1, 3) -(1, 4)-glucan degradation. Carbohydr. Res. 495:108081. https://doi.org/10.1016/j.carres.2020.108081

Mafa MS, Pletschke BI, Malgas S (2021a) Defining the frontier of synergism between cellulolytic enzymes for improved hydrolysis of lignocellulosic feedstocks. Catalysts 11 :1343. https://doi.org/10.3390/catal11111343

Malgas S, Mafa MS, Mkabayi L, Pletschke BI (2019) A mini review of xylanolytic enzymes with regards to their synergistic interactions during hetero-xylan degradation. World J. Microbiol. Biotechnol 35:1-13. https://doi.org/10.1007/s11274-019-2765-z

Malhotra M, Suman SK (2021) Laccase-mediated delignification and detoxification of lignocellulosic biomass: removing obstacles in energy generation. Environ.Sci.Pollut.Res 28:58929-58944. https://doi.org/10.1007/s11356-021-13283-0

Meier KK, Jones SM, Kaper T, Hansson H, Koetsier MJ, Karkehabadi S, Solomon EI, Sandgren M, Kelemen B (2017) Oxygen activation by Cu LPMOs in recalcitrant carbohydrate polysaccharide conversion to monomer sugars. Chem. Rev 118:2593-2635. https://doi.org/10.1021/acs.chemrev.7b00421

Min K, Kim YH, Kim J, Kim Y, Gong G, Um Y (2022). Effect of manganese peroxidase on the decomposition of cellulosic component: direct cellulolytic activity and synergistic effect with cellulase. Bioresour. Technol. 343:126138. https://doi.org/10.1016/j.biortech.2021.126138

Miranda MIV, Cascone O (1995). Horseradish peroxidase extraction and purification by aqueous two-phase partition. Appl. Biochem. Biotechnol 53:147-154. https://doi.org/10.1007/BF02788604

Mnich E, Bjarnholt N, Eudes A, Harholt J, Holland C, Jorgensen B, Larsen FH, Liu Manat R, Meyer AS, Mikkelsen JD (2020) Phenolic cross-links: building and de-constructing. Nat. Prod. Rep 37:919-961. https://doi: 10.1039/c9np00028c

Olsson L, Hahn-Hagerdal B (1996) Fermentation of lignocellulosic hydrolysates for ethanol production. Enzyme Microb. Technol. 18:312-331. https://doi.org/10.1016/0141-0229(95)00157-3

Park S, Baker JO, Himmel ME, Parilla PA, Johnson DK (2010) Cellulose crystallinity index: measurement techniques and their impact on interpreting cellulase performance. Biotechnol. Biofuels 3:1-10. https://doi.org/10.1186/1754-6834-3-10

Paul KG, Stigbrad T (1970) Four isoperoxidases from horseradish root. Acta Chem Scand 24:3607–3617.

Pengilly M, Joubert E, van Zyl WH, Botha A, Bloom M (2008) Enhancement of rooibos (Aspalathus linearis) aqueous extract and antioxidant yield with fungal enzymes. J. Agric. Food Chem 56:4047-4053. https://doi.org/10.1021/jf073095y

Rad AM, Ghourchian H, Moosavi-Movahedi AA, Hong J, Nazari K (2007) Spectrophotometric assay for horseradish peroxidase activity based on pyrocatechol–aniline coupling hydrogen donor. Anal. Biochem. 362:38-43. https://doi.org/10.1016/j.ab.2006.11.035

Chibbar RN, van Huystee RB (1984) Characterization of peroxidase in plant cells. Plant Physiol 75:956-958. https://doi.org/10.1104/pp.75.4.956

Sarika D, Kumar PSSA, Arshad S, Sukumaran MK (2015) Purification and evaluation of horseradish peroxidase activity. Int. j. curr. microbiol. appl. sci 4:367-375.

Silva-Sanzana C, Estevez JM, Blanco-Herrera F (2020) Influence of cell wall polymers and their modifying enzymes during plant–aphid interactions. J. Exp. Bot 71:3854-3864. https://doi.org/10.1093/jxb/erz550

Strother A, Fraser IM, Allahyari R, Tilton BE (1981) Metabolism of 8-aminoquinoline antimalarial agents. Bull. World Health Organ. 59:413.

Su Y, Yu X, Sun Y, Wang G, Chen H, Chen G (2018) Evaluation of screened lignin-degrading fungi for the biological pretreatment of corn stover. Sci. Rep 8:1-11. https://doi:10.1038/s41598-018-23626-6

Sulyman AO, Igunnu A, Malomo SO (2020) Isolation, purification, and characterization of cellulase produced by Aspergillus niger cultured on Arachis hypogaea shells. Heliyon, 6:e05668. https://doi.org/10.1016/j.heliyon.2020.e05668

Sun FH, Li J, Yuan YX, Yan ZY, Liu XF (2011) Effect of biological pretreatment with Trametes hirsuta yj9 on enzymatic hydrolysis of corn stover. Int. Biodeterior. Biodegradation 65:931-938. https://doi.org/10.1016/j.ibiod.2011.07.001

Thoresen M, Malgas S, Mafa MS, Pletschke BI (2021) Revisiting the phenomenon of cellulase action: Not all endo-and exo-cellulase interactions are synergistic. Catalysts 11:170. https://doi.org/10.3390/catal11020170

Van Dyk JS, Pletschke BI (2012) A review of lignocellulose bioconversion using enzymatic hydrolysis and synergistic cooperation between enzymes—factors affecting enzymes, conversion and synergy. Biotechnol. Adv. 30:1458-1480. https://doi:10.1016/j.biotechadv.2012.03.002

Walton PH, Davies GJ (2016) On the catalytic mechanisms of lytic polysaccharide monooxygenases. Curr Opin Chem Biol 31:195-207. http://dx.doi.org/10.1016/j.cbpa.2016.04.001

Zhang XZ, Zhang YHP (2013) Cellulases: characteristics, sources, production, and applications. Bioprocessing technologies in biorefinery for sustainable production of fuels, chemicals, and polymers (eds S.-T. Yang, H.A. El-Enshasy and N. Thongchul) 1:131-146. https://doi.org/10.1002/9781118642047.ch8

Supplementary data (Publication)

A

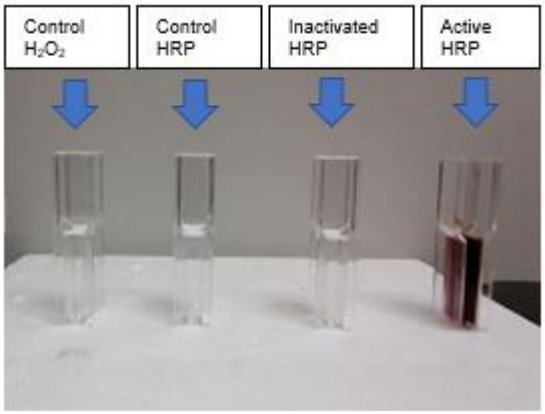

B

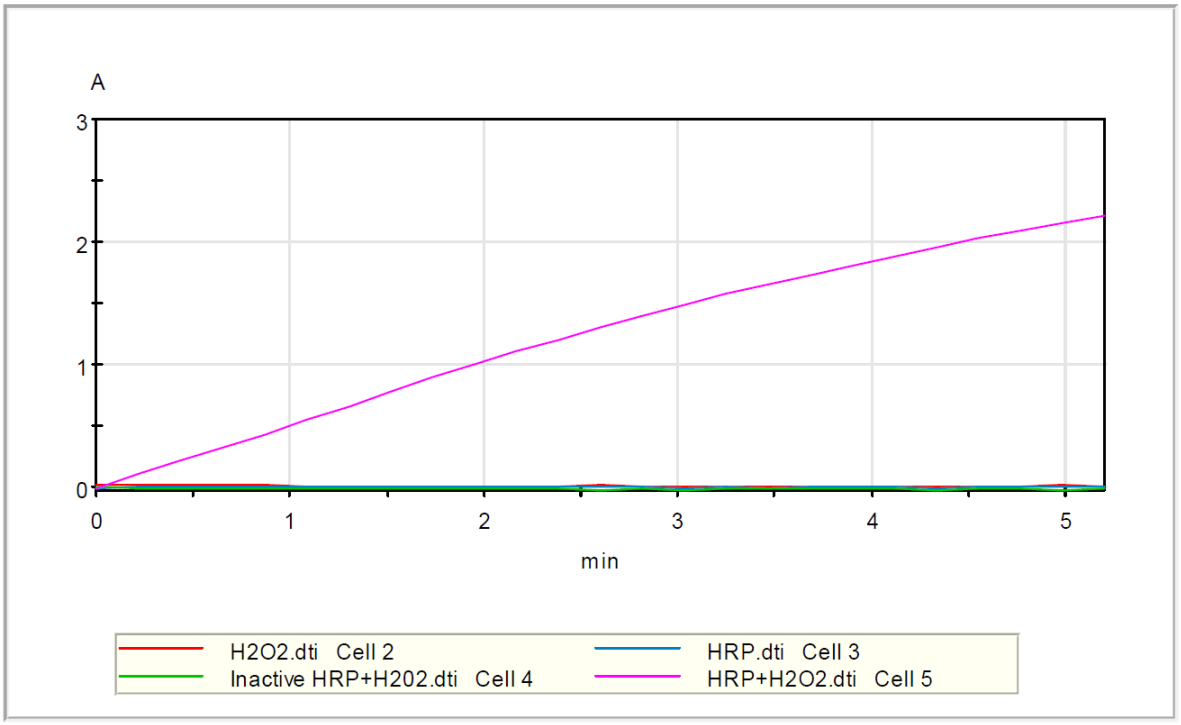

Red Line: Control H_2O_2 without HRP

Blue Line: Control HRP without H2O2

Green Line: Inactive HRP

Pink Line: active HRP

C

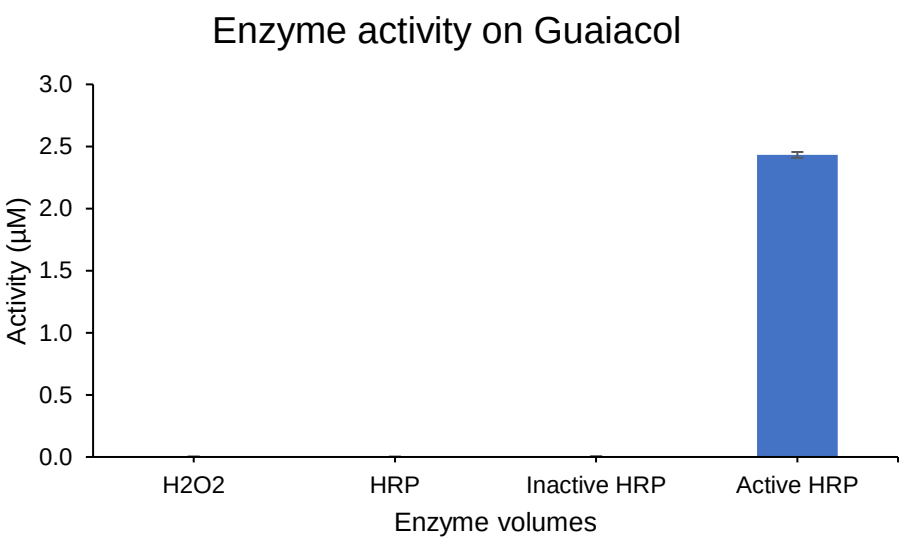

Fig.SI1 The activity of the HRP on the guaiacol substrate. A, B and C show the colour change due to the reaction, raw data from the kinetic read of the reaction, and the calculated HRP activity, respectively. The values represent the mean ± standard deviation. In C, The H_2O_2 is the control (H_2O_2 without enzyme); HRP is enzyme control without H_2O_2; inactive HRP+H_2O_2; and HRP activity.

A

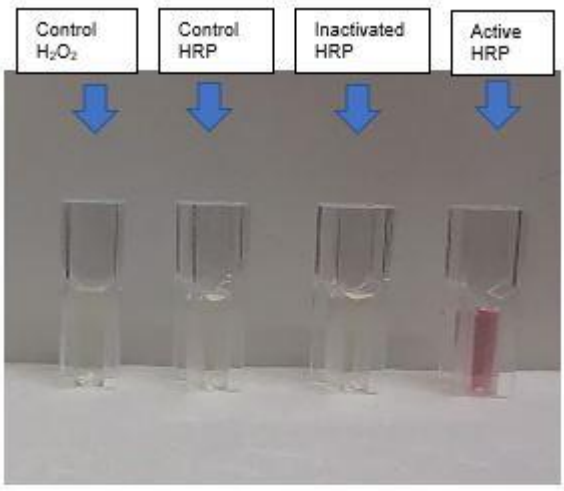

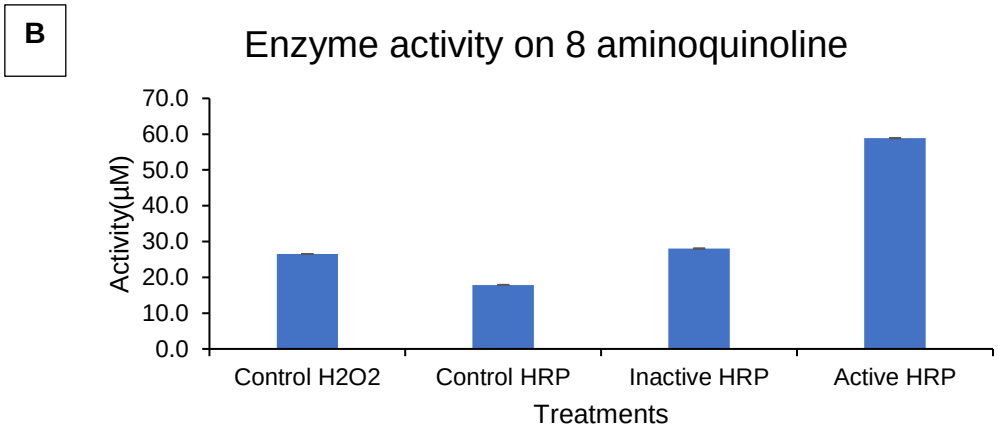

Fig.SI2 The activity of the HRP on the 8-aminoquinoline substrate. A and B show the color change due to the reaction, and the calculated HRP activity, respectively. The values represent the mean ± standard deviation. In B, the H_2O_2 is the control (H_2O_2 without enzyme); HRP is enzyme control without H_2O_2; inactive HRP+H_2O_2; and HRP activity.

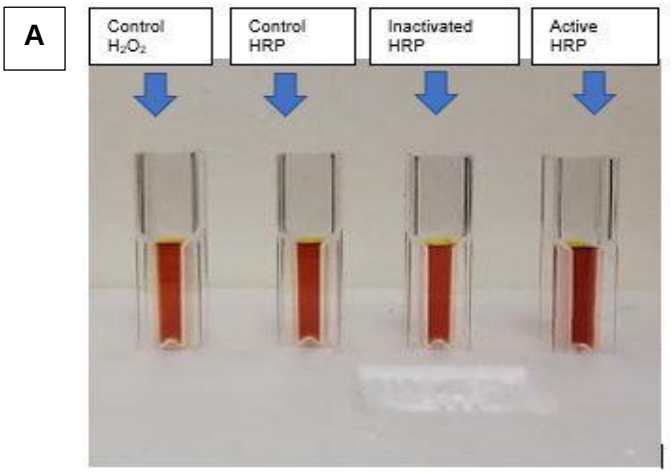

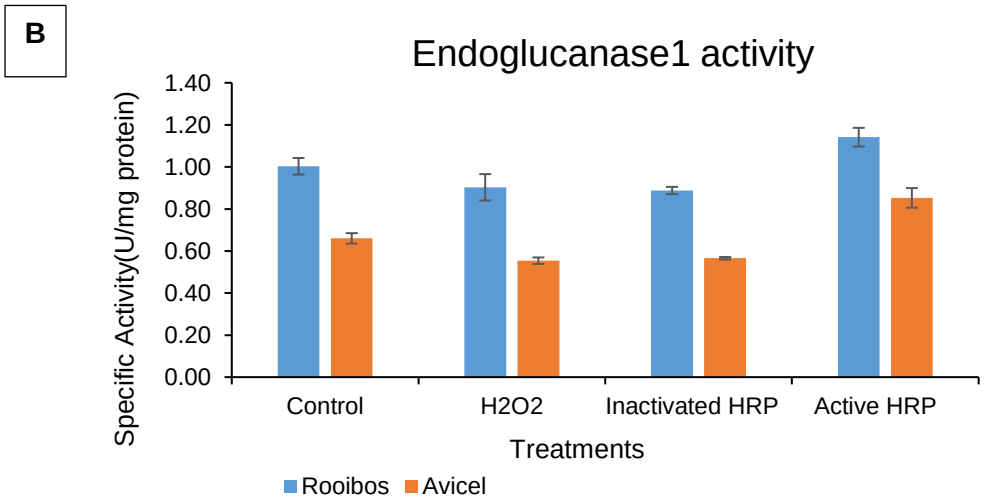

C

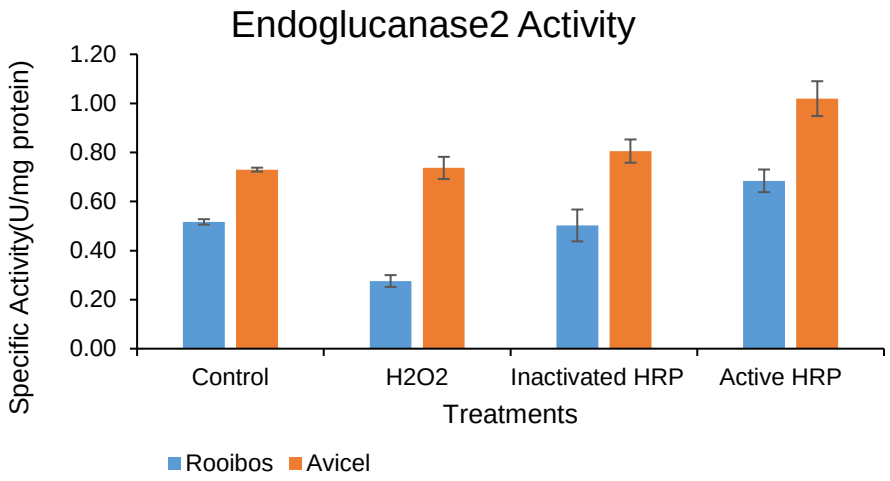

Fig.SI3 The effect of the HRP pretreatment on the endoglucanase (EG) activity. The HRP pretreated Avicel and rooibos or the controls (including the H2O2 and inactivated HRP) were catalysed by EG1 from *A. niger* and EG2 from *Aspergillus* sp. A shows the colour change due to EG releasing total reducing sugars, while A and B show the calculated activity of EG1 and EG2 on the biomass pretreated with controls or HRP enzymes. The values represent the mean ± standard deviation.

Chapter 4: Published article

Peroxidase application reduces microcrystalline cellulose recalcitrance towards cellulase hydrolysis in model cellulose substrates and rooibos biomass

Mamosela Marriam Mohotloane[1], Orbett Alexander[2], Vanthini Nelson Adoons[3], Brett Ivan Pletschke[4] and Mpho Stephen Mafa[1*]

1. Carbohydrates and Enzymology Laboratory (CHEM-LAB), Department of Plant Sciences, University of the Free State, P.O. Box 339, 9300 Bloemfontein, South Africa
2. Department of Chemistry, University of the Western Cape, Bellville, Cape Town, 7535, South Africa
3. Department of Physics, University of the Free State, QwaQwa Campus, Private Bag X 13, Phuthaditjhaba, 9866, South Africa
4. Enzyme Science Programme (ESP), Department of Biochemistry and Microbiology, Rhodes University, 6140 Makhanda, South Africa

*Corresponding author: Mpho S Mafa mafams@ufs.ac.za
https://doi.org/10.1016/j.carpta.2024.100426

Abstract

In our previous study we hypothesised that the HRP enzyme had microcrystalline cellulose modifying activity, which has not yet been explored. The current study investigated the effect of HRP pretreatment on microcrystalline cellulose substrates, Avicel and filter paper. Our SEM findings showed that HRP pretreatment resulted in the possible oxidation of the para-microcrystalline regions of Avicel, cracking, and opening of pores on the surface. On filter paper, HRP removed the para-microcrystalline regions exposing fibres. The peak height crystallinity index (CrI) method confirmed that HRP increased the CrI of Avicel from 49% to 54.19% and filter paper from 42% to 47%. The cellulose crystallite sizes increased from 45 to 47 nm at the 002 lattices in Avicel but decreased from 60.7 to 59.3 nm in filter paper. In addition, true endoglucanase displayed 1.15-fold increased activity on HRP-pretreated Avicel, but its activity was comparable to the control on pretreated filter paper. These findings showed that HRP pretreatment acted on cellulose II of Avicel, loosening crystalline cellulose to make

it accessible to enzymes. In conclusion, HRP pretreatment modified microcrystalline cellulose of model substrates, as well as rooibos biomass, resulting in a 95% yield of total reducing sugars at 25 mg enzyme loading/g biomass.

Keywords: cellulose; microcrystalline cellulose; horseradish peroxidase; biomass pretreatment; endoglucanase; enzyme cocktail

1. Introduction

Second-generation biofuels (2G) are produced from raw materials such as agricultural residues that can be utilised without affecting the food supply (Kumar, Bhardwaj, Agrawal, Chaturvedi, & Verma, 2020). However, it is challenging to produce biofuel from agricultural residues due to its complex lignocellulose structure, which interferes with the saccharification processes or combined saccharification and fermentation processes (Bagewadi, Mulla, & Ninnekar, 2017). The lignocellulosic biomass is composed of major components such as cellulose, hemicellulose, and lignin. The cellulose and hemicellulose components are made up of fermentable sugars, while lignin is a complex polymer made up of phenolic compounds. Lignin is well known for hindering CAZyme activities by forming a barrier that inhibits lignocellulosic biomass degradation through enzymatic application (Mnich *et al*., 2020). The hindrance of CAZyme activities directly influences the production of simple sugars, which can be fermented to produce biofuel (Bagewadi *et al.*, 2017).

The removal of lignin from biomass is essential for the successful production of bioethanol. Several chemical pretreatment methods have been developed for the removal of lignin. Most chemical pretreatment methods such as acids or alkaline biomass pretreatment successfully remove lignin from biomass. However, their disadvantages include expensive costs, corrosive nature, harm to the environment, and results in the production of inhibitory compounds that affect the production of fermentable sugars, (Badiei, Asim, Jahim, & Sopian, 2014, Bagewadi *et al.,* 2017, Behera, Arora, Nandhagopal, & Kumar, 2014, Harmsen, Huijgen, Bermudez, & Bakker, 2010, Limayem & Ricke, 2012). Physical and chemical methods such as evaporation, solvent extraction, ion exchange, and activated charcoal adsorption can be deployed to remove the toxic compounds; however, these processes are expensive and only add to the production costs (Bagewadi *et al.*, 2017*).* To align with Sustainable development goal number 12 regarding the production of green chemicals that have less negative effect on the environment, several studies have used enzymatic or microbial methods to de-lignify the biomass.

The use of biological pretreatments, such as ligninase, peroxidase, laccase, and carbohydrate esterase enzymes or microbes, is increasing and several researchers argue that it can be a preferable alternative to chemical pretreatment (Behera *et al.*, 2014, Kong *et al.*, 2017, Mohotloane, Alexander, Pletschke, & Mafa, 2023,). Biological pretreatments have attractive features, i.e. they are sustainable, environmentally friendly without producing inhibitory compounds, require low energy, and are highly selective, resulting in high yields of sugar products (Bagewadi *et al.*, 2017, Devi *et al.*, 2022, Sharma, Xu, & Qin, 2019, Wagner *et al.*, 2018). The current disadvantages of this method include a slow reaction process if microbes (fungi) are used for pretreatment, (Harmsen *et al.*, 2010, Hernández-Chaverri, Buenrostro-Figueroa, & Prado-Barragán, 2021, Limayem & Ricke, 2012), and growth conditions require careful optimization (Behera *et al.*, 2014, Menon and Rao, 2012). However, selected ligninase enzymes successfully reduced the lignin content from biomass, particularly lignin peroxidase (LiP: EC1.11.1.14), versatile peroxidase (VP: EC 1.11.1.16), manganese peroxidase (MnP: EC 1.11.1.13), and laccase (Lac: EC 1.10.3.2) (Behera *et al.*, 2014, Kersten, Kalyanaraman, Hammel, Reinhammar, & Kirk, 1990, Kong *et al.*, 2017, Kumar *et a.l*, 2020, Manavalan, Manavalan, & Heese, 2015, Mohotloane *et al.*, 2023).

Peroxidases are enzymes known to contain a heme group and are used in the catalysis of organic or inorganic compounds (Lavery *et al.*, 2010, Pandey, Awasthi, Singh, Tiwari, & Dwivedi, 2017, Veitch, 2004). As a widely used commercial enzyme, horseradish peroxidase (HRP) is produced in large quantities for use in clinical diagnostic tests (Veitch, 2004). Other applications include the treatment of wastewater by removing phenols and dyes, or the detoxification of foodstuffs and industrial effluents by removing peroxide (Lavery *et al.*, 2010). Additionally, our previous study demonstrated that HRP removed lignin from rooibos biomass and changed the structural properties of the rooibos biomass after pre-treatment (Mohotloane *et al.*, 2023). We confirmed that HRP pre-treatment decrystallised microcrystalline cellulose regions in rooibos samples, which resulted in a higher subsequent production of soluble sugars. These findings generated the following questions: can HRP pre-treatment remove lignin and decrystallise other woody biomass? Given that it decrystallised the microcrystalline cellulose of rooibos, does it have activity on cellulose? And if so, which mechanism does it employ to catalyse cellulose modification? To answer these questions, the model crystalline cellulose substrates, such as Avicel and filter paper, were used to delineate HRP action against cellulose.

Previous studies claimed that crystalline cellulose is recalcitrant to enzymatic activity, and that it generally inhibits endoglucanase activity (Mafa, Pletschke, & Malgas, 2021, Van Dyk & Pletschke, 2012). In contrast, para-crystalline (cellulose II) and amorphous cellulose are easily degraded by endoglucanases. Chemical pretreatments were used to reduce the recalcitrance of microcrystalline cellulose by exposing the amorphous cellulose or regenerating para-crystalline cellulose, resulting in increased enzyme activity (Mafa, Malgas, Rashamuse, & Pletschke, 2020a, Tian, Zhao, & Chen, 2018). The physicochemical changes of the biomass are measured using current technologies, which include scanning electron microscopy (SEM), Fourier Transform Infrared Spectroscopy (FTIR), and X-ray diffraction (XRD) (Khan *et al.*, 2018, Ling *et al.*, 2019, Vernon-Parry, 2000, Yu, Liu, Xu, Chen, & Gao, 2020, Zhou, Apkarian, Wang, & Joy, 2007).

Ling *et al.*, (2019) used various techniques, including SEM, FTIR, and XRD to show that ball milling has an effect on cotton cellulose by breaking the crystalline cellulose while exposing or regenerating the amorphous cellulose. Mohotloane *et al.*, (2023) used SEM to show the removal of lignin and topological surface changes in rooibos samples after HRP pretreatment. These findings were supported by FTIR and XRD analyses, which revealed that HRP pretreatment had an effect on the holocellulose region of the biomass and reduced its crystallinity index. The current study aims to elucidate how HRP pretreatment changes the physicochemical properties of microcrystalline cellulose substrates (Avicel and filter paper) and subsequently enhances the hydrolytic activity of CAZymes.

2. Materials and methods

2.1.Materials

Rooibos (*Aspalathus linearis*) samples were supplied by Rooibos Limited (Clanwilliam, Western Cape, South Africa). The horseradish root *(Armoracia rusticana)* was provided by Mr. Barry Newton and M.r John Parr from Yaxham farm situated in Tweespruit, Free State, South Africa. The commercial cellulase and xylanase enzymes, such as xylanase from *Aspergillus oryzae*, endoglucanase1 (EG1) from *Aspergillus niger*, endoglucanase2 (EG2) from *Aspergillus* sp., and β-glucosidase from *Aspergillus niger,* and commercial substrate Avicel were all purchased from Sigma (3050 spruce street, St Louis, MO, USA). The filter paper was purchased from Whatman International Limited (Springfield Mill, Maidstone, Kent, England). All the analytical chemicals used in the study were purchased from Sigma (3050 spruce street, St Louis, MO, USA) unless stated differently.

2.2.Effect of HRP on cellulose model substrates

2.2.1 Avicel and filter paper pretreatment with HRP

Filter paper was crushed using liquid nitrogen and an industrial blender (Mellerware: optima jug blender) to produce a biomass similar to cotton wool. The cellulose model substrates were pretreated with HRP to assess its effect on the cellulose region of the biomass. An amount of 2.5 g of Avicel and filter paper was dissolved in 50 mM sodium citrate buffer pH 4.5, and the reaction conditions were similar to the ones described by Mohotloane *et al*. (2023). HRP pretreated samples were dried, crushed, and stored in an airtight container for later use.

2.2.2 FTIR analysis of HPR pretreated cellulose substrate

FTIR spectroscopy was used to determine the chemical (functional group) changes of the HRP pretreated Avicel and filter paper samples. Peaks' functional groups were assigned, FTIR spectra were overlaid, and an absorbance mode was used to compare the changes between the control and pretreated samples, according to Mafa *et al*., (2020a).

2.2.3 XRD analysis of Avicel and filter paper

X-ray diffractograms were recorded with a Bruker D8 Advance diffractometer. All XRD measurements were performed using the reflectance technique. The incident X-ray radiation was the Cu Kα (λ = 1.54 Å) characteristic X-ray passing through a nickel (Ni) filter with a power of 40 kV and 40 mA. Both the air-scattering prevention slit and the divergence slit were 1°. The width of the detection slit was 0.6 mm. Counts were collected over a range of angles between 10^o and 80^o, with an increment of 0.01945^o for 1 hour. The X-ray source was a copper (Cu) target bombarded with electrons. All samples were fixed on the sample holder. Each crystalline peak was determined by the XRD deconvolution (curve fitting) method. Figure 4.1 shows the curve fitting of the Avicel control, which was used to measure the crystallinity index. In addition, the crystallinity index (CrI) was calculated using the Segal method by determining the ratio between the maximum peak height subtracting the minimum peak height (I_{002} - I_{AM}) and total maximum peak height (I_{002}) (Park *et al* 2010, Segal, Creely, Martin Jr, & Conrad, 1959).

$$CrI\% = \frac{(I002 - IAM)}{I002} x\ 100 \qquad (1)$$

Where CrI% is the percentage crystallinity index, I_{002} is the maximum peak height at 2θ = 22.8° and I_{AM} is the minimum peak height at 2θ = 18.5°

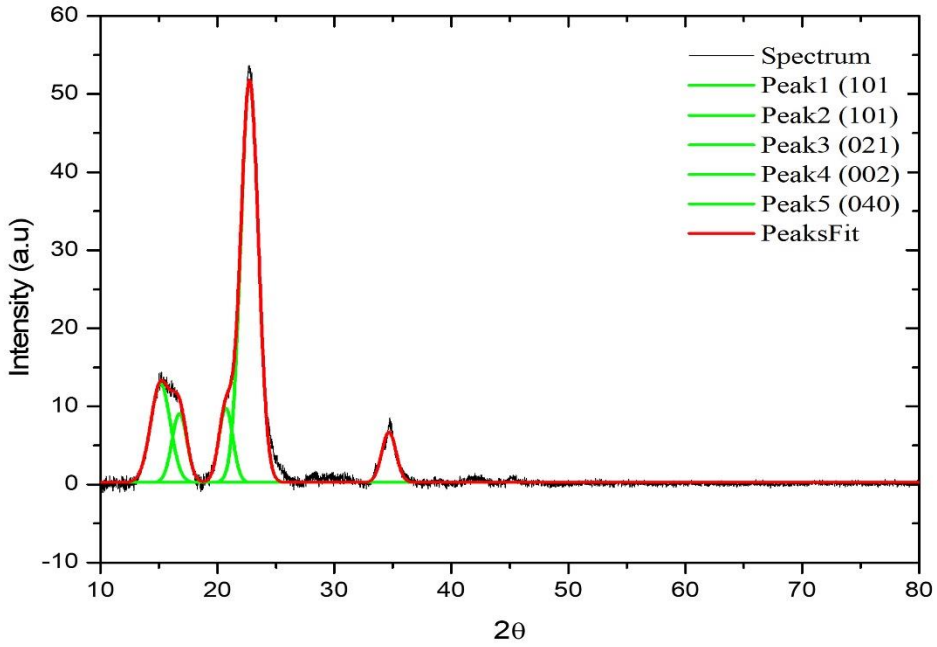

Figure 4.1: The Gaussian functions used to fit the X-ray diffraction data from an Avicel control.

The crystallite sizes of all samples were calculated based on the Scherrer equation (2) (Scherrer, 1918):

$$D = \frac{k\lambda}{\beta \cos\theta} \qquad (2)$$

where k is a constant whose value ranges between 0.9-0.99, λ is the incident an X-ray wavelength, β is full width at half maximum (FWHM) of diffraction peaks in radians and θ is the Bragg angle in degrees. The value of k used in equation (2) was 0.9.

The d-spacing values were calculated using Bragg's equation (3):

$n\lambda = 2d \sin\theta$ (3)

where n is an integer, λ is the wavelength of incident wavelength, d is the spacing between the planes in the atomic lattice, and θ is the angle between the incident ray and the scattering planes.

2.2.4 Topological studies of cellulose model substrates using SEM

SEM was used to determine the effect of HRP pretreatment on the topology of the microcrystalline cellulose model substrates Avicel and filter paper. Completely dry samples were mounted on aluminium pin stubs using double-sided carbon tape and coated with gold (2

μm) for conductivity using a Bio-Rad sputter coater (United Kingdom). Specimens were imaged at 5 kV using a JEOL JSM IT-200 SEM (Kyoto, Japan). The samples were analyzed with different magnifications ranging between 1000 and 10000x and photos were taken with a built-in camera to capture the results.

2.2.5 The effect of HRP pretreatment on Avicel and filter paper saccharification

Enzyme activity assays were conducted using EG1 (from *A. niger*) and EG2 (from *Aspergillus* sp.). The HRP pretreated Avicel and filter paper, and the untreated control were used as substrates. Each reaction consisted of about 1% (w/v) substrate (pretreated Avicel and filter paper dissolved in 50 mM sodium phosphate buffer pH 5) added to 0.1 mg/mL of EG1 and EG2 enzymes. All the reactions were incubated at 37ºC for about 0.5,1, 1.5, 2, and 24 hours. After the completion of the reactions, samples were centrifuged at 5 000 x *g*, and the total reducing sugars were quantified using the DNS method (Miller, 1959).

2.3.Improvement of the holocellulolytic enzyme cocktail

2.3.1 Formulation of the holocellulolytic enzyme cocktail

The most effective β-glucosidase concentration was determined using 1% (w/v) of pretreated Avicel and filter paper in 50 mM sodium citrate buffer pH 5, and the enzyme-loading combinations were 95, 90, 85, 80, 75, 70% for EG1, and 5, 10, 15, 20, 25, 30% for β-glucosidase, respectively. The enzyme concentration for all the combinations was kept constant at 2.5 μg/mL and incubation occurred for 24 hours at 37ºC. After the completion of the reactions, the total reducing sugars were detected using the DNS method.

The most effective concentration of β-glucosidase (i.e.,10%) was used in combination with EG1 and xylanase to formulate the holocellulolytic enzyme cocktail. The reaction consisted of 1% (w/v) HRP pretreated rooibos biomass in 50 mM sodium citrate buffer pH ,5 and the enzyme loading combinations between EG1, and xylanase were 100, 75, 50, 25, 0%, respectively. The enzyme combinations were kept at 2.5 μg/mL. The DNS method was used to measure the total reducing sugars produced.

2.3.2 HRP treated rooibos degradation with the holocellulolytic enzyme cocktail

The most effective holocellulolytic enzyme combination (50%:50%, EG1: xylanase) and (100%:0%, EG1: xylanase) were used to determine the required concentration (mg/g) to produce a high sugar yield percentage from HRP-treated biomass. The yield was determined

using 1% (w/v) HRP pretreated rooibos biomass in 50 mM sodium citrate buffer (pH 5) and using varying enzyme concentrations of 0.25, 0.5, 0.75, and 1 mg/mL, respectively. The reactions were incubated for 24 hours at 37ºC. All experiments were performed in triplicate. After the completion of the reactions, reducing sugars were detected using the DNS method.

3. Results

3.1 Determination of the topology using SEM

Our previous findings showed that HRP pretreatment not only removed lignin from fermented rooibos biomass, but that it also decreased the cellulose crystallinity (chapter 3). For a comprehensive understanding of this phenomenon, further studies were conducted to determine the effect of HRP pretreatment on the crystalline cellulose model substrates (Avicel and filter paper). SEM topological analysis showed that the Avicel control samples had a smooth surface layer of a fibre-like texture that was visible under 6000x magnification (Fig 4.2). However, the HRP-treated Avicel displayed a rough surface showing cracks and pores, with thick pieces of material that were seemingly being removed. The filter paper control had a smooth fibre-like surface, with a few thread-like structures visible on the surface layer. Interestingly, the HRP-treated filter paper exhibited a rough surface, showing the exposed microcrystalline cellulose fibre with pores between some fibres. These results show that the HRP had cellulase activity on the para-crystalline cellulose region, but that it could not hydrolyse the microcrystalline cellulose. The paracrystalline cellulose regions are referred to as cellulose II, while the crystalline cellulose was mostly cellulose I_{β}.

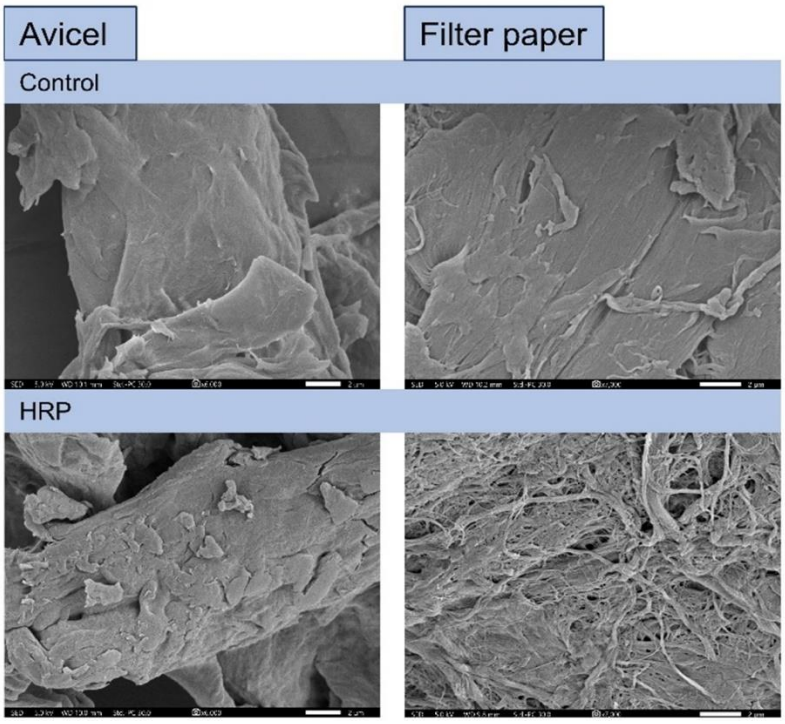

Figure 4.2: SEM topological analysis of Avicel and filter paper. The substrates pretreated with HRP (Avicel, bottom left and filter paper, bottom right images) were compared to the controls (Avicel, top left and filter paper, top right images). Avicel samples were analyzed at 6000-x magnification, while the filter paper samples were analyzed at 7000-x magnification; scale bar for all images is 2 μm.

3.2 FTIR analysis of the HRP pretreated cellulose model substrate.

FTIR analysis was used to determine the changes in the chemical functional groups of the untreated or pretreated Avicel and filter paper samples. The FTIR results confirmed the SEM findings by showing that HRP pretreatment modified the cellulose model substrates. The Avicel control showed a lower peak at 3330.82 cm^{-1} compared to the pretreated samples (Fig 4.3A). This peak corresponded to the presence of OH group in the sample, and it was broader in the microcrystalline cellulose-containing samples, because of the inter- and intra- hydrogen bonds that formed between the fibres containing OH groups. Interestingly, the same pattern was observed for the filter paper samples at peak 3330.82 cm^{-1}. The HRP pretreated samples displayed a significantly higher peak compared to the control (Fig 4.3B). Similar findings were observed at peak 1029.91 cm^{-1}, which represented the glycosidic bonds. The Avicel control had a lower peak, while the pretreated Avicel had a slight increase compared to the control at peak 1029.91 cm^{-1}. The HRP pretreated filter paper showed a substantial increase, compared to the control at the same peak. Thus, the SEM and FTIR findings suggest that the pretreatment

modified the structural and chemical properties of the two well-known cellulose model substrates.

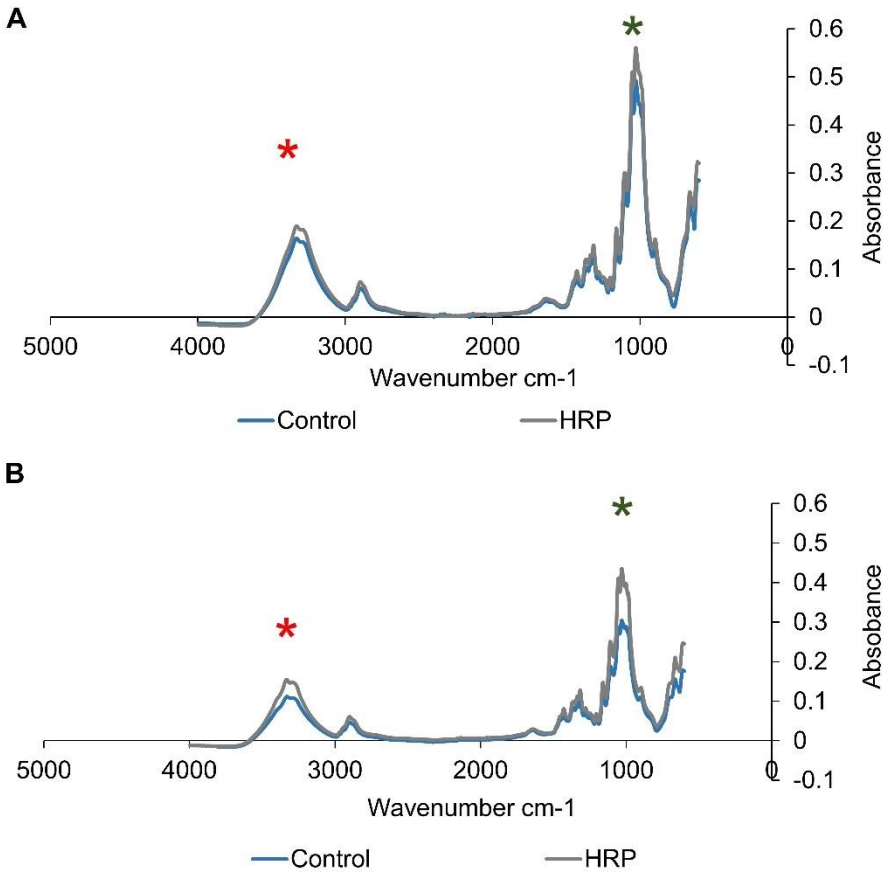

Figure 4.3: FTIR analysis of horseradish peroxidase (HRP) pretreated cellulose model substrates. The HRP treated Avicel (A) and filter paper (B) samples were compared to the controls by overlaying the spectra using the absorbance mode. Two regions of interest, the OH group, and glycosidic bonds regions, are represented by a red and green asterisk, respectively.

3.3 Crystallinity analysis of the HRP pretreated cellulose substrates

X-Ray diffraction (XRD) further supported the SEM and FTIR findings by showing that HRP pretreatment modified the crystallinity of the cellulose model substrates. Avicel and filter paper XRD diffractogram intensities showed clear differences between the HRP-treated and control. The pretreatment increased the peak intensity at the 101 and 002 lattice plane in the Avicel, compared to the control samples. The two lattice planes corresponded to cellulose II and cellulose Iβ, respectively. In the filter paper, the intensity values at the $10\bar{1}$ lattice plane were similar for the HRP treated samples and controls, but there was a significant increase in

the intensities of the pretreated samples, compared to the controls at the 002 lattice plane (Fig. 4.4A and 4.4B).

In addition, the peak height method showed that HRP pretreatment resulted in an increased crystallinity index (CrI) of about 54.19% and 47% in Avicel and filter paper, respectively, compared to a CrI of about 48.89 and 41.89% in the respective control samples (Table 4.1). It is worth noting that the crystallinity index determined with the deconvolution method showed a 1% change for the CrI of the Avicel samples. The control displayed a CrI of 71%, while the HRP pretreatment sample had a CrI of about 72%. The filter paper showed no change between the control and HRP pretreated samples, which had a CrI of about 93% for both samples.

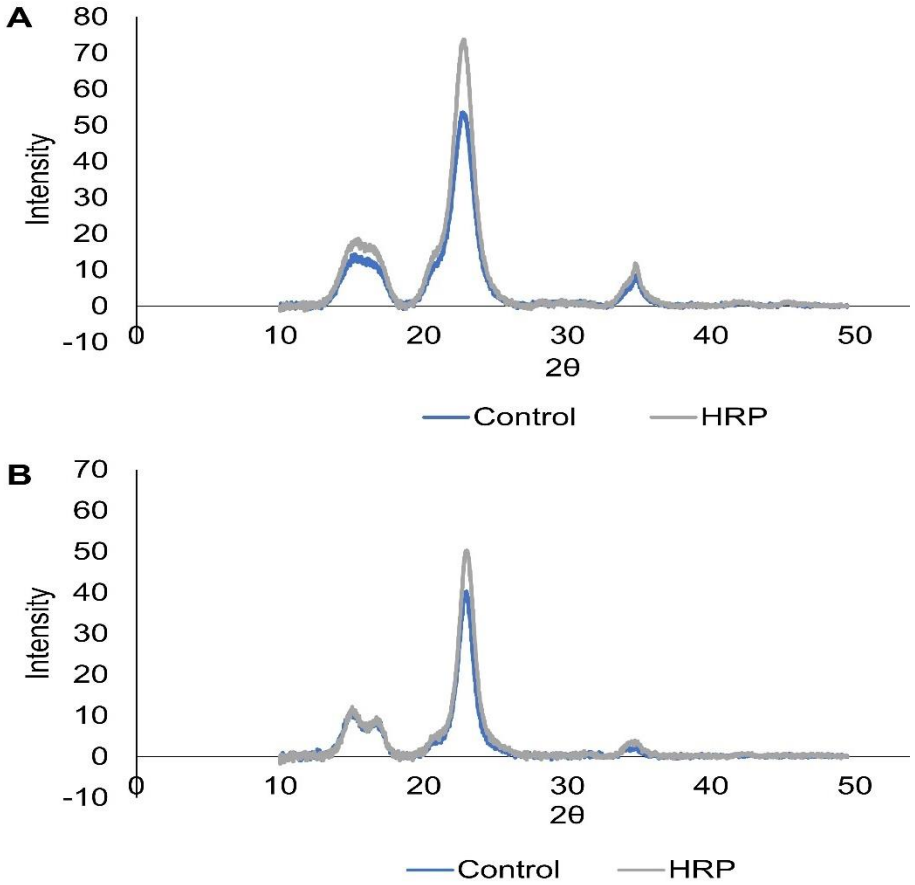

Figure 4.4: XRD diffractogram of the HRP-pretreatment cellulose model substrate Avicel (A) and filter paper (B). The spectra were overlaid to compare the differences between HRP-treated samples and the controls.

The determination of the crystallinity is not limited to the crystallinity index; there are other indicators to consider when determining cellulose crystallinity, such as crystallite sizes. The crystallite size was determined using the Scherrer equation and our results showed that the

HRP pretreatment has an effect on the crystallite sizes (Table 4.1). The HRP pretreated Avicel had reduced crystallite sizes (39.6 and 55.5 nm) at the 101 and 040 lattice planes compared to 40.6 and 58.1 nm in the controls. In contrast, the crystallite sizes of pretreated Avicel at the 021 and 002 lattice planes increased to 58.8 and 47.3 nm, compared to 57.5 and 45.7 nm in the controls. Interestingly, the crystallite size at peak $10\bar{1}$ showed no change in both the control and HRP pretreated Avicel and filter paper.

Additionally, the crystallite sizes at 002 and 040 lattices decreased to 59.3 and 62.9 nm in the HRP pretreated filter paper compared to 60.7 and 63.4 nm in the control, respectively. In contrast, the crystallite sizes at 101 and 021 lattices increased to 55.9 and 53.1 nm in HRP pretreated filter paper compared to 51.8 and 49.4 nm in the controls. The modification of the crystallite sizes further supports the hypothesis that the HRP pretreatment modified the physicochemical properties of the cellulose model substrates. The decreased d-spacing at the 101 and 002 lattice planes in the HRP pretreated filter paper samples (compared to the controls) confirmed the change in the structure of the biomass at the molecular level (Table 4.2).

Table 4.1: Mean crystallite size (C.S) calculated, computed (deconvolution) crystallinity indexing, and peak height crystallinity indexing for Avicel and filter paper samples

Miller Indices	**101**	**$10\bar{1}$**	**021**	**002**	**040**	**Peak height [CrI (%)]**	**deconvolution [CrI (%)]**
Sample	**C.S (Å)**	**C.S (Å)**	**C.S (Å)**	**C.S (Å)**	**C.S (Å)**		
Avicel (Control)	40.6	53.5	57.5	45.7	58.1	48.89	71
Avicel (HRP)	**39.6**	53.5	**58.8**	**47.3**	**55.5**	**54.19**	**72**
F. Paper (Control)	51.8	66.1	49.4	60.7	63.4	41.89	93
F. Paper (HRP)	**55.9**	66.1	**53.1**	**59.3**	**62.9**	**47.00**	93

1 nm is equal to 1 Å

Table 4.2: Position of maximum (2θ), *d*-spacing, and full width at half maximum intensity (FWHM) for Avicel and filter paper samples

Miller Indices	**101**		**$10\bar{1}$**		**021**		**002**		**040**	
Sample	**2θ**	**FWHM**	**2θ**	**FWHM**	**2θ**	**FWHM**	**2θ**	**FWHM**	**2θ**	**FWHM**
Avicel (Control)	15.135	1.972	16.753	1.499	20.724	1.404	22.751	1.772	34.665	1.433
***d*-spacing (nm)**	0.584		0.528		0.428		0.390		0.258	

Avicel (HRP)	15.122	**2.024**	16.776	**1.501**	20.738	**1.373**	22.756	**1.713**	34.632	**1.499**
***d*-spacing (nm)**	**0.585**		0.528		**0.427**		0.390		0.258	
F. Paper (Control)	15.034	1.545	16.726	1.215	21.138	1.634	22.933	1.335	34.469	1.311
***d*-spacing (nm)**	0,589		0,529		0,420		0,387		0,259	
F. Paper (HRP)	15.087	**1.433**	16.731	1.215	21.105	**1.521**	22.993	**1.366**	34.565	**1.322**
***d*-spacing (nm)**	**0.587**		0.529		**0.421**		**0.386**		0.259	

Note: C.S = Crystal size, FWHM = Full Width Half Maximum, 2θ = 2Theta

3.4 Endoglucanase activity on HRP treated cellulose model substrates

The SEM, FTIR, and XRD findings indicated that the HRP pretreatment modified the structural and chemical properties of microcrystalline cellulose model substrates. To test if these modifications were essential for higher enzymatic activity, endoglucanase 1 (EG1: from *A. niger*) and endoglucanase 2 (EG2: from *Aspergillus* sp.) were used to hydrolyse HRP pretreat Avicel and filter paper. Our findings showed that EG1 and EG2 activities significantly increased in the HRP pretreated Avicel and filter paper samples. EG1 showed a steadily increasing activity over time in both the control and the HRP pretreated Avicel samples (Fig 4.5A). The highest activity for this enzyme was recorded at 24 hours incubation, with an increase of 10% activity in the HRP pretreated Avicel, compared to the control. The second endoglucanase, EG2, showed little to no change over time with a sharp increase at 24 hours incubation in both the control and HRP pretreated Avicel samples (Fig 4.5B). EG2 had an increase of 20% activity in the HRP pretreated Avicel compared to the control. In contrast, the endoglucanase activities (EG1 and EG2) were comparable between HRP treated filter paper and the controls. The findings suggest that the filter paper was a much crystalline substrate compared to the Avicel (Fig 4.5C and D).

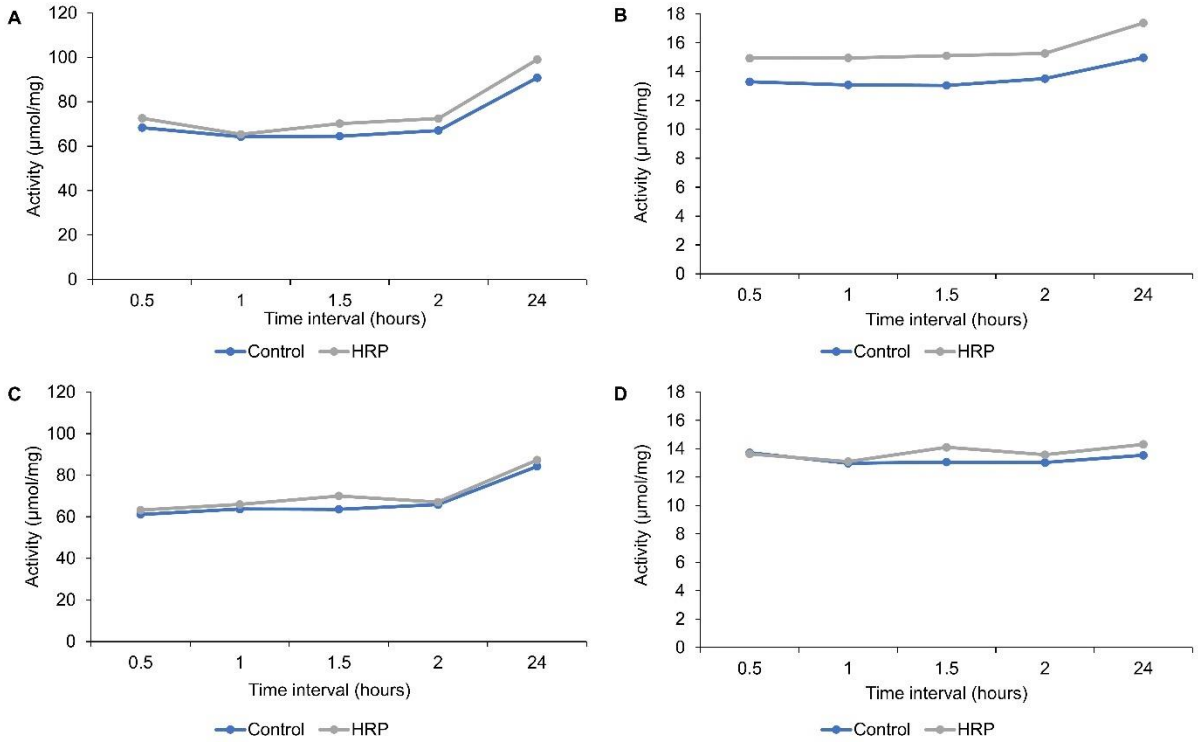

Figure 4.5: The endoglucanase-1 (EG1) and endoglucanase-2 (EG2) activity assays on HRP pretreated microcrystalline cellulose substrates (Avicel and filter paper). A and B represent EG1 and EG2 activities acting on Avicel, respectively, while C and D represent EG1 and EG2 activities on pretreated filter paper, respectively. Controls were used to confirm the effect of HRP treatment on the cellulose model substrates. The values represent the means ± standard deviation. Activity is equivalent to total reducing sugars produced EG during substrate hydrolysis (in umol/mg). One-way ANOVA ($p < 0.05$) was used to test for significant differences between HRP-treated and untreated Avicel and filter paper.

3.5 Cellulase synergy

The most effective β-glucosidase concentration was determined using varying combinations of EG1 and β-glucosidase on HRP pretreated Avicel (Fig 4.6A) and filter paper (Fig 4.6B), including the controls. The β-glucosidase showed a higher enzyme activity at 10% (v/v) enzyme loading when it hydrolysed the HRP treated Avicel; a slightly lower enzyme activity was observed at a loading of 20% β-glucosidase. In general, it is important to note that the addition of β-glucosidase to the reactions improved the enzymes activities of the treated Avicel substrate, compared to the controls. The HRP pretreated filter paper displayed significantly reduced enzyme activity compared to the controls (Fig 4.6B). However, for the control samples, the 10% β-glucosidase enzyme loading displayed the highest activity. In summary,

the findings above indicated that a 90% EG1/10% β-glucosidase enzyme loading was the optimal enzyme combination for hydrolysis on the cellulose model substrates.

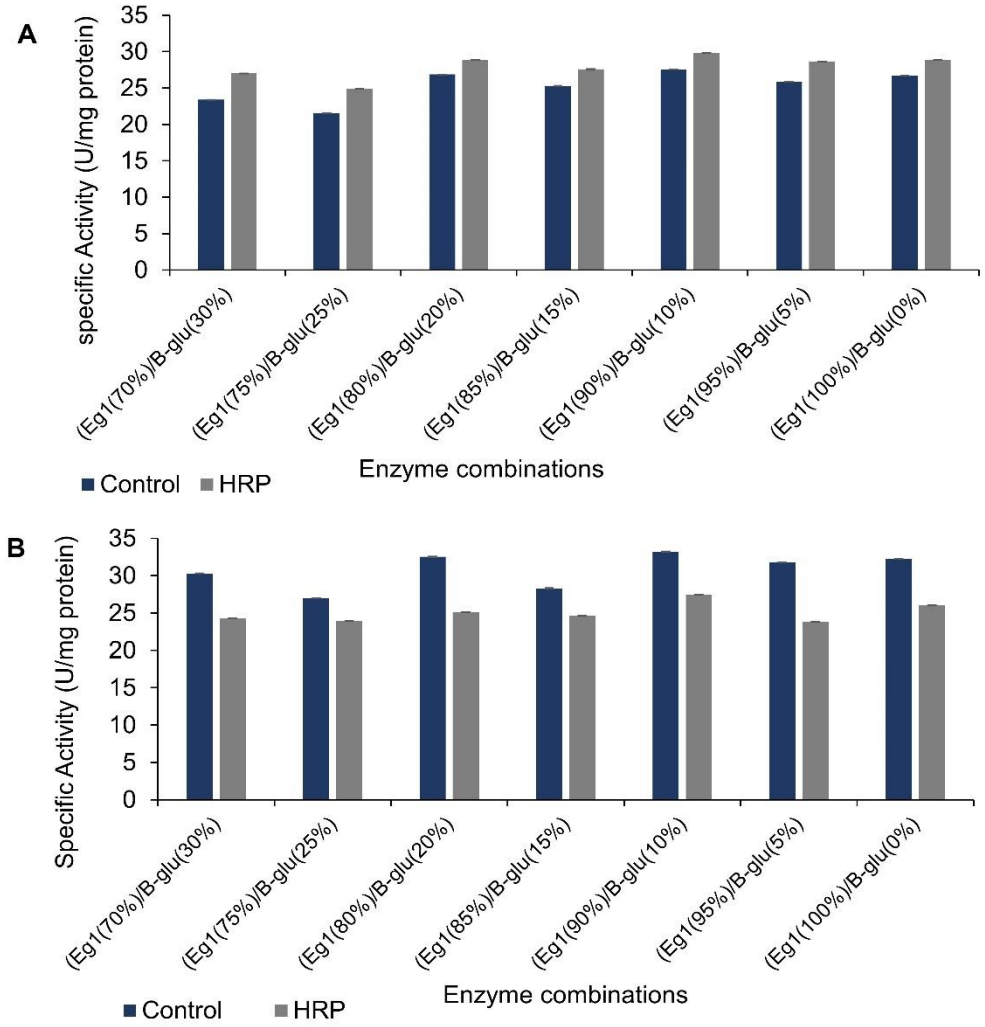

Figure 4.6: The synergy between EG1 and β-glucosidase tested using cellulose model substrates. The enzyme activity was determined using HRP-treated Avicel (A) and filter paper (B), and their controls. The U represent units, which is equal to μmol.h^{-1}.

3.6 Holocellulolytic enzyme formulation

After confirming the most effective β-glucosidase enzyme loading in combination with the EG1, we attempted to formulate the holocellulolytic enzyme cocktail that could improve the yield of soluble sugars from the HRP pretreated complex substrate (rooibos biomass). The results in Fig 4.7 showed that the most effective combinations were 50% EG1/50% xylanase, and 100% EG1/0% xylanase, which displayed 1.4-fold and 1.5-fold higher specific activities,

respectively, compared to their controls. In addition, the HRP-pretreated fermented rooibos was hydrolysed better than the controls, suggesting that β-glucosidase and EG1 or xylanase acted synergistically on the pretreated substrate.

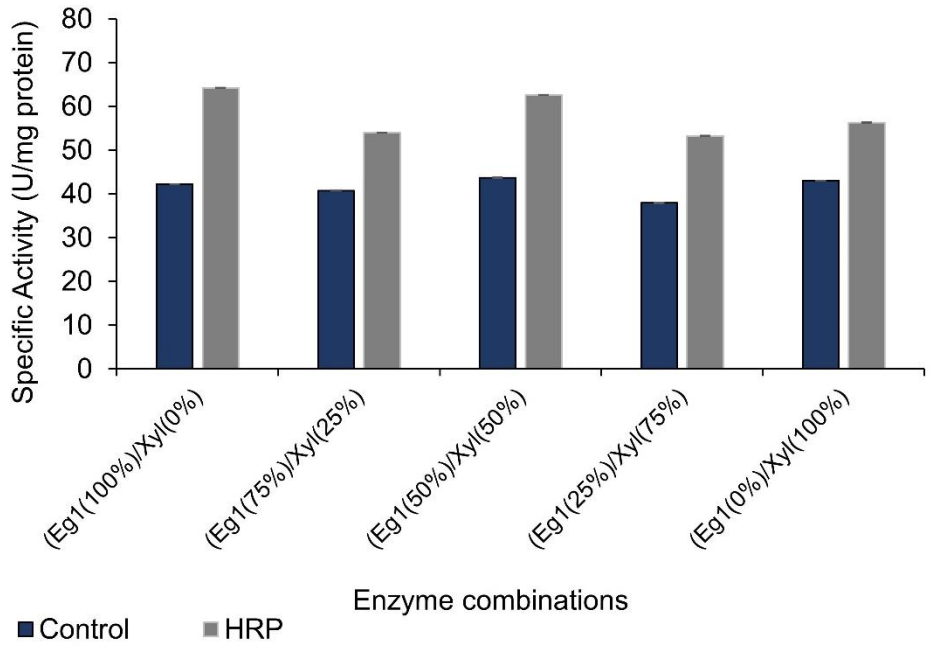

Figure 4.7: Formulations of the holocellulolytic enzyme cocktail using different combinations of endoglucanase 1 (EG1) and xylanase on fermented rooibos substrate. β-glucosidase was dosed at 10 % enzyme load relative to the concentrations of EG1 and xylanase. The values represent the means ± standard deviation. The U represent units, which is equal to μmol.h− 1 . One-way ANOVA ($p < 0.05$) was used to test for significant differences between HRP-treated and untreated Avicel and filter paper.

3.7 Producing soluble sugars from HRP treated biomass.

Quantification of the total amounts of soluble sugars was conducted using 1% (w/v) of the HRP-pretreated rooibos biomass. A 50% EG1/50% xylanase combination, and 100% EG1 (mixed with 10% β-glucosidase enzyme loading) were used in the production of soluble sugars, as they displayed high activity in the holocellulolytic enzyme formulation (Fig 4.7). Interestingly, the results indicated that the soluble sugar yield decreased as the enzyme loading concentration increased (Fig 4.8). The substrate hydrolysis with 100% EG1 (i.e. with no xylanase) showed a sharp decrease in the yield (Fig 4.8A), while 50% EG1 and 50% xylanase showed a steady decline until 75 mg/g biomass. Above 75 mg/g biomass concentration, the 100% EG1 enzyme rapidly lost activity and there was, consequently, a decline in yield at 100

mg/g. However, the 50% EG1 and 50% xylanase combinations only lost 11% in total reducing sugars yield at the same concentration. The 25 mg/g biomass was the effective concentration required to achieve 99% (Fig 4.8A) and 96% (Fig 4.8B) of total reducing sugar production.

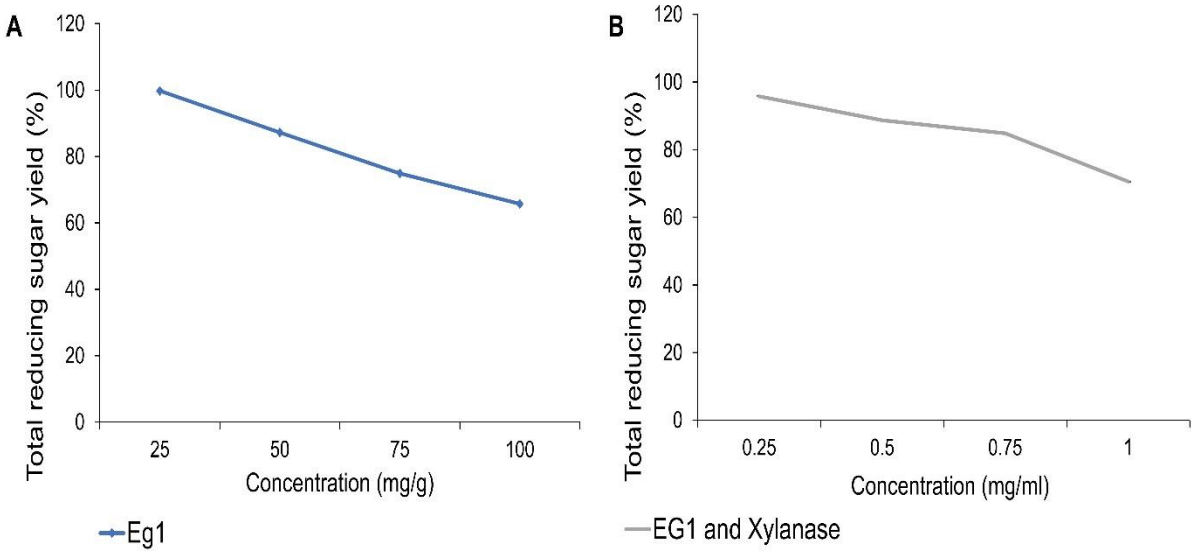

Figure 4.8: The application of the formulated cellulase and holocellulolytic enzyme cocktails using the most effective combinations, 100% endoglucanase 1 (EG1) (A), and 50% endoglucanase 1 (EG1)/50% Xylanase (B) on HRP pretreated fermented rooibos substrate.

4. Discussion

Agricultural biomass pre-treatment is vital for removing or modifying lignin, increasing enzymes accessibility to the biomass, and enhancing hydrolysis. In addition, pre-treatment reduces biomass crystallinity, which renders samples recalcitrant to enzyme hydrolysis (Mafa *et al.*, 2020b, Van Dyk & Pletschke, 2012). Therefore, the higher activity of the cellulases on the crystalline cellulose could be attributed to structural and chemical modification, which increases enzyme accessibility to the biomass (Van Dyk & Pletschke, 2012). Our previous study demonstrated that HRP pretreatment removed lignin and significantly decreased the crystallinity of rooibos biomass (Mohotloane et al., 2023). These observations led us to ask the following questions: Does HRP reduce the crystallinity of all the plant biomass samples, or is it specific to rooibos? Could the changes in the cellulose regions improve enzymatic activity on HRP-pretreated biomass? To understand the effects of HRP pretreatment on crystalline cellulose region of the biomass, we pretreated the cellulose model substrates, Avicel and filter paper.

The HRP pretreatment improved EG1 hydrolysis on Avicel and filter paper, as it had a higher activity compared to the control. Similarly, the true endoglucanase EG2 showed a lower enzyme activity on the Avicel and filter paper controls. However, the HRP pretreatment improved EG2 activity on both substrates. The EGs showed much higher activity on the Avicel compared to filter paper; suggesting that the pretreatment made Avicel a less crystalline biomass. Mohotloane *et al*., (2023) demonstrated that EG1 is a multifunctional enzyme because it was able to hydrolyse both cellulosic and hemicellulosic substrates. However, EG2 is a true endoglucanase that showed activity on the amorphous cellulose substrate (CMC) and had residual activity on the microcrystalline cellulose and hemicellulose substrates. Other oxidative enzymes such as lytic polysaccharide monooxygenases (LPMOs) act on the recalcitrant microcrystalline cellulose or chitin regions, increasing biomass accessibility for the GH enzymes (Chang et al., 2022, Levasseur, Drula, Lombard, Coutinho, & Henrissat, 2013., Min et al., 2022). In addition, LPMO application increased endoglucanase activity by minimizing the recalcitrant nature of microcrystalline cellulose, resulting in the improved production of soluble sugars (Monclaro & Ferreira Filho, 2017). Our findings showed that HRP pretreatment of the crystalline cellulose substrate Avicel increased surface area and enzyme accessibility to the biomass, resulting in improved endoglucanase activities.

SEM analysis showed that the HRP pretreatment structurally modified the crystalline cellulose substrates. The pretreated Avicel developed a rough surface layer, showing cracks and pores compared to the smooth surface observed in the control sample. The cracks and pores indicate that the HRP enzyme increased substrate accessibility, which resulted in higher hydrolytic efficiency for the endoglucanase enzymes. Similarly, HRP pretreatment removed the amorphous and paracrystalline cellulose from the filter paper samples, resulting in more exposed microcrystalline cellulose fibres compared to the control sample, which had a smooth surface. Min et al. (2022) also demonstrated that Avicel pretreatment with manganese peroxidase (MnP) had peeling effects on the surface of biomass that exposed cracks on the biomass. These observations support our findings, except that the filter paper results suggested that HRP pretreatment acted mostly on cellulose II (paracrystalline cellulose), exposing cellulose I_{β} (microcrystalline cellulose).

Generally, the FTIR peak reduction at 3000–3500 cm^{-1} implied that the crystalline region had been modified. The peak is assigned to OH groups and for the microcrystalline cellulose sample a broad peak indicated the presence of inter- and intra- hydrogen bonds between fibres. Several

studies have shown that the decreased IR absorbance values (due to biomass pretreatment) in this region (3000-3500 cm^{-1}) are associated with the regenerated amorphous cellulose, which resulted in increased cellulase activity (Mafa *et al.*, 2020b). Similarly, Ling *et al.* (2019) showed that the process of ball milling over time altered the bands (at 3000-3500 cm^{-1}) associated with cellulose Iα and Iβ, which suggested a modification of the crystalline structure, resulting in an increase in the amorphous region. In contrast, the HRP pretreatment increased the peak at 3330.82 cm^{-1} in Avicel and filter paper. These findings suggest that HRP was oxidising and removing the cellulose II (para-crystalline) regions and exposed the cellulose I_β (microcrystalline cellulose), supporting the SEM results obtained. However, the chemical and structural modification did not hinder enzyme hydrolysis by the endoglucanases.

The SEM and FTIR findings were confirmed by the XRD results, which showed that HRP pretreatment increased CrI in Avicel and filter paper. The commonly used peak height method by Segal *et al*. (1959) showed about a 5% increase in CrI of the pretreated samples, compared to the controls of Avicel and filter paper. Although peak height is the most commonly used method for determining CrI, a few studies caution against using CrI as a measure of biomass crystallinity, because it does not account for changes in the peak morphology/area, crystallite sizes, and d-spacing (Ju, Bowden, Brown, and Zhang, 2015, Nam, French, Condon, and Concha, 2016, Park et al., 2010). A study by Bommarius et al. (2008) also indicated that an increase in crystallinity index during Avicel pretreatment with ammonia, alkaline, and organo-solvent did not reduce cellulase activity. These observations from other studies and our findings with Avicel and filter paper CrI prompted us to determine other factors, such as crystallite size and d-spacing, to further understand the effect of HRP pretreatment at the molecular level.

Our findings show that there were significant changes at the molecular level after the HRP pretreatment of Avicel and filter paper. For Avicel there was a 1 nm decrease in the crystallite size and an increase of 0.001 nm d-spacing at the 101 lattice plane. These results suggest that HRP pretreatment acts on the cellulose crystallites and breaks down the intermolecular hydrogen bonds, leading to increased distance between the crystallites (Table 1 and 2). In addition, crystallite size at the 002 lattice-plane increased by about 1.6 nm, but there was no change in the d-spacing between the crystallites. We propose that these changes at the molecular level are directly correlated to the improved hydrolysis of HRP pre-treated Avicel by the endoglucanases.

For HRP pretreated filter paper, there was a significant (4 nm) increase in the crystallite size and 0.002 nm d-spacing at the 101 lattice plane (Tables 1 and 2). However, at the 002 lattices there was about a 1 nm decrease in the crystallite size and 0.001 nm in d-spacing. The 101 lattice plane corresponds to the presence of cellulose II, while 002 represents cellulose I allomorphs. The increased crystallite size of cellulose II confirmed our hypothesis that suggested that the HRP enzyme showed higher activity on the cellulose II allomorph and exposes crystalline cellulose I_{β}. These imply that there was an increase in the microcrystalline fibres in filter paper samples, leading to less endoglucanase biomass accessibility and activity. In addition, several studies have shown that samples which have large crystallites will have two distinct peaks at 101 and $10\bar{1}$ lattice planes, while samples with small crystallites have a broad peak combining the two peaks of 101 and $10\bar{1}$ (Garvey, Parker, & Simon, 2005, Ju et al., 2015, Ling, Chen, Zhang, & Xu, 2017). Ju et al. (2015) also argued that the increment in d-spacing and crystallite sizes showed that the biomass crystals were loosening while the decrease in d-spacing and crystallite size indicated a more compared biomass. These observations confirmed that HRP pretreatment was essential for changing the loosening Avicel structures, while it compacted the biomass of the filter paper.

After determining the effects of HRP pretreatment on the physicochemical properties of the cellulose model substrates, we formulated an enzyme cocktail by including 10% (v/v) β-glucosidase and increasing enzyme loading to improve the production of total reducing sugars. β-glucosidase is known as a cellulase enzyme that plays a role in degrading cellobiose, which is known to inhibit endoglucanase and exoglucanase activities (Zhang & Zhang, 2013). The previously formulated enzyme cocktail produced 10% total reducing sugars in the HRP pretreated rooibos (Mohotloane *et al.*, 2023), which prompted the need to formulate an enzyme cocktail with improved sugar production. The holocellulolytic enzyme cocktail resulted in two effective combinations that were used at varying enzyme concentrations to quantify the percentage yield produced per gram of biomass. The enzyme cocktails effectivity produced over 95% total reducing sugars at a lower concentration of 25 mg/g biomass, validating the efficacy of the HRP pretreatment in structurally and chemically modifying the biomass. Mafa *et al.* (2020b) demonstrated that NaOH pretreatment effectivity removed lignin from corncob and sweet sorghum bagasse, which improved the hydrolytic activity of the formulated enzyme cocktail obtained from termite metagenome. Similarly, Malgas *et al.* (2017) formulated a

holocellulolytic enzyme with superior hydrolytic efficiency on pretreated hardwoods, which resulted in high sugar conversion and yield.

5. Conclusion

Horseradish peroxidase (HRP) modifies the structural and chemical properties of microcrystalline cellulose. SEM analysis showed that the HRP had a peeling effect on Avicel, exposing cracks and pores, while it removed the amorphous and para-crystalline cellulose from filter paper, exposing the crystalline fibres (cellulose I). In addition, the FTIR and XRD analysis confirmed that after pretreatment, Avicel and filter paper increased in crystallinity index, supporting the hypothesis that the HRP enzymes oxidized and reduced cellulose II and exposed cellulose I_{β}. This claim was supported by the HRP pretreatment's ability to increase d-spacing and crystallite sizes at the 101 and 002 lattice planes in the cellulose model substrates. These physicochemical changes improved the activity of EGs on the Avicel and reduced the activity on the more crystalline cellulose substrate (filter paper). This information was important for understanding how HRP removes lignin and decreases the crystallinity of the rooibos substrate. Lastly, the formulated cellulases and hollocellulolytic enzyme cocktails achieved a yield of more than 95% of total reducing sugars per 25 mg enzyme loading/g biomass.

Acknowledgements

This research was supported by the University of the Free State, Department of Plant Science and Centre for Graduate Support. This research was also partially supported by the South African National Research Foundation through a Thuthuka grant awarded to Dr. Mpho S Mafa.

Author contribution

MMM and MSM designed the research; MMM conducted the experiments and prepared the original draft of the manuscript; MSM, MMM, OA, and BIP analysed the data and edited the paper; and MSM had primary responsibility for the final content.

Funding

Ms. MMM received a MSc bursary from the University of the Free State Centre for Graduate Support, MSM received a NRF-Thuthuka grant (TTK2204102938).

References

Badiei, M., Asim, N., Jahim, J.M. and Sopian, K., 2014. Comparison of chemical pretreatment methods for cellulosic biomass. APCBEE procedia, 9, pp.170-174.

Bagewadi, Z.K., Mulla, S.I. and Ninnekar, H.Z., 2017. Optimization of laccase production and its application in delignification of biomass. International Journal of Recycling of Organic Waste in Agriculture, 6, pp.351-365.

Behera, S., Arora, R., Nandhagopal, N. and Kumar, S., 2014. Importance of chemical pretreatment for bioconversion of lignocellulosic biomass. Renewable and Sustainable energy reviews, 36, pp.91-106.

Bommarius, A.S., Katona, A., Cheben, S.E., Patel, A.S., Ragauskas, A.J., Knudson, K. and Pu, Y., 2008. Cellulase kinetics as a function of cellulose pretreatment. Metabolic Engineering, 10(6), pp.370-381.

Chang, H., Gacias Amengual, N., Botz, A., Schwaiger, L., Kracher, D., Scheiblbrandner, S., Csarman, F. and Ludwig, R., 2022. Investigating lytic polysaccharide monooxygenase-assisted wood cell wall degradation with microsensors. Nature Communications, 13(1), p.6258.

Devi, A., Bajar, S., Kour, H., Kothari, R., Pant, D. and Singh, A., 2022. Lignocellulosic biomass valorization for bioethanol production: a circular bioeconomy approach. Bioenergy Research, 15(4), pp.1820-1841.

Garvey, C.J., Parker, I.H. and Simon, G.P., 2005. On the interpretation of X-ray diffraction powder patterns in terms of the nanostructure of cellulose I fibres. Macromolecular Chemistry and Physics, 206(15), pp.1568-1575.

Harmsen, P.F., Huijgen, W., Bermudez, L. and Bakker, R., 2010. Literature review of physical and chemical pretreatment processes for lignocellulosic biomass (No. 1184). Wageningen UR-Food & Biobased Research.

Hernández-Chaverri, R.A., Buenrostro-Figueroa, J.J and Prado-Barragán, L.A., 2021. Biomass: biorefinery as a model to boost the bioeconomy in Costa Rica, a review. *Agronomía Mesoamericana, 32*(3), pp.1047-1070.

Ju, X., Bowden, M., Brown, E.E. and Zhang, X., 2015. An improved X-ray diffraction method for cellulose crystallinity measurement. Carbohydrate Polymers, 123, pp.476-481.

Kersten, P.J., Kalyanaraman, B., Hammel, K.E., Reinhammar, B. and Kirk, T.K., 1990. Comparison of lignin peroxidase, horseradish peroxidase and laccase in the oxidation of methoxybenzenes. Biochemical Journal, 268(2), pp.475-480.

Khan, S.A., Khan, S.B., Khan, L.U., Farooq, A., Akhtar, K. and Asiri, A.M., 2018. Fourier transform infrared spectroscopy: fundamentals and application in functional groups and nanomaterials characterization. Handbook of materials characterization, pp.317-344.

Kong, W., Fu, X., Wang, L., Alhujaily, A., Zhang, J., Ma, F., Zhang, X. and Yu, H., 2017. A novel and efficient fungal delignification strategy based on versatile peroxidase for lignocellulose bioconversion. Biotechnology for Biofuels, 10(1), pp.1-15.

Kumar, B., Bhardwaj, N., Agrawal, K., Chaturvedi, V. and Verma, P., 2020. Current perspective on pretreatment technologies using lignocellulosic biomass: An emerging biorefinery concept. Fuel Processing Technology, 199, p.106244.

Lavery, C.B., MacInnis, M.C., MacDonald, M.J., Williams, J.B., Spencer, C.A., Burke, A.A., Irwin, D.J. and D'Cunha, G.B., 2010. Purification of peroxidase from horseradish (*Armoracia rusticana*) roots. Journal of Agricultural and Food Chemistry, 58(15), pp.8471-8476.

Levasseur, A., Drula, E., Lombard, V., Coutinho, P.M. and Henrissat, B., 2013. Expansion of the enzymatic repertoire of the CAZy database to integrate auxiliary redox enzymes. Biotechnology for Biofuels, 6(1), pp.1-14.

Limayem, A. and Ricke, S.C., 2012. Lignocellulosic biomass for bioethanol production: current perspectives, potential issues and future prospects. Progress in Energy and Combustion Science, 38(4), pp.449-467.

Ling, Z., Chen, S., Zhang, X. and Xu, F., 2017. Exploring crystalline-structural variations of cellulose during alkaline pretreatment for enhanced enzymatic hydrolysis. Bioresource Technology, 224, pp.611-617.

Ling, Z., Wang, T., Makarem, M., Santiago Cintrón, M., Cheng, H.N., Kang, X., Bacher, M., Potthast, A., Rosenau, T., King, H. and Delhom, C.D., 2019. Effects of ball milling on the structure of cotton cellulose. Cellulose, 26, pp.305-328.

Mafa, M.S., Malgas, S., Bhattacharya, A., Rashamuse, K. and Pletschke, B.I., 2020b. The effects of alkaline pretreatment on agricultural biomasses (corn cob and sweet sorghum bagasse) and their hydrolysis by a termite-derived enzyme cocktail. Agronomy, 10(8), p.1211.

Mafa, M.S., Malgas, S., Rashamuse, K. and Pletschke, B.I., 2020a. Delineating functional properties of a cello-oligosaccharide and β-glucan specific cellobiohydrolase (GH5_38): Its synergism with Cel6A and Cel7A for β-(1, 3)-(1, 4)-glucan degradation. Carbohydrate Research, 495, p.108081.

Mafa, M.S., Pletschke, B.I. and Malgas, S., 2021. Defining the frontiers of synergism between cellulolytic enzymes for improved hydrolysis of lignocellulosic feedstocks. Catalysts, 11(11), p.1343.

Malgas, S., Chandra, R., Van Dyk, J.S., Saddler, J.N. and Pletschke, B.I., 2017. Formulation of an optimized synergistic enzyme cocktail, HoloMix, for effective degradation of various pre-treated hardwoods. Bioresource Technology, 245, pp.52-65.

Manavalan, T., Manavalan, A. and Heese, K., 2015. Characterization of lignocellulolytic enzymes from white-rot fungi. Current Microbiology, 70, pp.485-498.

Menon, V. and Rao, M., 2012. Trends in bioconversion of lignocellulose: biofuels, platform chemicals & biorefinery concept. Progress in Energy and Combustion Science, 38(4), pp.522-550.

Miller, G.L., 1959. Use of dinitrosalicylic acid reagent for determination of reducing sugars. Analytical Chemistry 31.

Min, K., Kim, Y.H., Kim, J., Kim, Y., Gong, G. and Um, Y., 2022. Effect of manganese peroxidase on the decomposition of cellulosic components: Direct cellulolytic activity and synergistic effect with cellulase. Bioresource Technology, 343, p.126138.

Mnich, E., Bjarnholt, N., Eudes, A., Harholt, J., Holland, C., Jørgensen, B., Larsen, F.H., Liu, M., Manat, R., Meyer, A.S. and Mikkelsen, J.D., 2020. Phenolic cross-links: building and de-constructing the plant cell wall. Natural Product Reports, 37(7), pp.919-961.

Mohotloane, M.M., Alexander, O., Pletschke, B.I. and Mafa, M.S., 2023. Horseradish peroxidase delignification of fermented rooibos modifies biomass structural and chemical properties and improves holocellulolytic enzyme cocktail efficacy. Biologia 78, 1943–1959.

Monclaro, A.V. and Ferreira Filho, E.X., 2017. Fungal lytic polysaccharide monooxygenases from family AA9: recent developments and application in lignocelullose breakdown. International Journal of Biological Macromolecules, 102, pp.771-778.

Nam, S., French, A.D., Condon, B.D. and Concha, M., 2016. Segal crystallinity index revisited by the simulation of X-ray diffraction patterns of cotton cellulose Iβ and cellulose II. Carbohydrate Polymers, 135, pp.1-9.

Pandey, V.P., Awasthi, M., Singh, S., Tiwari, S. and Dwivedi, U.N., 2017. A comprehensive review on function and application of plant peroxidases. Biochem Anal Biochem, 6(1), p.308.

Park, S., Baker, J.O., Himmel, M.E., Parilla, P.A. and Johnson, D.K., 2010. Cellulose crystallinity index: measurement techniques and their impact on interpreting cellulase performance. Biotechnology for Biofuels, 3, pp.1-10.

Scherrer, P. (1918). Bestimmung der Größe und der inneren Struktur von Kolloidteilchen mittels Röntgenstrahlen. Nachrichten von der Gesellschaft der Wissenschaften zu Göttingen, 26, 98–100

Segal, L.G.J.M.A., Creely, J.J., Martin Jr, A.E. and Conrad, C.M., 1959. An empirical method for estimating the degree of crystallinity of native cellulose using the X-ray diffractometer. Textile Research Journal, 29(10), pp.786-794.

Sharma, H.K., Xu, C. and Qin, W., 2019. Biological pretreatment of lignocellulosic biomass for biofuels and bioproducts: an overview. Waste and Biomass Valorization, 10, pp.235-251.

Tian, S.Q., Zhao, R.Y. and Chen, Z.C., 2018. Review of the pretreatment and bioconversion of lignocellulosic biomass from wheat straw materials. Renewable and Sustainable Energy Reviews, 91, pp.483-489.

Van Dyk, J.S. and Pletschke, B., 2012. A review of lignocellulose bioconversion using enzymatic hydrolysis and synergistic cooperation between enzymes—factors affecting enzymes, conversion and synergy. Biotechnology Advances, 30(6), pp.1458-1480.

Veitch, N.C., 2004. Horseradish peroxidase: a modern view of a classic enzyme. Phytochemistry, 65(3), pp.249-259.

Wagner, A.O., Lackner, N., Mutschlechner, M., Prem, E.M., Markt, R. and Illmer, P., 2018. Biological pretreatment strategies for second-generation lignocellulosic resources to enhance biogas production. Energies, 11(7), p.1797.

Yu, S., Liu, Z., Xu, N., Chen, J. and Gao, Y., 2020. Influencing factors for determining the crystallinity of native cellulose by X-ray diffraction. Analytical Sciences, 36(8), pp.947-951.

Zhang, X.Z. and Zhang, Y.H.P., 2013. Cellulases: characteristics, sources, production, and applications. Bioprocessing technologies in biorefinery for sustainable production of fuels, chemicals, and polymers, pp.131-146.

Zhou, W., Apkarian, R., Wang, Z.L. and Joy, D., 2007. Fundamentals of scanning electron microscopy (SEM). Scanning Microscopy for Nanotechnology: Techniques and Applications, pp.1-40.

Chapter 5: General discussion and conclusion

Second generation biofuel (2G) is emerging as a renewable resource of choice because it does not compete with the food sources. However, it has been a challenge to close the loop (knowledge gap) in the circular economy, due to the presence of lignin in the agricultural residues and the limitations of the lignocellulose pretreatment methods that have been developed. Hence, in this study we explored the use of a sustainable and environmentally friendly biological pretreatment [partially purified horseradish peroxidase (HRP)]. Our results showed that this enzyme can catalyse several substrates, similar to LiP or VP. In addition, the findings showed HRP functions optimally under normal acidic condition and temperatures of 50℃ for less than an hour. Additionally, thermostability results revealed that this enzyme can be used for more than 24 hours at 37℃, making it suitable for overnight biomass pretreatment. The HRP physicochemical properties demonstrated that this enzyme does not use hash conditions like chemical pretreatments, which requires temperatures that are between 60 and 250℃.

The SEM, FTIR and XRD analyses showed HRP pretreatment modified the structural and chemical properties of the rooibos biomass. The HRP pretreatment showed efficiency in removing lignin, while also displaying LPMO-like activity because it reduced the recalcitrant nature of cellulose to endoglucanase activity. These findings prompted further research to elucidate the mechanism HRP used to modify structural and chemical properties of the microcrystalline cellulose. Hence, we used cellulose model substrates, i.e., Avicel and filter paper. The SEM analysis showed that HRP opened pores and cracks on the surface of the Avicel, while it efficiently hydrolysed the para-crystalline cellulose in the filter paper samples and exposed the crystalline fibres. These results were validated by the FTIR, which showed a significant increase in absorbance values of the broad peak between 3000 and 3600 cm^{-1} that is assigned to hydroxyl group, intra and intermolecular hydrogen bonds. Several studies including our research group have demonstrated that highly crystalline substrates have higher absorbance values in this region indicating strong intra and intermolecular hydrogen bonds. In contrast, pretreated samples displayed a lower absorbance value in this region, confirming the disruption of the intra and intermolecular hydrogen forces.

Surprisingly, both HRP treated Avicel and filter paper samples had increased CrI (crystallinity index) according to XRD analysis. Several studies suggested that higher CrI percentage was

correlated to higher cellulose crystallinity; therefore, the substrate will be more recalcitrant to enzymatic hydrolysis. However, Park et al. (2010) argued that the CrI generated using the Segal peak height method only explains the differences between the samples, as it does not consider the proportions of the amorphous and crystalline material within the sample. Therefore, we used the crystallite size, distance between the crystals (d spacing) and full width half-maximum (FWHM) to demonstrate the crystallinity and structural changes of cellulose in Avicel and filter paper after HRP pretreatment. Results showed that in Avicel the crystallite sizes at 002 lattice increased from 45.7 to 47.3 nm, while filter paper samples showed a general decrease of 1 nm, from 60.7 to 59.3 nm. Pretreated Avicel samples showed a significant decreased crystallite sizes (from 58.1 to 55.5 nm) at 040 lattice compared to a smaller decreased crystallite size from 63.4 to 62.9 nm. Both lattices 002 and 040 are attributed to cellulose-I (highly crystalline cellulose allomorph), thus, the crystallite size changes in Avicel, and filter paper suggest HRP reduce the crystallinity of the microcrystalline cellulose. Shao et al. (2023) argued that the increased grain sizes (at 002 lattice) suggested pretreatment loosened the crystalline structure of cellulose by destroying the intermolecular hydrogen bonds, which result in the decreased crystallinity. The FWHM and d-spacing also confirmed structural changes due to HRP treatment (chapter 4: Table 2).

Generally, endoglucanases do not effectively hydrolyse Avicel and filter paper microcrystalline cellulose regions. In our study, the endoglucanase displayed significantly higher activity on the HRP pretreated Avicel compared to the control. In contrast, the endoglucanase activity was reduced during the hydrolysis of filter paper. These patterns of endoglucanase activity corroborated the SEM results that showed HRP hydrolysed the para-crystalline regions of the filter paper exposing cellulose I_{β}. These findings imply the pretreatment increased the recalcitrance of filter paper towards endoglucanases but made Avicel easily accessible to the endoglucanase.

The complete removal of lignin and reduced cellulose crystallinity improving the subsequent hydrolysis processes with the formulated holocellulose enzyme cocktail (HEC). In chapter 3, the holocellulolytic enzyme cocktail was formulated with a combination of two endoglucanases (a multifunctional and a true endoglucanase), xylanase and β-glucosidase added at 10% (v/v). However, Cellobiohydrolase (CBHI) was not included in the HEC because it displayed anti-synergism with the endoglucanases, as the endoglucanase combination showed more activity than the combination containing CBHI. The application of the HEC on the delignified rooibos

resulted in 10% soluble sugars yield compared to 6% of the untreated rooibos. Therefore, for chapter 4 we aimed to improve the rooibos biomass conversion rate and improve soluble sugar production yields. We identified one of the challenges with the cocktail formulation method used in chapter 3 to be an underestimation of the enzyme concentration. One of commercial endoglucanases and xylanase were powders, as a result we determined their concentration by using weight per volume (w/v) method instead of measuring the enzyme concentration with Bradford method (Bradford 1976). The use of w/v method may not be accurate because we assumed that the weight that we measured is the correct concentration, instead the concentration was lower than expected. To solve the enzyme concentration challenge we decided to measure the concentrations of all enzymes used in chapter 4 by following Bradford method.

The higher enzyme loading (25 to 100 mg/g) of the multifunctional endoglucanase, xylanase and β-glucosidase added at 10% (v/v) was used to formulate the HEC. The best formulated HEC increased the conversion rate of HRP delignified rooibos over a period of 16 hours, resulting in 95% soluble sugar yield at 25 mg/g biomass. Thus, a higher enzyme concentration loading increased sugar conversion and improved the efficacy of the β-glucosidase in converting the short oligomers to monomeric sugars. These results demonstrated the effectiveness of HRP pretreatment on rooibos biomass, leading to formulation of less complex enzyme cocktail with higher biomass conversion rate.

In conclusion, the research presented in this MSc dissertation showed that rooibos biomass has the potential to be a feedstock for the production of value-added chemicals/products. Interestingly, the biomass was compatible with the type of biological pretreatment, resulting in a reduced pretreatment period (24-hour period) compared to other biological pretreatments (which take days or a week). The HRP also removed relatively more than 80% of the lignin from the biomass, changing both the structure and chemical properties. These modifications improved the enzyme hydrolysis/activity on the pretreated biomass. Finally, the HEC produced more than 90% yields of soluble sugars from the pretreatment biomass.

Future prospectives

1. Future work will focus on investigating the HRP pretreatment on the different fermented rooibos grades A to D, which we have in the CHEM-Lab.

2. The HRP pretreated rooibos biomasses will be investigated for the grade that can be used to produce the value-added chemicals at the large scale/pilot scale.
3. Comprehensive characterisation of the biomass (grades A to D) will be performed and used to select the biomass grade with better properties.
4. Can HRP, LiP and MnP synergize? We will also attempt to answer that question.

References

Abdelgalil, S.A., Attia, A.R., Reyed, R.M. and Soliman, N.A., 2020. Partial purification and biochemical characterization of a new highly acidic NYSO laccase from Alcaligenes faecalis. Journal of Genetic Engineering and Biotechnology, 18, pp.1-11.

Abraham, A., Mathew, A.K., Park, H., Choi, O., Sindhu, R., Parameswaran, B., Pandey, A., Park, J.H. and Sang, B.I., 2020. Pretreatment strategies for enhanced biogas production from lignocellulosic biomass. Bioresource Technology, 301, pp.122725.

Adsul, M., Sandhu, S.K., Singhania, R.R., Gupta, R., Puri, S.K. and Mathur, A., 2020. Designing a cellulolytic enzyme cocktail for the efficient and economical conversion of lignocellulosic biomass to biofuels. Enzyme and microbial technology, 133, pp.109442.

Adsul, M., Sandhu, S.K., Singhania, R.R., Gupta, R., Puri, S.K. and Mathur, A., 2020. Designing a cellulolytic enzyme cocktail for the efficient and economical conversion of lignocellulosic biomass to biofuels. Enzyme and microbial technology, 133, pp.109442.

Agrawal, K., Bhardwaj, N., Kumar, B., Chaturvedi, V. and Verma, P., 2019. Process optimization, purification and characterization of alkaline stable white laccase from Myrothecium verrucaria ITCC-8447 and its application in delignification of agroresidues. International journal of biological macromolecules, 125, pp.1042-1055.

Agrawal, K., Chaturvedi, V. and Verma, P., 2018. Fungal laccase discovered but yet undiscovered. Bioresources and Bioprocessing, 5(1), pp.1-12.

Al-Bagmi, M.S., Khan, M.S., Ismael, M.A., Al-Senaidy, A.M., Bacha, A.B., Husain, F.M. and Alamery, S.F., 2019. An efficient methodology for the purification of date palm peroxidase: Stability comparison with horseradish peroxidase (HRP). Saudi Journal of Biological Sciences, 26(2), pp.301-307.

Amit, K., Nakachew, M., Yilkal, B. and Mukesh, Y.J.R.J.C.E., 2018. A review of factors affecting enzymatic hydrolysis of pretreated lignocellulosic biomass. Res J Chem Environ, 22(7), pp.62-67.

Andlar, M., Rezić, T., Marđetko, N., Kracher, D., Ludwig, R. and Šantek, B., 2018. Lignocellulose degradation: An overview of fungi and fungal enzymes involved in lignocellulose degradation. Engineering in Life Sciences, 18(11), pp.768-778.

Asgher, M., Iqbal, H.M.N. and Irshad, M., 2012. Characterization of purified and xerogel immobilized novel lignin peroxidase produced from Trametes versicolor IBL-04 using solid state medium of corncobs. BMC biotechnology, 12, pp.1-8.

Auxenfans, T., Crônier, D., Chabbert, B. and Paës, G., 2017. Understanding the structural and chemical changes of plant biomass following steam explosion pretreatment. Biotechnology for biofuels, 10, pp.1-16.

Avanthi, A. and Banerjee, R., 2016. A strategic laccase mediated lignin degradation of lignocellulosic feedstocks for ethanol production. Industrial Crops and Products, 92, pp.174-185.

Badiei, M., Asim, N., Jahim, J.M. and Sopian, K., 2014. Comparison of chemical pretreatment methods for cellulosic biomass. APCBEE procedia, 9, pp.170-174.

Bagewadi, Z.K., Mulla, S.I. and Ninnekar, H.Z., 2016. Purification, characterization, gene cloning and expression of GH-10 xylanase (Penicillium citrinum isolate HZN13). 3 Biotech, 6, pp.1-9.

Bagewadi, Z.K., Mulla, S.I. and Ninnekar, H.Z., 2017. Optimization of laccase production and its application in delignification of biomass. International Journal of Recycling of Organic Waste in Agriculture, 6, pp.351-365.

Bai, H., Wang, H., Sun, J., Irfan, M., Han, M., Huang, Y., Han, X. and Yang, Q., 2013. Purification and characterization of beta 1, 4-glucanases from Penicillium simplicissimum H-11. BioResources, 8(3), pp.3657-3671.

Baker, J.O., King, M.R., Adney, W.S., Decker, S.R., Vinzant, T.B., Lantz, S.E., Nieves, R.E., Thomas, S.R., Li, L.C., Cosgrove, D.J. and Himmel, M.E., 2000. Investigation of the Cell-Wall

Loosening Protein Expansin as a Possible Additive in the Enzymatic Saccharification of Lignocellulosic Biomass. In: Finkelstein, M., Davison, B.H. (eds) Twenty-First Symposium on Biotechnology for Fuels and Chemicals. Applied Biochemistry and Biotechnology. Humana Press, Totowa, NJ, pp. 217-223.

Ballesteros, I., Negro, M.J., Oliva, J.M., Cabañas, A., Manzanares, P., Ballesteros, M. (2006). Ethanol Production From Steam-Explosion Pretreated Wheat Straw. In: McMillan, J.D., Adney, W.S., Mielenz, J.R., Klasson, K.T. (eds) Twenty-Seventh Symposium on Biotechnology for Fuels and Chemicals. ABAB Symposium. Humana Press, pp. 496-508.

Banerjee, R., Chintagunta, A.D. and Ray, S., 2019. Laccase mediated delignification of pineapple leaf waste: an ecofriendly sustainable attempt towards valorization. BMC chemistry, 13, pp.1-11.

Baruah, J., Nath, B.K., Sharma, R., Kumar, S., Deka, R.C., Baruah, D.C. and Kalita, E., 2018. Recent trends in the pretreatment of lignocellulosic biomass for value-added products. Frontiers in Energy Research, 6, pp.141.

Battistuzzi, G., Bellei, M., Bortolotti, C.A. and Sola, M., 2010. Redox properties of heme peroxidases. Archives of biochemistry and biophysics, 500(1), pp.21-36.

Behera, S., Arora, R., Nandhagopal, N. and Kumar, S., 2014. Importance of chemical pretreatment for bioconversion of lignocellulosic biomass. Renewable and sustainable energy reviews, 36, pp.91-106.

Bhatia, S.K., Jagtap, S.S., Bedekar, A.A., Bhatia, R.K., Patel, A.K., Pant, D., Banu, J.R., Rao, C.V., Kim, Y.G. and Yang, Y.H., 2020. Recent developments in pretreatment technologies on lignocellulosic biomass: effect of key parameters, technological improvements, and challenges. Bioresource technology, 300, pp.122724.

Bhattacharya, A.S., Bhattacharya, A. and Pletschke, B.I., 2015. Synergism of fungal and bacterial cellulases and hemicellulases: a novel perspective for enhanced bio-ethanol production. Biotechnology letters, 37, pp.1117-1129.

Bhutto, A.W., Qureshi, K., Harijan, K., Abro, R., Abbas, T., Bazmi, A.A., Karim, S. and Yu, G., 2017. Insight into progress in pre-treatment of lignocellulosic biomass. Energy, 122, pp.724-745.

Bilal, M., Rasheed, T., Iqbal, H.M. and Yan, Y., 2018. Peroxidases-assisted removal of environmentally-related hazardous pollutants with reference to the reaction mechanisms of industrial dyes. Science of the total environment, 644, pp.1-13.

Bradford, M.M., 1976. A rapid and sensitive method for the quantitation of microgram quantities of protein utilizing the principle of protein-dye binding. Analytical biochemistry, 72(1-2), pp.248-254.

Calderan-Rodrigues, M.J., Fonseca, J.G., de Moraes, F.E., VazSetem, L., CarmanhanisBegossi, A. and Labate, C.A., 2019. Plant cell wall proteomics: A focus on monocot species, Brachypodiumdistachyon, Saccharum spp. and Oryza sativa. International journal of molecular sciences, 20(8), pp1975.

Calderaro, F., Bevers, L.E. and van den Berg, M.A., 2021. Oxidative power: Tools for assessing LPMO activity on cellulose. Biomolecules, 11(8), pp.1098.

Chan, J.C., Paice, M. and Zhang, X., 2020. Enzymatic oxidation of lignin: challenges and barriers toward practical applications. ChemCatChem, 12(2), pp.401-425.

Chandel, A.K., Gonçalves, B.C., Strap, J.L. and da Silva, S.S., 2015. Biodelignification of lignocellulose substrates: An intrinsic and sustainable pretreatment strategy for clean energy production. Critical Reviews in Biotechnology, 35(3), pp.281-293.

Chaurasia, P.K., Yadav, R.S.S. and Yadava, S., 2013. A review on mechanism of laccase action. Res Rev Biosci, 7(2), pp.66-71.

Cheng, G., Varanasi, P., Li, C., Liu, H., Melnichenko, Y.B., Simmons, B.A., Kent, M.S. and Singh, S., 2011. Transition of cellulose crystalline structure and surface morphology of biomass as a function of ionic liquid pretreatment and its relation to enzymatic hydrolysis. Biomacromolecules, 12(4), pp.933-941.

Chylenski, P., Bissaro, B., Sørlie, M., Røhr, Å.K., Várnai, A., Horn, S.J. and Eijsink, V.G., 2019. Lytic polysaccharide monooxygenases in enzymatic processing of lignocellulosic biomass. ACS Catalysis, 9(6), pp.4970-4991.

Coetzee, G., Joubert, E., van Zyl, W.H. and Viljoen-Bloom, M., 2014. Improved extraction of phytochemicals from rooibos with enzyme treatment. Food and Bioproducts Processing, 92(4), pp.393-401.

Colom, X., Carrillo, F., Nogués, F. and Garriga, P., 2003. Structural analysis of photodegraded wood by means of FTIR spectroscopy. Polymer degradation and stability, 80(3), pp.543-549.

Coseri, S., 2017. Cellulose: To depolymerize. or not to?. Biotechnology advances, 35(2), pp251-266.

Cosgrove, D.J., 2000. Loosening of plant cell walls by expansins. Nature, 407(6802), pp321-326.

Cragg, S.M., Beckham, G.T., Bruce, N.C., Bugg, T.D., Distel, D.L., Dupree, P., Etxabe, A.G., Goodell, B.S., Jellison, J., McGeehan, J.E. and McQueen-Mason, S.J., 2015. Lignocellulose degradation mechanisms across the Tree of Life. Current opinion in chemical biology, 29, pp.108-119.

Daou, M., Bisotto, A., Haon, M., Oliveira Correia, L., Cottyn, B., Drula, E., Garajová, S., Bertrand, E., Record, E., Navarro, D. and Raouche, S., 2021. A putative lignin copper oxidase from Trichoderma reesei. Journal of Fungi, 7(8), pp.643.

de Gouvêa, P.F., Gerolamo, L.E., Bernardi, A.V., Pereira, L., Uyemura, S.A. and Dinamarco, T.M., 2019. Lytic polysaccharide monooxygenase from Aspergillus fumigatus can improve enzymatic cocktail activity during sugarcane bagasse hydrolysis. Protein and Peptide Letters, 26(5), pp.377-385.

de Oliveira, F.K., Santos, L.O. and Buffon, J.G., 2021. Mechanism of action, sources, and application of peroxidases. Food Research International, 143, pp.110266.

Derkacheva, O. and Sukhov, D. (2008), Investigation of Lignins by FTIR Spectroscopy. Macromol. Symp., 265: 61-68

Devi, A., Bajar, S., Kour, H., Kothari, R., Pant, D. and Singh, A., 2022. Lignocellulosic biomass valorization for bioethanol production: a circular bioeconomy approach. Bioenergy Research, 15(4), pp.1820-1841.

Dijkerman, R., Bhansing, D.C., den Camp, H.J.O., van der Drift, C. and Vogels, G.D., 1997. Degradation of structural polysaccharides by the plant cell-wall degrading enzyme system from anaerobic fungi: an application study. Enzyme and microbial technology, 21(2), pp.130-136.

Dos Santos, F.C., de Oliveira, M.A.S., Seixas, F.A.V. and Barbosa-Tessmann, I.P., 2020. A novel cellobiohydrolase I (CBHI) from Penicillium digitatum: Production, purification, and characterization. Applied Biochemistry and Biotechnology, 192, pp.257-282.

Duan, Y., Ma, Y., Zhao, X., Huang, R., Su, R., Qi, W. and He, Z., 2018. Real-time adsorption and action of expansin on cellulose. Biotechnology for biofuels, 11(1), pp.1-13.

Eijsink, V.G., Petrovic, D., Forsberg, Z., Mekasha, S., Røhr, Å.K., Várnai, A., Bissaro, B. and Vaaje-Kolstad, G., 2019. On the functional characterization of lytic polysaccharide monooxygenases (LPMOs). Biotechnology for biofuels, 12(1), pp.1-16.

Ertan, H., Siddiqui, K.S., Muenchhoff, J., Charlton, T. and Cavicchioli, R., 2012. Kinetic and thermodynamic characterization of the functional properties of a hybrid versatile peroxidase using isothermal titration calorimetry: insight into manganese peroxidase activation and lignin peroxidase inhibition. Biochimie, 94(5), pp.1221-1231.

Falade, A.O., Mabinya, L.V., Okoh, A.I. and Nwodo, U.U., 2019. Biochemical and molecular characterization of a novel dye-decolourizing peroxidase from Raoultella ornithinolytica OKOH-1. International journal of biological macromolecules, 121, pp.454-462.

Fernandes, C.G., Sawant, S.C., Mule, T.A., Khadye, V.S., Lali, A.M. and Odaneth, A.A., 2022. Enhancing cellulases through synergistic β-glucosidases for intensifying cellulose hydrolysis. Process Biochemistry, 120, pp.202-212.

Filiatrault-Chastel, C., Navarro, D., Haon, M., Grisel, S., Herpoël-Gimbert, I., Chevret, D., Fanuel, M., Henrissat, B., Heiss-Blanquet, S., Margeot, A. and Berrin, J.G., 2019. AA16, a new lytic polysaccharide monooxygenase family identified in fungal secretomes. Biotechnology for biofuels, 12(1), pp.1-15.

Forsberg, Z., Sørlie, M., Petrović, D., Courtade, G., Aachmann, F.L., Vaaje-Kolstad, G., Bissaro, B., Røhr, Å.K. and Eijsink, V.G., 2019. Polysaccharide degradation by lytic polysaccharide monooxygenases. Current Opinion in Structural Biology, 59, pp.54-64.

García-Cubero, M.T., González-Benito, G., Indacoechea, I., Coca, M. and Bolado, S., 2009. Effect of ozonolysis pretreatment on enzymatic digestibility of wheat and rye straw. Bioresource technology, 100(4), pp.1608-1613.

Garvey, C.J., Parker, I.H. and Simon, G.P., 2005. On the interpretation of X-ray diffraction powder patterns in terms of the nanostructure of cellulose I fibres. Macromolecular Chemistry and Physics, 206(15), pp.1568-1575.

Georgelis, N., Nikolaidis, N. and Cosgrove, D.J., 2015. Bacterial expansins and related proteins from the world of microbes. Applied microbiology and biotechnology, 99, pp.3807-3823.

Ghodake, G.S., Kalme, S.D., Jadhav, J.P. and Govindwar, S.P., 2009. Purification and partial characterization of lignin peroxidase from Acinetobacter calcoaceticus NCIM 2890 and its application in decolorization of textile dyes. Applied biochemistry and biotechnology, 152, pp.6-14.

Giacobbe, S., Pezzella, C., Lettera, V., Sannia, G. and Piscitelli, A., 2018. Laccase pretreatment for agrofood wastes valorization. Bioresource technology, 265, pp.59-65.

Guo, X., Yuan, H., Xiao, T. and Wu, Y., 2019. Application of micro-FTIR spectroscopy to study molecular association of adsorbed water with lignin. International journal of biological macromolecules, 131, pp.1038-1043.

Haldar, D. and Purkait, M.K., 2021. A review on the environment-friendly emerging techniques for pretreatment of lignocellulosic biomass: Mechanistic insight and advancements. Chemosphere, 264, pp.128523.

Harmsen, P.F., Huijgen, W., Bermudez, L. and Bakker, R., 2010. Literature review of physical and chemical pretreatment processes for lignocellulosic biomass (No. 1184). Wageningen UR-Food & Biobased Research.

Harris, P.V., Welner, D., McFarland, K.C., Re, E., Navarro Poulsen, J.C., Brown, K., Salbo, R., Ding, H., Vlasenko, E., Merino, S. and Xu, F., 2010. Stimulation of lignocellulosic biomass hydrolysis by proteins of glycoside hydrolase family 61: structure and function of a large, enigmatic family. Biochemistry, 49(15), pp.3305-3316.

Hassan, S.S., Williams, G.A. and Jaiswal, A.K., 2018. Emerging technologies for the pretreatment of lignocellulosic biomass. Bioresource technology, 262, pp.310-318.

Hendriks, A.T.W.M. and Zeeman, G., 2009. Pretreatments to enhance the digestibility of lignocellulosic biomass. Bioresource technology, 100(1), pp.10-18.

Hernández-Chaverri, R.A., Buenrostro-Figueroa, J.J. and Prado-Barragán, L.A., 2021. Biomass: biorefinery as a model to boost the bioeconomy in Costa Rica, a review. Agronomy Mesoamerican, 32(3), pp.1047-1070.

Hiner, A.N., Raven, E.L., Thorneley, R.N., García-Cánovas, F. and Rodríguez-López, J.N., 2002. Mechanisms of compound I formation in heme peroxidases. Journal of inorganic biochemistry, 91(1), pp.27-34.

Houghton, J., 2005. Global warming. Reports on progress in physics, 68(6), pp.1343.

Howard, R.L., Abotsi, E.L.J.R., Van Rensburg, E.J. and Howard, S., 2003. Lignocellulose biotechnology: issues of bioconversion and enzyme production. African Journal of biotechnology, 2(12), pp.602-619.

Huang, J., Xia, T., Li, G., Li, X., Li, Y., Wang, Y., Wang, Y., Chen, Y., Xie, G., Bai, F.W. and Peng, L., 2019. Overproduction of native endo-β-1, 4-glucanases leads to largely enhanced biomass saccharification and bioethanol production by specific modification of cellulose features in transgenic rice. Biotechnology for Biofuels, 12, pp.1-15.

Hübsch, Z., Van Vuuren, S.F. and Van Zyl, R.L., 2014. Can rooibos (Aspalathus linearis) tea have an effect on conventional antimicrobial therapies?. South African Journal of Botany, 93, pp.148-156.

I.P.C.C. Climate change (2007) The physical science basis. Agenda 6(07), pp333

Imai, T., Naruse, M., Horikawa, Y., Yaoi, K., Miyazaki, K. and Sugiyama, J., 2023. Disturbance of the hydrogen bonding in cellulose by bacterial expansin. Cellulose, 30(13), pp.8423-8438.

Jouili, H., Bouazizi, H. and El Ferjani, E., 2011. Plant peroxidases: biomarkers of metallic stress. Acta Physiologiae Plantarum, 33, pp.2075-2082.

Ju, X., Bowden, M., Brown, E.E. and Zhang, X., 2015. An improved X-ray diffraction method for cellulose crystallinity measurement. Carbohydrate polymers, 123, pp.476-481.

Kalyani, D.C., Phugare, S.S., Shedbalkar, U.U. and Jadhav, J.P., 2011. Purification and characterization of a bacterial peroxidase from the isolated strain Pseudomonas sp. SUK1 and its application for textile dye decolorization. Annals of Microbiology, 61(3), pp.483-491.

Karnaouri, A., Muraleedharan, M.N., Dimarogona, M., Topakas, E., Rova, U., Sandgren, M. and Christakopoulos, P., 2017. Recombinant expression of thermostable processive Mt EG5 endoglucanase and its synergism with Mt LPMO from Myceliophthora thermophila during the hydrolysis of lignocellulosic substrates. Biotechnology for biofuels, 10, pp.1-17.

Keller, M.B., Badino, S.F., Røjel, N., Sørensen, T.H., Kari, J., McBrayer, B., Borch, K., Blossom, B.M. and Westh, P., 2021. A comparative biochemical investigation of the impeding effect of C1-oxidizing LPMOs on cellobiohydrolases. Journal of Biological Chemistry, Volume 296, pp100504.

Khan, S.A., Khan, S.B., Khan, L.U., Farooq, A., Akhtar, K. and Asiri, A.M., 2018. Fourier transform infrared spectroscopy: fundamentals and application in functional groups and nanomaterials characterization. Handbook of materials characterization, pp.317-344.

Khatun, S., Ashraduzzaman, M., Karim, M.R., Pervin, F., Absar, N. and Rosma, A., 2012. Purification and characterization of peroxidase from Moringa oleifera L. leaves. BioResources, 7(3), pp.3237-3251.

Kim, E.S., Lee, H.J., Bang, W.G., Choi, I.G. and Kim, K.H., 2009. Functional characterization of a bacterial expansin from Bacillus subtilis for enhanced enzymatic hydrolysis of cellulose. Biotechnology and bioengineering, 102(5), pp.1342-1353.

Kim, H., Ahn, Y. and Kwak, S.Y., 2016. Comparing the influence of acetate and chloride anions on the structure of ionic liquid pretreated lignocellulosic biomass. Biomass and Bioenergy, 93, pp.243-253.

Kim, I.J., Lee, H.J., Choi, I.G. and Kim, K.H., 2014. Synergistic proteins for the enhanced enzymatic hydrolysis of cellulose by cellulase. Applied microbiology and biotechnology, 98, pp.8469-8480.

Kong, W., Fu, X., Wang, L., Alhujaily, A., Zhang, J., Ma, F., Zhang, X. and Yu, H., 2017. A novel and efficient fungal delignification strategy based on versatile peroxidase for lignocellulose bioconversion. Biotechnology for biofuels, 10(1), pp.1-15.

Koupaie, E.H., Dahadha, S., Lakeh, A.B., Azizi, A. and Elbeshbishy, E., 2019. Enzymatic pretreatment of lignocellulosic biomass for enhanced biomethane production-A review. Journal of environmental management, 233, pp.774-784.

Kumar, A. and Chandra, R., 2020. Ligninolytic enzymes and its mechanisms for degradation of lignocellulosic waste in environment. Heliyon, 6(2), pp.e03170.

Kumar, B., Bhardwaj, N., Agrawal, K., Chaturvedi, V. and Verma, P., 2020. Current perspective on pretreatment technologies using lignocellulosic biomass: An emerging biorefinery concept. Fuel Processing Technology, 199, pp.106244.

Lee J, 1997. Biological conversion of lignocellulosic biomass to ethanol. J Biotechnol, 56, pp1-24.

Lee, J.M., Shi, J., Venditti, R.A. and Jameel, H., 2009. Autohydrolysis pretreatment of Coastal Bermuda grass for increased enzyme hydrolysis. Bioresource Technology, 100(24), pp.6434-6441.

Li, B.Z., Balan, V., Yuan, Y.J. and Dale, B.E., 2010. Process optimization to convert forage and sweet sorghum bagasse to ethanol based on ammonia fiber expansion (AFEX) pretreatment. Bioresource technology, 101(4), pp.1285-1292.

Li, F., Ma, F., Zhao, H., Zhang, S., Wang, L., Zhang, X. and Yu, H., 2019. A lytic polysaccharide monooxygenase from a white-rot fungus drives the degradation of lignin by a versatile peroxidase. Applied and environmental microbiology, 85(9), pp.e02803-18.

Li, L., Yu, S.T., Liu, F.S., Xie, C.X. and Xu, C.Z., 2011. Efficient enzymatic in situ saccharification of cellulose in aqueous-ionic liquid media by microwave pretreatment. BioResources, 6(4).

Li, X., Shi, Y., Kong, W., Wei, J., Song, W. and Wang, S., 2022. Improving enzymatic hydrolysis of lignocellulosic biomass by bio-coordinated physicochemical pretreatment—A review. Energy Reports, 8, pp.696-709.

Limayem, A. and Ricke, S.C., 2012. Lignocellulosic biomass for bioethanol production: current perspectives, potential issues, and future prospects. Progress in energy and combustion science, 38(4), pp.449-467.

Linares, N.C., Dilokpimol, A., Stålbrand, H., Mäkelä, M.R. and De Vries, R.P., 2020. Recombinant production and characterization of six novel GH27 and GH36 α-galactosidases from Penicillium subrubescens and their synergism with a commercial mannanase during the hydrolysis of lignocellulosic biomass. Bioresource Technology, 295, pp.122258.

Ling, Z., Chen, S., Zhang, X., Takabe, K. and Xu, F., 2017. Unraveling variations of crystalline cellulose induced by ionic liquid and their effects on enzymatic hydrolysis. Scientific Reports, 7(1), pp.10230.

Ling, Z., Wang, T., Makarem, M., Santiago Cintrón, M., Cheng, H.N., Kang, X., Bacher, M., Potthast, A., Rosenau, T., King, H. and Delhom, C.D., 2019. Effects of ball milling on the structure of cotton cellulose. Cellulose, 26, pp.305-328.

Liu, X., Renard, C.M., Bureau, S. and Le Bourvellec, C., 2021. Revisiting the contribution of ATR-FTIR spectroscopy to characterize plant cell wall polysaccharides. Carbohydrate Polymers, 262, pp.117935.

Liu, Z., Shao, T., Li, Y., Wu, B., Jia, H. and Hao, N., 2021. Expression, characterization and its deinking potential of a thermostable xylanase from Planomicrobium glaciei CHR43. Frontiers in bioengineering and biotechnology, 9,p p.618979.

Luo, X., Liu, J., Zheng, P., Li, M., Zhou, Y., Huang, L., Chen, L. and Shuai, L., 2019. Promoting enzymatic hydrolysis of lignocellulosic biomass by inexpensive soy protein. Biotechnology for biofuels, 12(1), pp.1-13.

Mafa, M.S. and Malgas, S., 2023. Towards an understanding of the enzymatic degradation of complex plant mannan structures. World Journal of Microbiology and Biotechnology, 39(11),pp.302.

Mafa, M.S. Pletschke, B.I, Malgas, S, 2021a. Defining the frontier of synergism between cellulolytic enzymes for improved hydrolysis of lignocellulosic feedstocks. Catalysts,11 (11), pp1343

Mafa, M.S., Lebusa, N., Gumani, T.F., Kemp, G., Visser, B., Boshoff, W.H. and Castelyn, H.D., 2023. Accumulation of complex oligosaccharides and CAZymes activity under acid conditions constitute the Thatcher+ Lr9 defence responses to Puccinia triticina. Biologia, 78, pp1929–1941.

Mafa, M.S., Malgas, S., and Pletschke, B.I., 2021b. Feruloyl esterase (FAE-1) sourced from a termite hindgut and GH10 xylanases synergy improves degradation of arabinoxylan. AMB Express, 11(1), pp1-9.

Mafa, M.S., Malgas, S., Bhattacharya, A., Rashamuse, K. and Pletschke, B.I., 2020b. The effects of alkaline pretreatment on agricultural biomasses (corn cob and sweet sorghum bagasse) and their hydrolysis by a termite-derived enzyme cocktail. Agronomy, 10(8), pp.1211.

Mafa, M.S., Malgas, S., Rashamuse, K. and Pletschke, B.I., 2020a. Delineating functional properties of a cello-oligosaccharide and β-glucan specific cellobiohydrolase (GH5_38): Its synergism with Cel6A and Cel7A for β-(1, 3)-(1, 4)-glucan degradation. Carbohydrate Research, 495, pp.108081.

Mafa, M.S., Rufetu, E., Alexander, O., Kemp, G. and Mohase, L., 2022. Cell-wall structural carbohydrates reinforcements are part of the defence mechanisms of wheat against Russian wheat aphid (Diuraphis noxia) infestation. Plant Physiology and Biochemistry, 179, pp.168-178.

Maity, S.K., Gayen, K. and Bhowmick, T.K. eds., 2021. Hydrocarbon biorefinery: sustainable processing of biomass for hydrocarbon biofuels. Elsevier.

Malgas, S., Mafa, M.S., Mathibe, B.N. and Pletschke, B.I., 2021. Unraveling synergism between various GH family xylanases and debranching enzymes during hetero-xylan degradation. Molecules, 26(22), pp.6770.

Malgas, S., Mafa, M.S., Mkabayi, L. and Pletschke, B.I., 2019. A mini review of xylanolytic enzymes with regards to their synergistic interactions during hetero-xylan degradation. World Journal of Microbiology and Biotechnology, 35(12), pp.187.

Malgas, S., Mkabayi, L., Mathibe, B.N., Thoresen, M., Mafa, M.S., Le Roes-Hill, M., van Zyl, W.H.E. and Pletschke, B.I., 2020b. Enzymatic path to bioconversion of lignocellulosic biomass. In Recent Advances in Bioconversion of Lignocellulose to Biofuels and Value-Added Chemicals within the Biorefinery Concept (pp5-32). Elsevier.

Malgas, S., Rose, S.H., van Zyl, W.H. and Pletschke, B.I., 2020a. Enzymatic hydrolysis of softwood derived paper sludge by an in vitro recombinant cellulase cocktail for the production of fermentable sugars. Catalysts, 10(7), pp.775.

Malgas, S., van Dyk, J.S. and Pletschke, B.I., 2015. A review of the enzymatic hydrolysis of mannans and synergistic interactions between β-mannanase, β-mannosidase and α-galactosidase. World journal of microbiology and biotechnology, 31, pp.1167-1175.

Malhotra, M. and Suman, S.K., 2021. Laccase-mediated delignification and detoxification of lignocellulosic biomass: removing obstacles in energy generation. Environmental Science and Pollution Research, 28, pp.58929-58944.

Meier, K.K., Jones, S.M., Kaper, T., Hansson, H., Koetsier, M.J., Karkehabadi, S., Solomon, E.I., Sandgren, M. and Kelemen, B., 2017. Oxygen activation by Cu LPMOs in recalcitrant carbohydrate polysaccharide conversion to monomer sugars. Chemical reviews, 118(5), pp.2593-2635.

Menon, V. and Rao, M., 2012. Trends in bioconversion of lignocellulose: biofuels, platform chemicals & biorefinery concept. Progress in energy and combustion science, 38(4), pp.522-550.

Merino, S.T. and Cherry, J., 2007. Progress and challenges in enzyme development for biomass utilization. Biofuels, vol 108, pp.95-120.

Miller, G.L., 1959. Use of dinitrosalicylic acid reagent for determination of reducing sugar. Analytical chemistry, 31(3), pp.426-428.

Min, C.H.E.N., Shanjing, Y.A.O., Zhang, H. and Liang, X., 2010. Purification and characterization of a versatile peroxidase from edible mushroom Pleurotus eryngii. Chinese journal of chemical engineering, 18(5), pp.824-829.

Min, K., Kim, Y.H., Kim, J., Kim, Y., Gong, G. and Um, Y., 2022. Effect of manganese peroxidase on the decomposition of cellulosic components: Direct cellulolytic activity and synergistic effect with cellulase. Bioresource Technology, 343, pp.126138.

Mnich, E., Bjarnholt, N., Eudes, A., Harholt, J., Holland, C., Jørgensen, B., Larsen, F.H., Liu, M., Manat, R., Meyer, A.S. and Mikkelsen, J.D., 2020. Phenolic cross-links: building and de-constructing the plant cell wall. Natural product reports, 37(7), pp.919-961.

Mohotloane, M.M., Alexander, O., Pletschke, B.I. and Mafa, M.S., 2023. Horseradish peroxidase delignification of fermented rooibos modifies biomass structural and chemical properties and improves holocellulolytic enzyme cocktail efficacy. Biologia, 78, 1943–1959.

Moon, M., Lee, J.P., Park, G.W., Lee, J.S., Park, H.J. and Min, K., 2022. Lytic polysaccharide monooxygenase (LPMO)-derived saccharification of lignocellulosic biomass. Bioresource Technology, 359, pp.127501.

Morsi, R., Bilal, M., Iqbal, H.M. and Ashraf, S.S., 2020. Laccases and peroxidases: the smart, greener and futuristic biocatalytic tools to mitigate recalcitrant emerging pollutants. Science of the total environment, 714, pp.136572.

Mukhopadhyay, M. and Banerjee, R., 2015. Purification and biochemical characterization of a newly produced yellow laccase from Lentinus squarrosulus MR13. 3 Biotech, 5(3), pp.227-236.

Mustafa, A.H., Rashid, S.S., Rahim, M.H.A., Roslan, R., Musa, W.A.M., Sikder, B.H. and Sasi, A.A., 2022. Enzymatic pretreatment of lignocellulosic biomass: an overview. Journal of Chemical Engineering and Industrial Biotechnology, 8(1), pp.1-7.

Nargotra, P., Sharma, V., Lee, Y.C., Tsai, Y.H., Liu, Y.C., Shieh, C.J., Tsai, M.L., Dong, C.D. and Kuo, C.H., 2022. Microbial Lignocellulolytic enzymes for the effective valorization of lignocellulosic biomass: a review. Catalysts, 13(1), pp.83.

Neelkant, K.S., Shankar, K., Jayalakshmi, S.K. and Sreeramulu, K., 2020. Purification, biochemical characterization, and facile immobilization of laccase from Sphingobacterium ksn-11 and its application in transformation of diclofenac. Applied Biochemistry and Biotechnology, 192, pp.831-844.

Nuruddin, M., Hosur, M., Uddin, M.J., Baah, D. and Jeelani, S., 2016. A novel approach for extracting cellulose nanofibers from lignocellulosic biomass by ball milling combined with chemical treatment. Journal of Applied Polymer Science, 133(9) ,pp42990.

Olsson, L. and Hahn-Hägerdal, B., 1996. Fermentation of lignocellulosic hydrolysates for ethanol production. Enzyme and Microbial technology, 18(5), pp.312-331.

Pandey, V.P. and Dwivedi, U.N., 2011. Purification and characterization of peroxidase from Leucaena leucocephala, a tree legume. Journal of Molecular Catalysis B: Enzymatic, 68(2), pp.168-173.

Pandey, V.P., Awasthi, M., Singh, S., Tiwari, S. and Dwivedi, U.N., 2017. A comprehensive review on function and application of plant peroxidases. Biochem Anal Biochem, 6(1), pp.308.

Pandey, V.P., Singh, S., Singh, R. and Dwivedi, U.N., 2012. Purification and characterization of peroxidase from papaya (Carica papaya) fruit. Applied biochemistry and biotechnology, 167, pp.367-376.

Park, S., Baker, J.O., Himmel, M.E., Parilla, P.A. and Johnson, D.K., 2010. Cellulose crystallinity index: measurement techniques and their impact on interpreting cellulase performance. Biotechnology for biofuels, 3, pp.1-10.

Pengilly, M., Joubert, E., van Zyl, W.H., Botha, A. and Bloom, M., 2008. Enhancement of rooibos (Aspalathus linearis) aqueous extract and antioxidant yield with fungal enzymes. Journal of agricultural and food chemistry, 56(11), pp.4047-4053.

Rajak, R.C. and Banerjee, R., 2015. Enzymatic delignification: an attempt for lignin degradation from lignocellulosic feedstock. RSC Advances, 5(92), pp.75281-75291.

Rajak, R.C. and Banerjee, R., 2016. Enzyme mediated biomass pretreatment and hydrolysis: a biotechnological venture towards bioethanol production. Rsc Advances, 6(66), pp.61301-61311.

Rajeswari, G. and Jacob, S., 2020. Deciphering the aloe vera leaf rind as potent feedstock for bioethanol through enzymatic delignification and its enhanced saccharification. Industrial Crops and Products, 143, pp.111876.

Ravichandran, A., Rao, R.G., Thammaiah, V., Gopinath, S.M. and Sridhar, M., 2019. A versatile peroxidase from Lentinus squarrosulus towards enhanced delignification and in vitro digestibility of crop residues. BioResources, 14(3), pp.5132-5149.

Rekik, H., Nadia, Z.J., Bejar, W., Kourdali, S., Belhoul, M., Hmidi, M., Benkiar, A., Badis, A., Sallem, N., Bejar, S. and Jaouadi, B., 2015. Characterization of a purified decolorizing detergent-stable peroxidase from Streptomyces griseosporeus SN9. International journal of biological macromolecules, 73, pp.253-263.

Ren, W., Zhu, J., Guo, F., Guo, J., Zhang, X., Wang, H. and Yu, Y., 2022. Structural evolution of cellulose from bamboo fibers and parenchyma cells during ionic liquid pretreatment for enhanced hydrolysis. Biomacromolecules, 23(5), pp.1938-1948.

Saravanan, A., Kumar, P.S., Jeevanantham, S., Karishma, S. and Vo, D.V.N., 2022. Recent advances and sustainable development of biofuels production from lignocellulosic biomass. Bioresource Technology, 344, pp.126203.

Sarika, D., Kumar, P.S.S.A., Arshad, S. and Sukumaran, M.K., 2015. Purification and evaluation of horseradish peroxidase activity. International Journal of Current Microbiology and Applied Sciences, 4(7), pp.367-375.

Schilling, J.S., Ai, J., Blanchette, R.A., Duncan, S.M., Filley, T.R. and Tschirner, U.W., 2012. Lignocellulose modifications by brown rot fungi and their effects, as pretreatments, on cellulolysis. Bioresource Technology, 116, pp.147-154.

Schmitz, E., Leontakianakou, S., Norlander, S., Karlsson, E.N. and Adlercreutz, P., 2022. Lignocellulose degradation for the bioeconomy: The potential of enzyme synergies between xylanases, ferulic acid esterase and laccase for the production of arabinoxylo-oligosaccharides. Bioresource Technology, 343, pp.126114.

Segal, L.G.J.M.A., Creely, J.J., Martin Jr, A.E. and Conrad, C.M., 1959. An empirical method for estimating the degree of crystallinity of native cellulose using the X-ray diffractometer. Textile research journal, 29(10), pp.786-794.

Shao, B., Han, Z., Pang, R., Wu, D., Xie, B. and Su, Y., 2023. The crystalline structure transition and hydrogen bonds shift determining enhanced enzymatic digestibility of cellulose treated by ultrasonication. Science of The Total Environment, 876, pp.162631.

Sharma, H.K., Xu, C. and Qin, W., 2019. Biological pretreatment of lignocellulosic biomass for biofuels and bioproducts: an overview. Waste and Biomass Valorization, 10, pp.235-251.

Sharma, S., Sharma, V., Nargotra, P. and Bajaj, B.K., 2018. Process desired functional attributes of an endoxylanase of GH10 family from a new strain of Aspergillus terreus S9. International journal of biological macromolecules, 115, pp.663-671.

Sheng, Y., Lam, S.S., Wu, Y., Ge, S., Wu, J., Cai, L., Huang, Z., Van Le, Q., Sonne, C. and Xia, C., 2021. Enzymatic conversion of pretreated lignocellulosic biomass: A review on influence of structural changes of lignin. Bioresource technology, 324, pp.124631.

Shi, J., Sharma-Shivappa, R.R. and Chinn, M.S., 2009. Microbial pretreatment of cotton stalks by submerged cultivation of Phanerochaete chrysosporium. Bioresource technology, 100(19), pp.4388-4395.

Shirkavand, E., Baroutian, S., Gapes, D.J. and Young, B.R., 2016. Combination of fungal and physicochemical processes for lignocellulosic biomass pretreatment–a review. Renewable and Sustainable Energy Reviews, 54, pp.217-234.

Sidana, A. and Yadav, S.K., 2022. Recent developments in lignocellulosic biomass pretreatment with a focus on eco-friendly, non-conventional methods. Journal of Cleaner Production, 335, pp.130286.

Silva-Sanzana, C., Estevez. J.M., and. Blanco-Herrera, F., 2020. Influence of cell wall polymers and their modifying enzymes during plant–aphid interactions. Journal of experimental botany, 71(13), pp3854-3864

Singh, P., Suman, A., Tiwari, P., Arya, N., Gaur, A. and Shrivastava, A.K., 2008. Biological pretreatment of sugarcane trash for its conversion to fermentable sugars. World Journal of Microbiology and Biotechnology, 24, pp.667-673.

Singhania, R.R., Dixit, P., Patel, A.K., Giri, B.S., Kuo, C.H., Chen, C.W. and Di Dong, C., 2021. Role and significance of lytic polysaccharide monooxygenases (LPMOs) in lignocellulose deconstruction. Bioresource Technology, 335, pp.125261.

Singhania, R.R., Patel, A.K., Raj, T., Chen, C.W., Ponnusamy, V.K., Tahir, N., Kim, S.H. and Dong, C.D., 2022. Lignin valorisation via enzymes: A sustainable approach. Fuel, 311, pp.122608.

Sugiura, M., Hirai, H. and Nishida, T., 2003. Purification and characterization of a novel lignin peroxidase from white-rot fungus Phanerochaete sordida YK-624. FEMS microbiology letters, 224(2), pp.285-290.

Sun, H., Cui, X., Li, R., Guo, J. and Dong, R., 2021. Ensiling process for efficient biogas production from lignocellulosic substrates: Methods, mechanisms, and measures. Bioresource Technology, 342, pp.125928.

Sun, Y. and Cheng, J., 2002. Hydrolysis of lignocellulosic materials for ethanol production: a review. Bioresource technology, 83(1), pp.1-11.

Taboada-Puig, R., Lú-Chau, T., Moreira, M.T., Feijoo, G., Martínez, M.J. and Lema, J.M., 2011. A new strain of Bjerkandera sp. production, purification and characterization of versatile peroxidase. World Journal of Microbiology and Biotechnology, 27, pp.115-122.

Tayyab, M., Noman, A., Islam, W., Waheed, S., Arafat, Y., Ali, F., Zaynab, M., Lin, S., Zhang, H. and Lin, W., 2018. Bioethanol production from lignocellulosic biomass by environment-friendly pretreatment methods: a review. Applied Ecology & Environmental Research, 16(1), pp225-249.

Thoresen, M., Malgas, S., Mafa, M.S. and Pletschke, B.I., 2021. Revisiting the phenomenon of cellulase action: Not all endo-and exo-cellulase interactions are synergistic. Catalysts, 11(2), pp.170.

Tian, S.Q., Zhao, R.Y. and Chen, Z.C., 2018. Review of the pretreatment and bioconversion of lignocellulosic biomass from wheat straw materials. Renewable and Sustainable Energy Reviews, 91, pp.483-489.

Tiwari, A., Chen, C.W., Haldar, D., Patel, A.K., Dong, C.D. and Singhania, R.R., 2023. Laccase in Biorefinery of Lignocellulosic Biomass. Applied Sciences, 13(8), pp.4673.

Tõlgo, M., Hegnar, O.A., Østby, H., Várnai, A., Vilaplana, F., Eijsink, V.G. and Olsson, L., 2022. Comparison of six lytic polysaccharide monooxygenases from Thermothielavioides terrestris shows that functional variation underlies the multiplicity of LPMO genes in filamentous fungi. Applied and Environmental Microbiology, 88(6), pp.e00096-22.

Tsegaye, B., Balomajumder, C. and Roy, P., 2019. Microbial delignification and hydrolysis of lignocellulosic biomass to enhance biofuel production: an overview and future prospect. Bulletin of the National Research Centre, 43(1), pp.1-16.

Twala, P.P., Mitema, A., Baburam, C. and Feto, N.A., 2020. Breakthroughs in the discovery and use of different peroxidase isoforms of microbial origin. AIMS microbiology, 6(3), pp.330.

Ürek, R.Ö. and Pazarlioğlu, N.K., 2004. Purification and partial characterization of manganese peroxidase from immobilized Phanerochaete chrysosporium. Process Biochemistry, 39(12), pp.2061-2068.

Vaaje-Kolstad, G., Forsberg, Z., Loose, J.S., Bissaro, B. and Eijsink, V.G., 2017. Structural diversity of lytic polysaccharide monooxygenases. Current opinion in structural biology, 44, pp.67-76.

van Bloois, E., Torres Pazmiño, D.E., Winter, R.T. and Fraaije, M.W., 2010. A robust and extracellular heme-containing peroxidase from Thermobifida fusca as prototype of a bacterial peroxidase superfamily. Applied microbiology and biotechnology, 86, pp.1419-1430.

Van Dyk, J.S. and Pletschke, B., 2012. A review of lignocellulose bioconversion using enzymatic hydrolysis and synergistic cooperation between enzymes—factors affecting enzymes, conversion and synergy. Biotechnology advances, 30(6), pp.1458-1480.

Vermaas, J.V., Crowley, M.F., Beckham, G.T. and Payne, C.M., 2015. Effects of lytic polysaccharide monooxygenase oxidation on cellulose structure and binding of oxidized cellulose oligomers to cellulases. The Journal of Physical Chemistry B, 119(20), pp.6129-6143.
Vernon-Parry, K.D., 2000. Scanning electron microscopy: an introduction. III-Vs review, 13(4), pp.40-44.

Waghmare, P.R., Khandare, R.V., Jeon, B.H. and Govindwar, S.P., 2018. Enzymatic hydrolysis of biologically pretreated sorghum husk for bioethanol production. BIOFUEL RESEARCH JOURNAL-BRJ, 5(3), pp.846-853.

Wagner, A.O., Lackner, N., Mutschlechner, M., Prem, E.M., Markt, R. and Illmer, P., 2018. Biological pretreatment strategies for second-generation lignocellulosic resources to enhance biogas production. Energies, 11(7), pp.1797.

Walton, P.H. and Davies, G.J., 2016. On the catalytic mechanisms of lytic polysaccharide monooxygenases. Current opinion in chemical biology, 31, pp.195-207.

Wan, C. and Li, Y., 2010. Microbial pretreatment of corn stover with Ceriporiopsis subvermispora for enzymatic hydrolysis and ethanol production. Bioresource technology, 101(16), pp.6398-6403.

Wang, J., Zhu, J., Huang, R. and Yang, Y., 2012. Investigation of cell wall composition related to stem lodging resistance in wheat (Triticum aestivum L.) by FTIR spectroscopy. Plant signaling & behavior, 7(7), pp.856-863.

Weng, C., Peng, X. and Han, Y., 2021. Depolymerization and conversion of lignin to value-added bioproducts by microbial and enzymatic catalysis. Biotechnology for Biofuels, 14(1), pp.1-22.

Wu, D., Wei, Z., Mohamed, T.A., Zheng, G., Qu, F., Wang, F., Zhao, Y. and Song, C., 2022. Lignocellulose biomass bioconversion during composting: Mechanism of action of lignocellulase, pretreatment methods and future perspectives. Chemosphere, 286, pp.131635.

Yang, J., Yuan, H., Wang, H. and Chen, W., 2005. Purification and characterization of lignin peroxidases from Penicillium decumbens P6. World Journal of microbiology and Biotechnology, 21, pp.435-440.

Yu, S., Liu, Z., Xu, N., Chen, J. and Gao, Y., 2020. Influencing factors for determining the crystallinity of native cellulose by X-ray diffraction. Analytical Sciences, 36(8), pp.947-951.
Zabed, H., Sahu, J.N., Boyce, A.N. and Faruq, G., 2016. Fuel ethanol production from lignocellulosic biomass: an overview on feedstocks and technological approaches. Renewable and sustainable energy reviews, 66, pp.751-774.

Zabed, H.M., Akter, S., Yun, J., Zhang, G., Awad, F.N., Qi, X. and Sahu, J.N., 2019. Recent advances in biological pretreatment of microalgae and lignocellulosic biomass for biofuel production. Renewable and Sustainable Energy Reviews, 105, pp.105-128.

Zhang, K., Xu, R., Abomohra, A.E.F., Xie, S., Yu, Z., Guo, Q., Liu, P., Peng, L. and Li, X., 2019. A sustainable approach for efficient conversion of lignin into biodiesel accompanied by biological pretreatment of corn straw. Energy conversion and management, 199, pp.111928.

Zhang, P., Cui, M., Huang, R., Qi, W., Thielemans, W., He, Z. and Su, R., 2021. Enhanced enzymatic hydrolysis of cellulose by endoglucanase via expansin pretreatment and the addition of zinc ions. Bioresource Technology, 333, pp.125139.

Zhang, S., Dong, Z., Shi, J., Yang, C., Fang, Y., Chen, G., Chen, H. and Tian, C., 2022. Enzymatic hydrolysis of corn stover lignin by laccase, lignin peroxidase, and manganese peroxidase. Bioresource Technology, 361, pp.127699.

Zhou, W., Apkarian, R., Wang, Z.L. and Joy, D., 2007. Fundamentals of scanning electron microscopy (SEM). Scanning Microscopy for Nanotechnology: Techniques and Applications, pp.1-40.

Zhou, Z., Ju, X., Chen, J., Wang, R., Zhong, Y. and Li, L., 2021. Charge-oriented strategies of tunable substrate affinity based on cellulase and biomass for improving in situ saccharification: A review. Bioresource Technology, 319, pp.124159.

Appendices

Table A1: Biochemical characterisation of ligninolytic and holocellulolytic enzymes

Types of enzymes	Names of the enzymes	Source	pH optimum	Temperature optimum	Thermostability	Reference
Ligninolytic enzymes						
	dye-decolourizing peroxidase	*Raoultella ornithinolytica* OKOH-1	pH 6	50°C	50°C	Falade *et al.* (2019)
	Laccase	*Sphingobacterium* ksn-11	pH 4.5	40°C	-	Neelkant *et al.* (2020)
	laccase	*Alcaligenes faecalis*	pH 4	55°C	-	Abdelgalil *et al.* (2020)
	yellow laccase	*Lentinus squarrosulus* MR13	pH 4-9	40°C	25-55°C	Mukhopadhyay and Banerjee (2015)
	Bacterial peroxidase	*Thermobifida fusca*	pH 3.5	25°C	60°C	van Bloois *et al.* (2010)
	Bacterial peroxidase	isolated strain *Pseudomonas* sp. SUK1	pH 3	40°C	-	Kalyani *et al.* (2011)
	Manganese peroxidase	*Phanerochaete chrysosporium*	pH 4.5	30°C	25-40°C	Ürek and Pazarlioğlu, (2004)
	free and immobilized Lignin peroxidase	*Trametes versicolor* IBL-04	pH 6 and 5, respectively	60°C and 80°C, respectively	20-60°C and 20-80°C, respectively	Asgher *et al.* (2012)
	Lignin peroxidase	*Acinetobacter calcoaceticus* NCIM 2890	pH 1.0	40–70°C	-	Ghodake *et al.* (2009)
	hybrid versatile peroxidase (Lignin	*Bjerkandera adusta*	pH 3.0-3.5 for LiP and pH 4.5 for MnP	40°C for LiP and 60°C for MnP	-	Ertan *et al.* (2012)

and Manganese peroxidase)					
Peroxidase	Moringa *Oleifers* L leaves	pH 6	50°C	50°C	Khatun *et al.* (2012)
Peroxidase from date palm	*Phoenix dactylifera* leaves	pH 3–5, with optima at around pH 4.5	-	75°C	Al-Bagmi *et al.* (2019)
Horseradish peroxidase	*Armoracia rusticana*	pH 4.5	-	37°C	Mohotloane *et al.,* 2023
Peroxidase	*Leucaena Leucocephala*	pH 5	55°C	65°C for 20 min	Pandey and Dwivedi, (2011)
Peroxidase	*Carica papaya*	pH 7	40°C	60°C for 1 hour	Pandey *et al.* (2012).
Holocellulolytic enzymes					
Thermostable xylanase	*Planomicrobium glaciei* CHR43	pH 9	80°C	50 -90°C	Liu *et al.* (2021)
GH10 xylanase	*Penicillium citrinum* isolate HZN13	pH 3.5-5	65°C	55-75°C	Bagewadi, *et al.* (2016)
Cellobiohydrolase I (CBHI)	*Penicillium digitatum*	pH 5.2	60°C	-	Dos Santos *et al.* (2020)
β-1,4-Glucanases from	*Penicillium simplicissimum* H-11	pH 3.2	60°C	50°C	Bai *et al.* (2013)
GH10 Endoxylanase	*Aspergillus terreus* S9	pH 9	80°C	60°C	Sharma *et al.* (2018)

Table A2: Chemical composition (as a percentage) of various biomass materials used for biofuel production.

Lignocellulosic materials	**Major components of the lignocellulosic material**			**Reference**
	Cellulose (%)	**Hemicellulose (%)**	**Lignin (%)**	
Sugarcane Bagasse	43	25	24	Merino and Cherry (2007)
Sweet sorghum bagasse	27	14	14	Li *et al.* (2010)
Corn stover (Zea mays)	38	23	20	Wan and Li (2010)
Corn cobs	45	35	15	Sun and Cheng (2002)
Wheat straw	30	22	17	Ballesteros *et al.* (2006)
Rice straw	32.1	24 1	18	Howard at al., (2003)
Sugarcane leaves	45	25	18	Singh *et al.* (2008)

Cotton stalk	67	16	13	Kim *et al.* (2016)
Rye straw	31	22	25	García-Cubero *et al.,* 2009
Switchgrass	31	24	18	Lee *et al.* (2009)

Table A3: Functional group assignment of biomass components

Wavenumber (1/cm)	**Functional group assignment and biomass component identification.**	**References (Mafa et al., 2020a, b)**
3600–3000	OH, stretching vibration; broad peak represents intra/inter hydrogen bonds: Microcrystalline cellulose region.	Nuruddin *et al.,* 2016 Guo *et al.,* 2019 Mafa *et al. 2020a, b*
3000–2600	2960-2850 C-H stretching (cellulose).	Nuruddin *et al.,* 2016 Mafa *et al. 2020a, b*
1800–1500	1775-1730 ester bond, lignin hemicellulose conjugation region. 1675–1655 C=O stretching vibration: lignin region. 1630–1593 Aromatic skeletal plus C=O stretching vibration: Lignin region.	Nuruddin *et al.,* 2016 Derkacheva and Sukhov 2008 Guo *et al.,* 2019
1500–1300	1428 CH_2 symmetric bending (cellulose). 1367 C–H vibrations and CH_2 bending. (Cellulose, hemicelluloses). 1331-1320 Bending of O–H groups in pyranose ring.	Nuruddin *et al.,* 2016 Guo *et al.,* 2019 Liu *et al.,* 2021 Mafa *et al. 2020a, b*
1300–1200	1200 C-C plus C-O plus C=O stretching vibration; carbohydrates and lignin.	Guo *et al.,* 2019 Derkacheva and Sukhov 2008
1200–900	1057-1030 ether/glyosidic bonds, with shoulders at 1109 and 1165 related to the polysaccharide components.	Wang *et al.,* 2012 Liu *et al.,* 2021
900–700	900 celluloses	Nuruddin *et al.,* 2016

	890 hemicellulose 886 β-1,3-glucan	Liu *et al.*, 2021

adapted from Mafa *et al*., 2020a, b

Standard curves

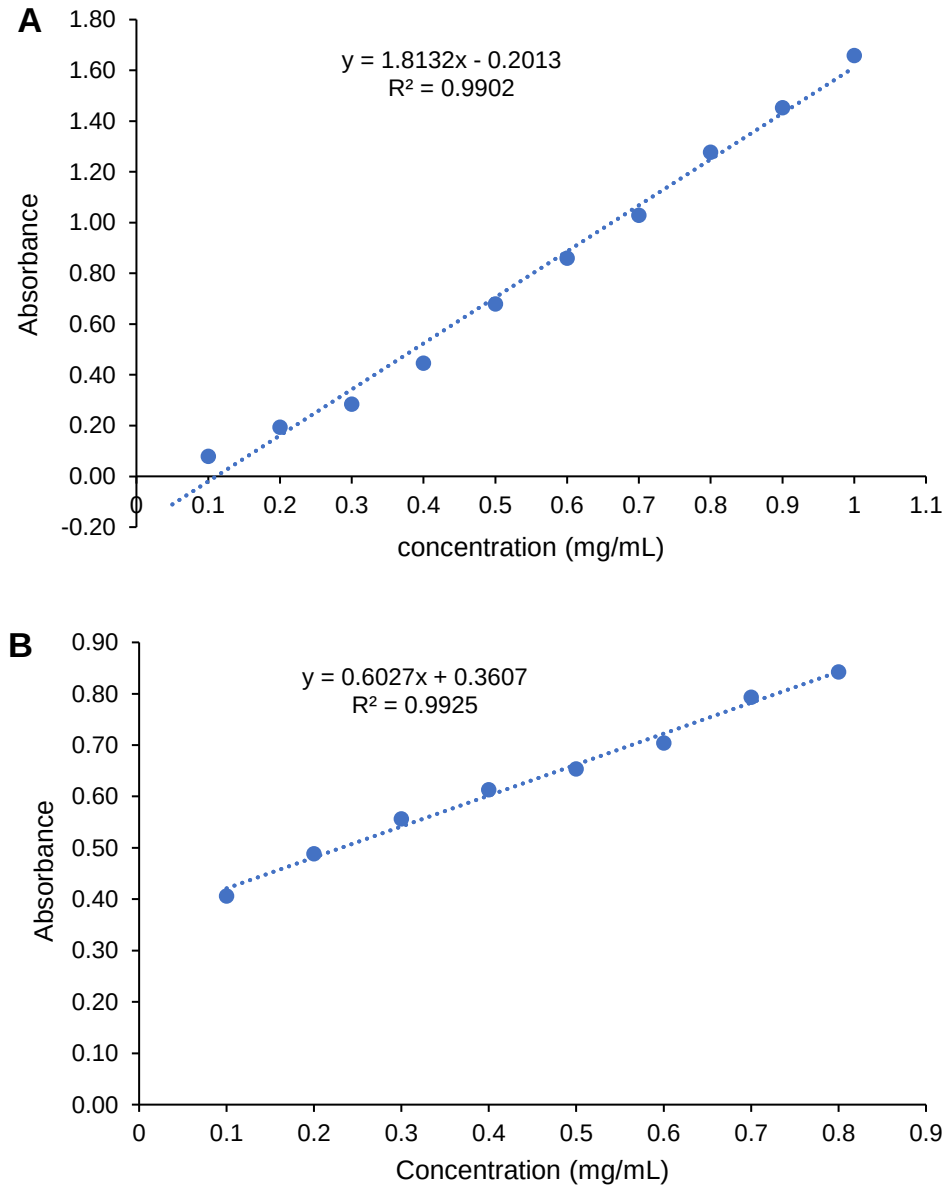

Figure A1: A representation of the DNS (glucose) assay (A) and Bradford assay (B) standard curves